PERIÓDICO TCHÊ QUÍMICA

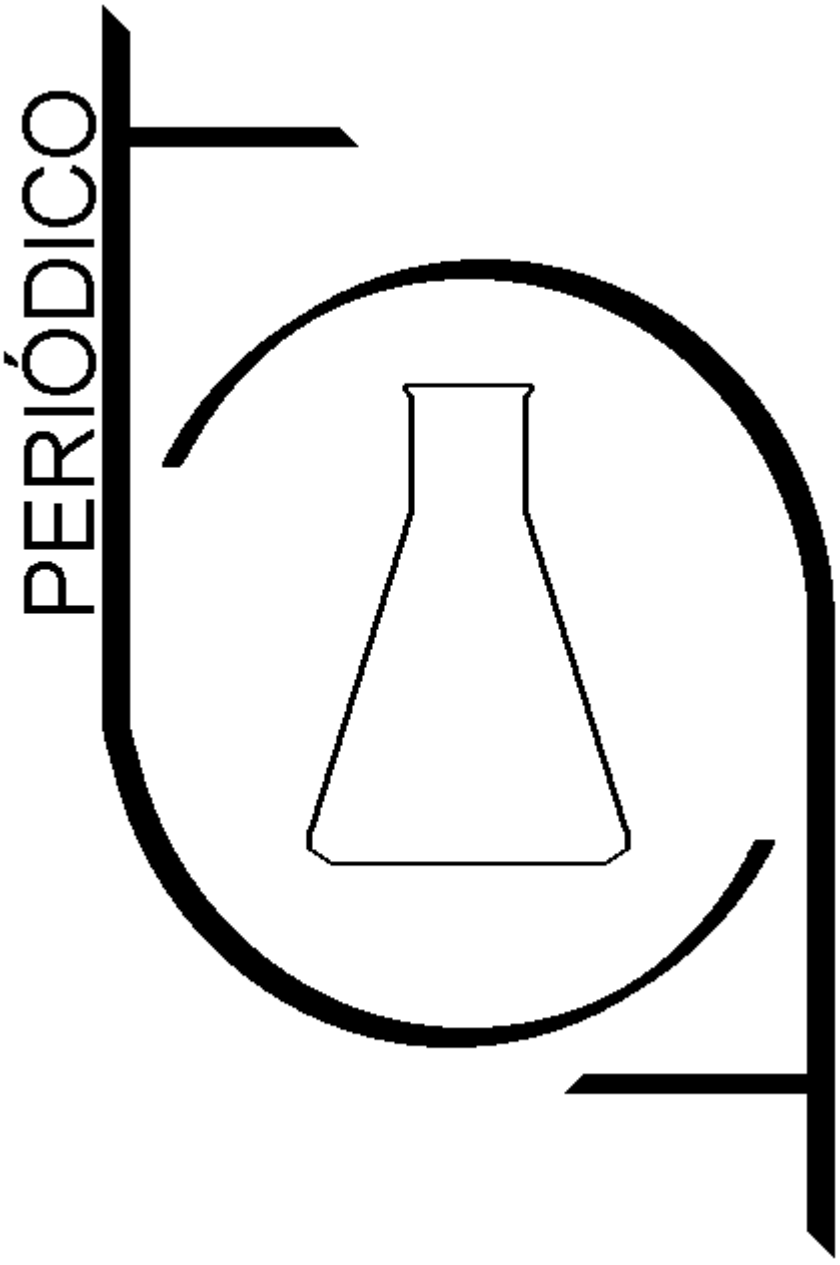

Volume 19 - Número 42 - 2022 ISSN 2179-0302

Órgão de divulgação científica e informativa

www.periodico.tchequimica.com

PERIÓDICO TCHÊ QUÍMICA

ISSN - 1806-0374 (Impresso) ISSN - 2179-0302 (Online)

Volume 19 **Número 42 – 2022** **ISSN 2179 - 0302**

Órgão de divulgação científica e informativa.

Dados Internacionais de Catalogação na Publicação (CIP)

Periódico Tchê Química: órgão de divulgação científica e informativa [recurso eletrônico] / Grupo Tchê Química – Vol. 1, n. 1 (Jan. 2004) – Porto Alegre: Grupo Tchê Química, 2005 - Semestral.
Sistema requerido: Adobe Acrobat Reader.
Modo de acesso: World Wide Web:
<http://www.tchequimica.com>
Descrição baseada em: Vol. 19, n. 41 (Jun. 2022).
ISSN 1806-0374
ISSN 2179-0302
1.Química. 2. Física. 3. Biologia. 4. Ciências Naturais. 5. Farmacologia. 6. Ciências exatas. 7. Ciências aplicadas. 8. Ciências. I. Grupo Tchê Química.

UDC 001

Bibliotecário Responsável
Ednei de Freitas Silveira
CRB 10/1262

Welcome to PERIÓDICO TCHÊ QUÍMICA
International multidisciplinary scientific journal

Periodico Tchê Quimica publishes Research Article/Original Article, Review Article, Short Report, Technical Notes, Case Studies, Interview, Book review and Forum article. Articles suitable for publication at Periodico Tchê Quimica are those that cover the traditional fields of ***Chemistry, Biology/Biochemistry, Pharmaceutical Chemistry, Medicinal Chemistry, Chemical Engineering, Chemometrics/Statistics, phisics/Phisical chemistry, and Science Education****. We are especially interested in those submissions that are highly relevant to theoretical and* ***applied contributions in the area of chemistry and related disciplines.***

PERIÓDICO TCHÊ QUÍMICA

Volume 19 Número 42 – 2022 ISSN 2179 - 0302

Órgão de divulgação científica e informativa.

Periódico Tchê Química

ISSN - 1806-0374 (Print)
ISSN - 2179-0302 (Online)

LCCN: 2010240735

Divulgação *on-line* em
http://www.periodico.tchequimica.com
http://www.journal.tchequimica.com
http://www.tchequimica.com

Esta revista é indexada e resumida pelo CAS, EBSCO, Index Copernicus, EJL, Reaxys, Latindex, Web of Science (ESCI), OAJI.net, CAB Abstracts, ROAD, and Sumários.

Missão

O Periódico Tchê Química (PTQ) publica artigos de pesquisa originais, artigos de revisão, notas curtas (publicações científicas), revisões de livros, artigos de fórum, editoriais e entrevistas. Pesquisadores de todos os países são convidados a publicar nas páginas do PTQ.

A responsabilidade sobre os artigos é de exclusividade dos autores.

Correspondências:

Rua Anita Garibaldi, 359/603.
Bairro Mon't Serrat. CEP: 90450-001
Porto Alegre – RS. Brasil.
Skype: tchequimica
www.periodico.tchequimica.com
journal.tq@gmail.com

Índice / Index

2023 CALL FOR PAPER

CHAMADA PARA TRABALHOS 2023

e-mail: journal.tq@gmail.com

As the world is going through a difficult period, the Periódico Tchê Química would like to make its part to improve it through scientific divulgation. Therefore, for **2023** all the manuscripts dealing with **food, drug, or energy production** will be published without publication fees as long as they follow the journal instructions on the website.

Including, **but not limited to**:

- raw-materials;
- production;
- quality-control;
- shelf life;
- energy efficiency;
- Production of fertilizers;
- biotechnology for food and drugs;
- industrial process.

We look forward to hearing from you and are grateful for your support in sharing this message with your friends.

Thank you very much.

Editors.

Como o mundo está passando por um período difícil, o Periódico Tchê Química gostaria de fazer sua parte para melhorá-lo através da divulgação científica. Portanto, para **2023**, todos os manuscritos que tratam da **produção de alimentos, medicamentos ou energia** serão publicados sem taxas de publicação, desde que sigam as instruções do jornal disponíveis no site.

Incluindo, **mas não limitado a**:

- matérias-primas;
- Produção;
- controle de qualidade;
- validade;
- Eficiência energética;
- Produção de fertilizantes;
- biotecnologia para alimentos e medicamentos

Estamos ansiosos para ouvir de você e somos gratos por seu apoio em compartilhar esta mensagem com seus amigos.

Muito obrigado.

Editores.

PERIÓDICO TCHÊ QUÍMICA
ARTIGO ORIGINAL

USO DO RGB COMO MÉTODO QUANTITATIVO APLICADO AO ENSINO DE QUÍMICA ANALÍTICA

USE OF RGB AS A QUANTITATIVE METHOD APPLIED TO THE TEACHING OF ANALYTICAL CHEMISTRY

VELOSO, Pedro Henrique Fonseca[1*], SACRAMENTO, Veronica de Melo[2], ROYO, Vanessa de Andrade[1,2]

[1] Universidade Estadual de Montes Claros (Unimontes), Departamento de Biologia Geral, Montes Claros - Brasil.

[2] Universidade Estadual de Montes Claros (Unimontes), Programa de Pós-Graduação em Biotecnologia, Montes Claros - Brasil.

** Autor correspondente*
e-mail: pedrofonsecambc@gmail.com

Received 20 Augst 2022; received in revised form 20 September 2022; accepted 26 September 2022

RESUMO

Introdução: A utilização de alternativas para o ensino de química analítica na graduação tem sido um desafio para professores, uma vez que a maior parte dos métodos demandam de equipamentos de alto custo e habilidades analíticas funcionais. Este trabalho apresenta o uso do RGB, um sistema de cores aditivas presentes em médios digitais como método de quantificação de um determinado analito em amostras. **Objetivo**: Analisar diferentes amostras contendo distintas concentrações de café, comparando-as por meio de duas técnicas: 1) espectrofotometria e 2) RGB, e posteriormente realizar os cálculos para a determinação de uma concentração desconhecida. **Métodos:** Oito amostras foram preparadas, seis com concentrações definidas de café, uma em branco e uma sem concentração definida. O método 1 utilizou o espectrofotômetro para leitura da absorvância no comprimento de onda 420 nm para a leitura das melanoidinas, no método 2 foi utilizado o RGB, posicionando cubetas em frente uma tela digital emitindo luz no comprimento de onda correspondente. O Microsoft Powerpoint foi utilizado para coleta dos dados RGB e o Microsoft Excel para o tratamento dos dados. **Resultados:** Os dados obtidos por meio do equipamento analítico, bem como os obtidos via RGB foram capazes de estimar a concentração desconhecida de café, ambas as técnicas estimaram uma concentração entre 3 e 4%, ambos com equação da reta e r^2 capazes de estimar valores correspondentes as concentrações das amostras. **Discussão:** A técnica RGB vem sendo estudada nas últimas décadas, principalmente para análises colorimétricas, uma vez possibilita de forma acessível o estudo ou experiencias laboratoriais. Aproximando o discente da técnica espectrofotométrica, promovendo desenvolvimento científico e a elaboração de hipótese sobre o uso da tecnologia como ferramenta de análise. **Conclusões:** As práticas experimentais promovem o desenvolvimento de investigação, que orientam tanto o docente como o discente na utilização de novas tecnologias e no desenvolvimento de novas atividades voltadas para o ensino, este trabalho em questão abre um leque para a utilização de ferramentas e métodos de fácil acesso e baixo custo.

Palavras-chave: *Café, Melanoidinas, Métodos de quantificação, espectrofotometria, RGB.*

ABSTRACT

Background: The use of alternatives for teaching analytical chemistry in undergraduate studies has been a challenge for teachers since most methods require high-cost equipment and functional analytical skills. This work presents the use of RGB, an additive color system n digital media, as a method of quantifying of a given analyte in samples. **Aim:** To analyze different samples containing different concentrations of coffee, comparing them using two techniques: 1) spectrophotometry and 2) RGB, and then perform the calculations for the determination of an unknown concentration. **Methods:** Eight samples were prepared, six with defined concentrations of coffee, one in white, and one without a defined concentration. Method 1 used the spectrophotometer to read the absorbance at 420 nm wavelength for melanoidin reading, in method 2 the RGB was used, positioning buckets in front of a digital screen emitting light at the corresponding wavelength. Microsoft Powerpoint was used to collect RGB and Microsoft Excel data for data processing. **Results:** The data obtained through the analytical equipment, as well as those obtained via RGB, were able to estimate the unknown concentration of coffee, both techniques estimated a concentration between 3 and 4%, both with the equation of the line and r^2 capable of estimating

DOI: 10.52571/PTQ.v19.n42.2022.01_VELOSO_pgs_01_12.pdf

values corresponding to the concentrations of the samples. **Discussion:** The RGB technique has been studied in recent decades, mainly for colorimetric analyses, since it makes the study or laboratory experiments available in an accessible way. Bringing the student closer to the spectrophotometric technique, promoting scientific development, and elaborating the hypothesis about using technology as an analysis tool. **Conclusions:** Experimental practices promote the development of research, which guide both teachers and students in the use of new technologies and in the development of new activities aimed at teaching, this work in question opens a range for the use of tools and methods of easy access and low cost.

Keywords: *Coffee, Melanoidins, Quantification Methods, Spectrophotometry, RGB*

1. INTRODUÇÃO:

A química analítica pode ser definida como um processo autossuficiente, capaz de gerar dados qualitativos e quantitativos dentro de uma amostra ou material, no qual obtém-se informações sobre a composição química, estrutura presente, arranjo e volume de átomos de uma amostra (Cammann,1992). É uma disciplina ofertada em diversas graduações, incluindo cursos das áreas das ciências exatas, biológicas, naturais, saúde e tecnologia. De forma generalista o ensino de química é frequentemente relatado como algo difícil, isso se dá principalmente pela utilização de termos técnicos complexos diretamente relacionados a linguagem científica (Mönch e Markic, 2022). Dentre as principais barreiras do ensino de químicas estão as dificuldades de realização de práticas experimentais, principalmente no que diz respeito da contextualização da teoria junto a prática (Moisés *et al*., 2022).

Nessa perspectiva, gerar o conhecimento e desenvolvimento científico se faz necessário para o bom desempenho acadêmico do aluno na vida cotidiana bem como no profissional. O conhecimento científico exerce influência no cotidiano da sociedade e do meio ambiente. Na tentativa de conhecer os fenômenos e descrevê-los torna-se comum a realização de práticas experimentais que de forma extensa e controlada que impulsionam o desenvolvimento nos mais diversos setores tornando-os mais atraentes, acessíveis e promovendo o avanço tecnológico de materiais e processos como na indústria de medicamentos, na agricultura, na alimentação, na comunicação, entre outros (Coelho e Marques, 2007)

Os laboratórios exercem uma grande importância no contexto do ensino, através dele é possível fornecer treinamento e observação no qual estímulos e curiosidade podem ser treinados, uma vez que a utilização deste espaço configura uma importante abordagem para o desenvolvimento intelectual do aluno, considerada uma experiencia popular e valiosa tanto para professores quanto para alunos (Salta, Ntalakou e Tsiortos, 2022). Neste cenário, a contextualização das atividades experimentais auxilia e contempla a educação científica ao promover entre os discentes descobertas, interações e participações ativas de forma reflexiva e dialógica, e promovem o desenvolvimento de conhecimentos e habilidades, afastando a premissa de que práticas laboratoriais requerem equipamentos e materiais caros e inacessíveis (Diógenes *et al*., 2020; Pucinelli *et al*., 2021)

A espectrofotometria é uma técnica analítica quantitativa, que tem como objetivo a absorção de luz em espectros do ultravioleta ou luz visível por espécies químicas, tanto em solução quanto em fase gasosa (Worsfold, 2017), é uma técnica ensinada a alunos do ensino médio (Silva *et al*., 2021) e graduação, sendo aplicada na caracterização de compostos químicos (Lietard *et al*., 2021). Desta forma a técnica é definida como a quantificação de um determinado composto a partir da luz emitida ou absorvida pelos constituintes presentes em uma amostra. Concomitantemente, aplica-se a Lei de Lambert-Beer, que é usada na determinação da concentração (Paristiowati *et al*., 2021). Trabalhos já publicados sobre a utilização da espectrofotometria de forma didática (Wang *et al*., 2022; Destino e Cunninghan, 2020; Angarita-Rivera *et al*., 2019; Arrebola *et al*., 2020; Dooling *et al*., 2013) trazem método como peça-chave ou como uma ferramenta estratégica que busca aproximar o discente de situações que simulem o ambiente do laboratório. A utilização da Webcam (Silva *et al*., 2021) e construção do próprio espectrofotômetro tem sido uma das maneiras de desmistificar a técnica analítica e aproximá-la dos discentes (Diawati *et al*., 2018).

Segundo Paulo Freire (1996), é necessário que o processo de ensino-aprendizagem contemple a realidade histórico-social do aluno, como principal meio para a sua autonomia (Freire, 1996). Logo, buscar o uso de elementos do

cotidiano para facilitar a compreensão dos conceitos é essencial. Neste contexto, insere-se o café, bebida altamente apreciada no Brasil, que é o maior produtor e exportador destes grãos no mundo, ocupando a segunda posição em consumo no ocidente (Brasil, 2022). Os aspectos relativos às propriedades do café e sua composição química pode ser uma ferramenta utilizado no processo ensino-aprendizagem visto que há possibilidade da aproximação de uma situação conteudista a algo prático no cotidiano do discente.

A determinação da qualidade do café é realizada a partir das características organolépticas do produto, tal qual a aparência física e os constituintes químicos (Tolessa *et al*., 2017) dentre os constituintes químicos de maior relevância estão o ácido clorogênico (figura 1), a cafeína (figura 2), a trigonelina (figura 3) e as melanoidinas (figura4)(Monteiro e Trugo, 2005), essas responsáveis pela cor e aroma, com o percentual de até 25% da matéria seca do produto (Tolessa *et al*., 2017). O processo pirolítico é induzido pela torrefação dos polissacarídeos presentes na parece celular do café, como as arabinogalactanas que correspondem a 47% das melanoidinas formadas (Rufián-Henares e Pastoriza, 2015), aquecimento também provoca a redução dos teores de ácido clorogênico e trigonelina, que são compostos termolábeis, com consequente formação de melanoidinas por meio da Reação de Maillard (Marcucci *et al*., 2013).

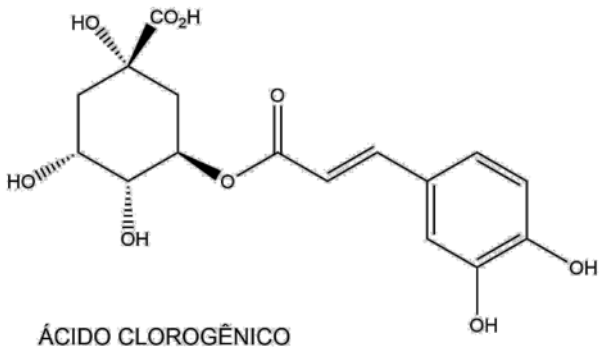

Figura 1. *Estrutura do Ácido Clorogênico. Fonte: autores.*

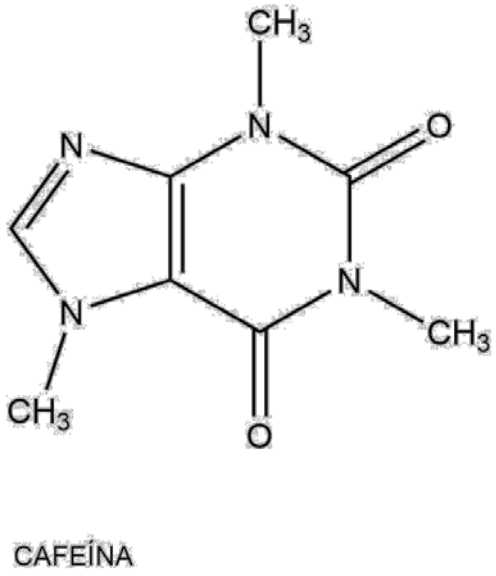

Figura 2. *Estrutura da Cafeína. Fonte: autores.*

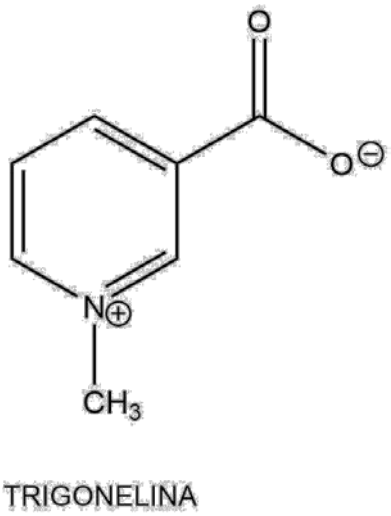

Figura 3. *Estrutura da Trigonelina. Fonte: autores.*

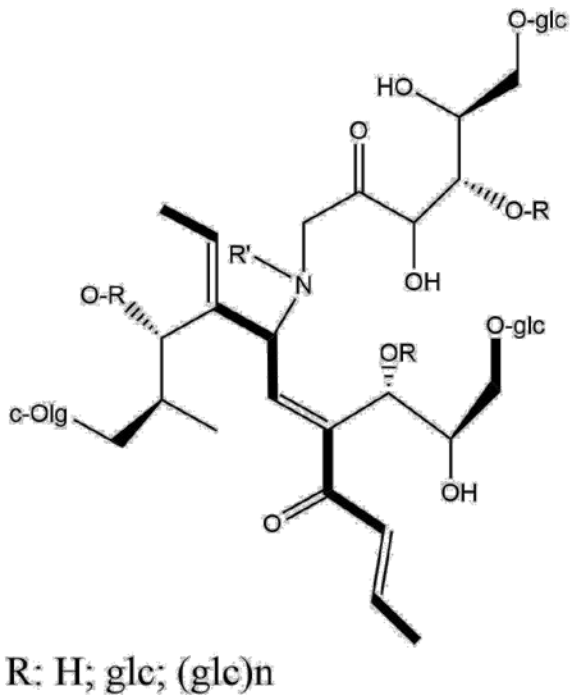

Figura 4. *Estrutura básica das melanoidinas. Fonte: autores, adaptado de Cämmerer, Jalyschkov e Kroh (2002)*

A reação de Maillard, (RM) é definida como uma cascata de reações químicas que envolve aminoácidos ou proteínas em conjunto com açúcares redutores, não enzimáticas, ocorre em altas temperaturas (Su *et al*., 2012), e como resultado há a formação de compostos que conferem cor, sabor e aroma aos alimentos (Starowicz e Zieliński, 2019). Dentre os produtos obtidos pela RM, destacam-se as melanoidinas, compostos de alto peso molecular formadas na última etapa da RM, são reconhecidas estruturalmente pela presença de nitrogênio entre o grupo carbonila dos açúcares redutores e o grupo amino dos aminoácidos ou proteínas e pela cor marrom e dourada que confere aos alimentos (Johnson *et al*., 2019)

As cores e os corantes possuem papéis notáveis em nossa vida, seja pelo fascínio que a sociedade atribui a eles, ou pela sua utilização antes da era comum, pelas civilizações mais remotas, que os utilizavam para os tingimentos e pinturas (Goldani, 2005). As melanoidinas não são classificadas como corantes, mas especificamente as encontradas no café exercem funções próximas, uma vez que possui a capacidade de deixar manchas de tons marrom nos tecidos nos quais teve contato direto.

Visando uma abordagem simplificada e de fácil realização, o objetivo da experiência é demonstrar a técnica espectrofotométrica de forma simples, a partir das cores expressas em diferentes concentrações das soluções de café. Utilizando como ferramenta de leitura o sistema de cores RGB (*red, green, blue*). O foco do experimento é observar as diferentes diluições das soluções, avaliando as utilizações de ferramentais digitais como estratégia didática.

2. PARTE EXPERIMENTAL:

O Café (*Coffea arabica* L.) torrado e moído, do tipo torra escura (extra forte), foi adquirido no comércio da cidade de Montes Claros em Minas Gerais - Brasil.

2.1. Obtenção da solução estoque

A preparação da solução estoque foi realizada adicionando 10 gramas do pó de café, em funil com filtro de papel, em seguida foram vertidos 100 mL de água mineral a aproximadamente 90 ºC sobre o pó (Santos *et al*., 2007; Yen *et al*., 2005). O método utilização para a extração das melanoidinas foi a líquido-sólido, no qual por meio do processo de filtração o líquido foi coletado e armazenado para análise posterior. Diferente da líquido-líquido que utiliza-se dois líquidos, geralmente uma fase aquosa e uma orgânica, no qual há a transferência de solutos de uma solução para outra, que posteriormente são separadas por um funil de separação (Polli, Prochnow e Tamanini, 1998).

2.2. Análises experimentais

As análises experimentais se deram em cinco etapas:

1) Diluição da solução estoque em água nas concentrações de 1, 2, 3, 4, 5, 6% e uma amostra desconhecida, completadas com água filtrada até a alíquota de 2 mL de uma cubeta. Para o branco foi utilizado água filtrada.

2) Análise das amostras no espectrofotômetro Shimadzu UV-VIS (Spectrophotometer UV-VIS 2550, Tókio, Japão) no comprimento de onda 420 nm.

3) Alocação das imagens sobre um fundo de tela colorido equivalente ao comprimento de onda desejado por meio de conversão on-line do comprimento de onda para RGB (Gee *et al*. 2017), para a análise foi utilizado o comprimento de 420 nm, comumente utilizado para avaliação de melanoidinas (figura 6).

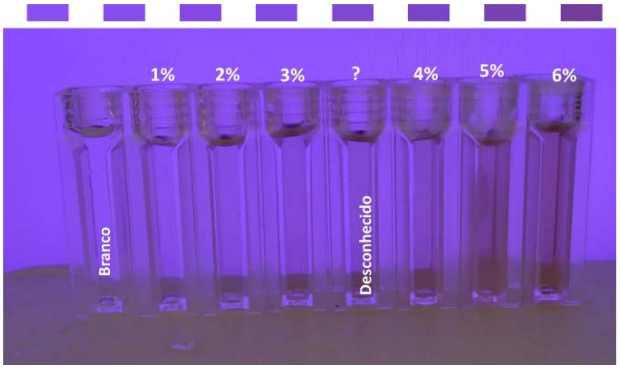

Figura 6. *Amostras em frente a um fundo como RGB equivalente ao comprimento de onda de 420 nm. Fonte: autores*

4) Aquisição das imagens utilizando smartphone Xiaomi Mi A2 provido de flash (12 megapixels com resolução de 4000 x 3000 pixels). A análise das imagens foi realizada por meio do *software Microsoft Powerpoint 365* (versão 16.0.15028.20160), no qual inseriu-se o formato retângulo por meio do menu "inserir> ilustrações> formas> retângulo" e utilizou-se a ferramenta conta gotas "forma de formato>estilos de forma> preenchimento de formas> conta-gotas". Foi selecionada a forma retângulo e posteriormente preenchida por meio do conta-gotas através do padrão sólido da cor de cada amostra (figura 7).

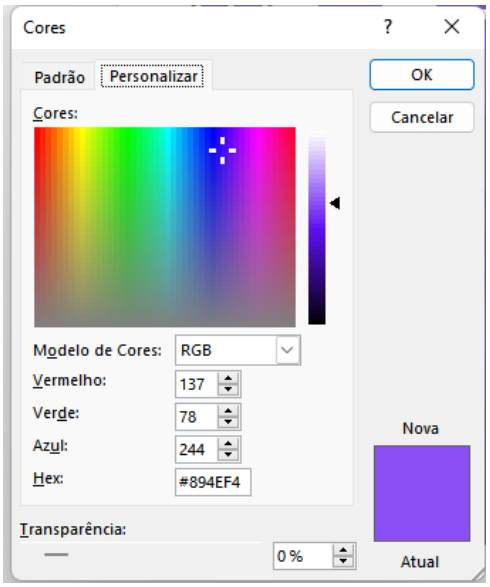

Figura 7. *Janela do Powerpoint utilizada para coleta dos dados. R: 137, G: 78 e B: 244 referentes a amostra "branco". Fonte: autores.*

5) Comparação dos resultados obtidos por meio do sistema RGB utilizando o Microsoft Excel 365 (versão 16.0.15028.20160), e os dados obtidos por meio da espectrofotometria. O cálculo das concentrações através da equação da reta e a estimativa da concentração desconhecida. No qual foi plotado os gráficos, com equação da reta, linha tendencia e R^2 (Gee *et al*., 2017).

2.3 Análise de Dados

Os resultados da aborvância foram calculados utilizando a equação 1 (Gee *et al*., 2017):

$$A = -\log (I_n/I_{branco}) \qquad \text{(Eq. 1)}$$

No qual, o I_n é correspondente aos valores de RGB, que são adaptados com os melhores resultados dentre os obtidos. I_{branco} é o valor RGB para água filtrada.

3. RESULTADOS E DISCUSSÃO:

3.1. Resultados

As análises realizadas por meio do espectrofotômetro foram concisas com a atividade proposta, as leituras no comprimento de onda 420 nm foram eficientes, capazes de apresentar a equação da reta necessária para revelar a concentração desconhecida (figura 7). A medição da concentração desconhecida foi realizada após a análise das concentrações conhecidas, que apresentou a aborvância de 0,414. O branco foi realizado com água filtrada.

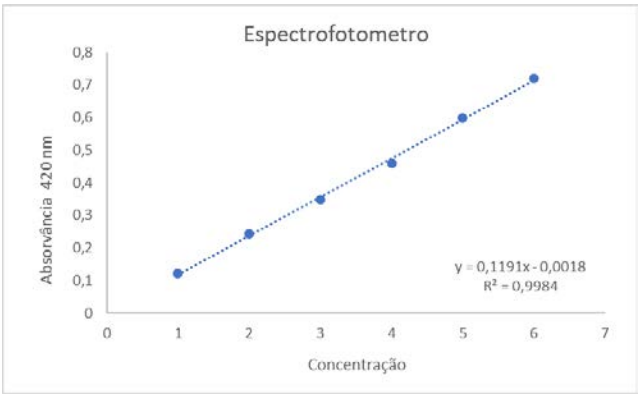

Figura 8. *Gráfico com as medidas de aborvâncias no espectrofotômetro das concentrações conhecidas. Fonte: autores*

Os resultados obtidos por meio da utilização de uma tela, com a cor equivalente ao comprimento de onda de 420 nm, apresentou eficiência na organização dos dados, originando a equação da reta necessária para o cálculo do ponto desconhecido (figura 8). O branco foi realizado com água filtrada (R: 137, G: 78, B:244).

A medição da concentração desconhecida foi realizada após a análise das concentrações conhecidas, que apresentou a aborvância de 0,065.

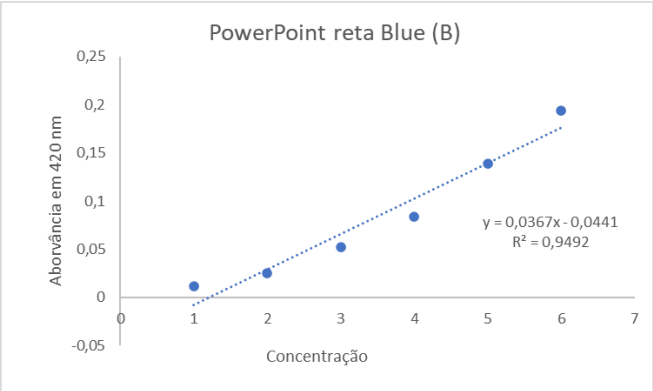

Figura 9. *Gráfico com as medidas de aborvâncias RGB – B no Powerpoint das concentrações conhecidas. Fonte: autores*

Os cálculos foram realizados por meio das equações da reta referentes a cada um dos métodos. Para o cálculo referente à espectrofotometria foi utilizada a equação 2:

$y = 0{,}1191x - 0{,}0018 \quad R^2: 0{,}9984 \quad$ (Eq. 2)

Para o cálculo referente ao RGB- B foi utilizada a equação 3:

$Y = 0{,}0367x - 0{,}0441 \quad R^2: 0{,}9492 \quad$ (Eq. 3)

Os resultados equivalentes as técnicas utilizadas foram expressas nas tabelas 1 e 2, respectivamente leitura no espectrofotômetro e leitura no RGB-B para a determinação da concentração desconhecida.

Tabela 1. *Resultados da análise espectrofotométrica.*

Equação da reta espectrofotômetro: y = 0,1191x - 0,0018 R² = 0,9984		
Concentração inicial	Absorbância	Concentração final
1%	0,121	1,0
2%	0,243	2,0
3%	0,349	2,9
4%	0,459	3,86
5%	0,599	5,0
6%	0,719	6,0
Concentração desconhecida	0,414	3,49

Fonte: autores

Tabela 2. *Resultado da análise em RBG - B*

Equação da reta RGB (B) Powerpoint: y = 0,0367x - 0,0441 R² = 0,9492		
Concentração inicial	Absorbância	Concentração estimada no RBG
1%	0,012	1,52
2%	0,025	1,88
3%	0,052	2,61
4%	0,084	3,49
5%	0,139	4,9
6%	0,194	6,4
Concentração desconhecida	0,065	2,97

Fonte: autores

3.2. Discussão

A atividade realizada proporcionou experiência importante sobre o uso de duas ferramentas para estimar a concentração de café, por meio das melanoidinas. Ambas as técnicas utilizadas apresentaram resultados significativos no que se diz respeito sobre a determinação de concentração de uma amostra desconhecida, por meio da equação da reta.

O conceito de cor luz pode ser traduzida como a cor que enxergamos refletidas em um determinado objeto, isto é, reflete a que se encontra do mesmo comprimento de onda e absorve aquelas fora do espectro, nesse conceito há denominação de três cores primárias, o azul, verde e vermelho (Zimmermann, 2005). Nos meios digitais é usado esses mesmos sistemas de cores aditivos, o RGB, R= vermelho, G: verde e B: azul.

Na análise realizada pelo método RGB demostrou eficiência tanto para a leitura quanto para a estimativa de concentração, com ressalvas uma vez que a técnica não é tão precisa quanto um equipamento analítico, mas é capaz de gerar estimativas em concordância com diferentes concentração, como pode ser observado na figura 7 e tabela 2. A linear adotada para a realização do estudo foi a B, que refere-se a cor azul, que apresentou melhores resultados, próximos aos encontrados das obtidas do espectrofotômetro. A definição de qual é o melhor canal de cor (R, G ou B) deve ser utilizada com base nos resultados que apresentam uma maior faixa dinâmica (Gee *et al*., 2017).

A utilização de RGB já foi utilizada em inúmeros estudos colorimétricos, o uso tem sido implicado na realização de experimentos de baixo custo, quando comparado ao uso do espectrofotômetro. A técnica já foi aplicada na quantificação de curcuminóides em cúrcuma, no

qual os resultados obtidos foram muito próximos, não havendo diferenças significativas quando comparado com os resultados obtidos via espectrofotometria (Supannarach e Thanapatay, 2008). A mesma metodologia, aplicada a variação e intensidade de cor foi utilizada no monitoramento do crescimento da alga *Chlorella vulgaris* (Peter *et al*., 2021).

Mais especificamente para a análise do café, foram realizadas análises em sala de aula onde o RGB foi aplicado para verificar diferentes intensidades, teores de fenólicos e o poder redutor, mostrando eficácia do método, além do baixo valor agregado as análises (Barreto, 2019). Em nossa pesquisa análise de diferentes concentrações de café por meio do RGB foi uma estratégia do ensino da espectrofotometria de forma simplificada, que pode ser realizada tanto em laboratório, sala de aula ou em casa, fazendo-se possível realizar as leituras, e confeccionar as curvas de regressão linear e estimar a absorbância de cada amostra.

Práticas experimentais promovem o desenvolvimento de posturas investigativas e a construção dos saberes científicos que podem ocorrer de forma contextualizada. Assim, a experimentação vai além do preconceito relativo a uma simples aplicação de "receita" que tem como resultado um relatório pré-determinado. Na óptica proposta, neste trabalho, o discente e o docente envolvem-se na experimentação de forma cooperativa, investigativa e dinâmica com a utilização de tecnologia que usam os padrões RBG que são funcionais como estratégia para o ensino da espectrofotometria, especialmente durante as aulas não presenciais. Na experimentação investigativa há a discussão por parte dos alunos no processo da elaboração de hipóteses, e o auxílio do professor responsável, mediando as ideias, para o exercício da capacidade de argumentação (Oliveira *et al*., 2011)

4. CONCLUSÕES:

A diluição das amostras, a análise colorimétrica e o cálculo de absorção são exercícios importantes para o desenvolvimento crítico do aluno e aulas experimentais como esta trata-se de estratégias didáticas para o ensino de química, a partir destas surgem investigações que possibilitam a criação de hipóteses sobre as atividades a serem realizadas, aproximando-os do método científico na prática.

Concluímos que a utilização do RGB em sala de aula como um método alternativo ao espectrofotômetro é eficiente, barato e de fácil realização. Unindo a teoria por traz da espectrofotometria de forma clara utilizando materiais presentes no cotidiano.

5. DECLARAÇÕES

5.1. Limitações do estudo

O estudo é limitado as amostras analisadas e aos ensaios realizados.

5.2. Agradecimentos

Laboratório de Produtos Naturais (LPN) - Universidade Estadual de Montes Claros.

5.3. Funding source

Esta pesquisa foi financiada pelos próprios autores.

5.4. Competing Interests

Os autores declaram que não há conflito de interesses.

6. REFERÊNCIAS:

1. Angarita-Rivera, P. A., Gabbard, D. B., Main, K. A., Timmermann, K. M., Kinkade, K. B., Wilson, K. J., & Doçi, C. L. (2019). Vitamin C as a Model for a Novel and Approachable Experimental Framework for Investigating Spectrophotometry. In Journal of Chemical Education (Vol. 96, Issue 11, pp. 2578–2583). American Chemical Society (ACS). https://doi.org/10.1021/acs.jchemed.9b00197

2. Arrebola, J. C., Rodríguez-Fernández, N., & Caballero, Á. (2020). Decontamination of Wastewater Using Activated Biochar from Agricultural Waste: A Practical Experiment for Environmental Sciences Students. In Journal of Chemical Education (Vol. 97, Issue 11, pp. 4137–4144). American Chemical Society (ACS). https://doi.org/10.1021/acs.jchemed.0c00202.

3. BARRETO, M. S. (2019). Método analítico inovador para determinação de compostos fenólicos e atividade antioxidante do café. 2019. 55 f. Dissertação (Mestrado em Química em Rede Nacional) - Universidade Federal de Viçosa, Viçosa-MG.

4. Brasil, Ministério da Agricultura, Pecuária e Abastecimento, Café no Brasil, 2018. Disponível em: http://www.agricultura.gov.br/assuntos/politicaagricola/cafe/cafeicultura-brasileira. Acesso em: 10 abr. 2022.

5. Cammann, K. (1992). Analytical Chemistry ? today's definition and interpretation. In Fresenius' Journal of Analytical Chemistry (Vol. 343, Issue 11, pp. 812–813). Springer Science and Business Media LLC. https://doi.org/10.1007/bf00328560

6. Cämmerer, B., Jalyschkov, V., & Kroh, L. W. (2002). Carbohydrate structures as part of the melanoidin skeleton. In International Congress Series (Vol. 1245, pp. 269–273). Elsevier BV. https://doi.org/10.1016/s0531-5131(02)00890-7

7. Coelho, J. C., Marques, C. A. (2007). Contribuições freireanas para a contextualização no ensino de Química. Ensaio Pesquisa em Educação em Ciências (Belo Horizonte), 9, 59-75. https://doi.org/10.1590/1983-21172007090105

8. Destino, J. F., & Cunningham, K. (2020). At-Home Colorimetric and Absorbance-Based Analyses: An Opportunity for Inquiry-Based, Laboratory-Style Learning. In Journal of Chemical Education (Vol. 97, Issue 9, pp. 2960–2966). American Chemical Society (ACS). https://doi.org/10.1021/acs.jchemed.0c00604.

9. Diawati, C., Liliasari, Setiabudi, A., & Buchari. (2018). Using Project-Based Learning To Design, Build, and Test Student-Made Photometer by Measuring the Unknown Concentration of Colored Substances. In Journal of Chemical Education (Vol. 95, Issue 3, pp. 468–475). American Chemical Society (ACS). https://doi.org/10.1021/acs.jchemed.7b00025

10. Diógenes, L. M. M. B., Pinheiro, M. C. D., Rolim, K. M. C., Albuquerque, F. H. S., Firmes, M. da P. R., Castro, C. S. C., Sampaio, C. S. M., & Oliveira, B. K. F. (2020). Painel integrado: Recurso didático-pedagógico no processo ensino-aprendizagem. In Brazilian Journal of Development (Vol. 6, Issue 4, pp. 20426–20474). Brazilian Journal of Development. https://doi.org/10.34117/bjdv6n4-282

11. Dooling, K., Bodenstedt, K., & Page, M. F. Z. (2013). A Caffeinated Boost on UV Spectrophotometry: A Lab for High School Chemistry or an Introductory University Chemistry Course. In Journal of Chemical Education (Vol. 90, Issue 7, pp. 914–917). American Chemical Society (ACS). https://doi.org/10.1021/ed300654u

12. Freire, P. Pedagogia da autonomia: saberes necessários à prática educativa. São Paulo, Paz e Terra, 1996.

13. Gee, C. T., Kehoe, E., Pomerantz, W. C. K., & Penn, R. L. (2017). Quantifying Protein Concentrations Using Smartphone Colorimetry: A New Method for an Established Test. In Journal of Chemical Education (Vol. 94, Issue 7, pp. 941–945). American Chemical Society (ACS). https://doi.org/10.1021/acs.jchemed.6b00676

14. GOLDANI, E. (2005). DYES: COLORS AND THEIR FASCINATION IN SOCIETY.

Em Periódico Tchê Química (Vol. 03, Issue 2, p. 61–66). Dr. D. Scientific Consulting. https://doi.org/10.52571/ptq.v2.n03.2005.janeiro/9_pgs_61_66.pdf

15. Johnson, I., Sithik Ali, M. A., & Kumar, M. (2019). Cyanobacteria/Microalgae for Distillery Wastewater Treatment- Past, Present and the Future. In Microbial Wastewater Treatment (pp. 195–236). Elsevier. https://doi.org/10.1016/b978-0-12-816809-7.00010-5

16. Lietard, A., Screen, M. A., Flindt, D. L., Jordan, C. J. C., Robson, J. M., & Verlet, J. R. R. (2021). A Combined Spectrophotometer and Fluorometer to Demonstrate the Principles of Absorption Spectroscopy. In Journal of Chemical Education (Vol. 98, Issue 12, pp. 3871–3877). American Chemical Society (ACS). https://doi.org/10.1021/acs.jchemed.1c00742.

17. Marcucci, C. T., Benassi, M. de T., Almeida, M. B., & Nixdorf, S. L. (2013). Teores de trigonelina, ácido 5-cafeoilquínico, cafeína e melanoidinas em cafés solúveis comerciais brasileiros. In Química Nova (Vol. 36, Issue 4, pp. 544–548). FapUNIFESP (SciELO). https://doi.org/10.1590/s0100-40422013000400011

18. Moisés, L. J. A., Nunes, J. D. S., Souza, L. M. de, Lira, A. de L., & Simões, A. S. de M. (2022). Experimentação no ensino de ciências: possibilidades e desafios. In Revista Brasileira da Educação Profissional e Tecnológica (Vol. 1, Issue 22, p. e12562). Instituto Federal de Educacao, Ciencia e Tecnologia do Rio Grande do Norte (IFRN). https://doi.org/10.15628/rbept.2022.12562

19. Mönch, C., & Markic, S. (2022). Exploring Pre-Service Chemistry Teachers' Pedagogical Scientific Language Knowledge. In Education Sciences (Vol. 12, Issue 4, p. 244). MDPI AG. https://doi.org/10.3390/educsci12040244

20. Monteiro, M. C., & Trugo, L. C. (2005). Determinação de compostos bioativos em amostras comerciais de café torrado. In Química Nova (Vol. 28, Issue 4, pp. 637–641). FapUNIFESP (SciELO). https://doi.org/10.1590/s0100-40422005000400001

21. OLIVEIRA, N., BENEDETI, F. E., FIORUCCI, A. R., BENEDETTI, L. P. dos S., & BELOTO, M. R. M. de O. (2011). USE OF SIMULATORS FOR LABORATORY EQUIPMENT IN ACTIVITY OF INVESTIGATIVE PLAYFUL EXPERIMENTATION IN SECONDARY SCHOOLS. In Periódico Tchê Química (Vol. 08, Issue 16, pp. 32–41). Dr. D. Scientific Consulting. https://doi.org/10.52571/ptq.v8.n16.2011.32_periodico16_pgs_32_41.pdf

22. Paristiowati, M., Moersilah, M., Nurjayadi, M., & Fitria, A. N. (2021). RGB-ColorMeter on smartphones as a simple spectrophotometer: An alternative method of teaching spectrophotometry at the vocational high school of chemical analysts. In Journal of Physics: Conference Series (Vol. 1869, Issue 1, p. 012064). IOP Publishing. https://doi.org/10.1088/1742-6596/1869/1/012064.

23. Peter, A. P., Chew, K. W., Koyande, A. K., Yuk-Heng, S., Ting, H. Y., Rajendran, S., Munawaroh, H. S. H., Yoo, C. K., & Show, P. L. (2021). Cultivation of Chlorella vulgaris on dairy waste using vision imaging for biomass growth monitoring. In Bioresource Technology (Vol. 341, p. 125892). Elsevier BV. https://doi.org/10.1016/j.biortech.2021.125892

24. Polli, V. R. G., Prochnow, A. R., & Tamanini, J. Z. (1998). EXTRACTION OF COLORED SUBSTANCES FROM MATE (ILEX PARAGUARIENSIS). Em SOUTHERN BRAZILIAN JOURNAL OF CHEMISTRY (Vol. 6, Issue 6, p. 45–51). Southern Brazilian Journal of Chemistry. https://doi.org/10.48141/sbjchem.v6.n6.1998.47_1998.pdf

25. Pucinelli, R. H., Kassab, Y., & Ramos, C. (2021). METODOLOGIAS ATIVAS NO ENSINO SUPERIOR: UMA ANÁLISE BIBLIOMÉTRICA / ACTIVE

METHODOLOGIES IN HIGHER EDUCATION: A BIBLIOMETRIC ANALYSIS. In Brazilian Journal of Development (Vol. 7, Issue 2, pp. 12495–12509). Brazilian Journal of Development. https://doi.org/10.34117/bjdv7n2-051

26. Rufián-Henares, J. A., & Pastoriza, S. (2015). Melanoidins in Coffee. In Coffee in Health and Disease Prevention (pp. 183–188). Elsevier. https://doi.org/10.1016/b978-0-12-409517-5.00020-6

27. Salta, K., Ntalakou, E., & Tsiortos, Z. (2022). Review of Hands-On Laboratory Experiments Employing Household Supplies. In Journal of Chemical Education (Vol. 99, Issue 7, pp. 2563–2571). American Chemical Society (ACS). https://doi.org/10.1021/acs.jchemed.2c00037

28. Santos, M. H. dos, Batista, B. L., Duarte, S. M. da S., Abreu, C. M. P. de, & Gouvêa, C. M. C. P. (2007). Influência do processamento e da torrefação sobre a atividade antioxidante do café (Coffea arabica). In Química Nova (Vol. 30, Issue 3, pp. 604–610). FapUNIFESP (SciELO). https://doi.org/10.1590/s0100-40422007000300020

29. Silva, W. R. F., Suarez, W. T., Reis, C., dos Santos, V. B., Carvalho, F. A., Reis, E. L., & Vicentini, F. C. (2021). Multifunctional Webcam Spectrophotometer for Performing Analytical Determination and Measurements of Emission, Absorption, and Fluorescence Spectra. In Journal of Chemical Education (Vol. 98, Issue 4, pp. 1442–1447). American Chemical Society (ACS). https://doi.org/10.1021/acs.jchemed.0c01085

30. Starowicz, M., & Zieliński, H. (2019). How Maillard Reaction Influences Sensorial Properties (Color, Flavor and Texture) of Food Products? In Food Reviews International (Vol. 35, Issue 8, pp. 707–725). Informa UK Limited. https://doi.org/10.1080/87559129.2019.1600538

31. Su, J.-F., Yuan, X.-Y., Huang, Z., Wang, X.-Y., Lu, X.-Z., Zhang, L.-D., & Wang, S.-B. (2012). Physicochemical properties of soy protein isolate/carboxymethyl cellulose blend films crosslinked by Maillard reactions: Color, transparency and heat-sealing ability. In Materials Science and Engineering: C (Vol. 32, Issue 1, pp. 40–46). Elsevier BV. https://doi.org/10.1016/j.msec.2011.09.009

32. Supannarach, S., & Thanapatay, D. (2008). The study of using RGB color sensor to measure the Curcuminiods amount in Turmeric (Curcuma longa Linn.) and Zedoary (Curcuma Zedoarie Rose.) by comparing colors with HSL system. In 2008 5th International Conference on Electrical Engineering/Electronics, Computer, Telecommunications and Information Technology. 2008 5th International Conference on Electrical Engineering/Electronics, Computer, Telecommunications and Information Technology (ECTI-CON). IEEE. https://doi.org/10.1109/ecticon.2008.4600487

33. Tolessa, K., D'heer, J., Duchateau, L., & Boeckx, P. (2016). Influence of growing altitude, shade and harvest period on quality and biochemical composition of Ethiopian specialty coffee. In Journal of the Science of Food and Agriculture (Vol. 97, Issue 9, pp. 2849–2857). Wiley. https://doi.org/10.1002/jsfa.8114.

34. Wang, J., Zhou, W., Yu, M., Zhu, Z., & Li, Y. (2021). Adsorption of Additives in Cola Beverages: A Safe and Improved Experiment Exploring Beer's Law and Adsorption Process. In Journal of Chemical Education (Vol. 99, Issue 2, pp. 924–931). American Chemical Society (ACS). https://doi.org/10.1021/acs.jchemed.1c00471.

35. Worsfold, Paul. J., & Zagatto, Elias. A. G. (2017). Spectrophotometry: Overview ☆. In Reference Module in Chemistry, Molecular Sciences and Chemical Engineering. Elsevier.

https://doi.org/10.1016/b978-0-12-409547-2.14265-9

36. Yen, W.-J., Wang, B.-S., Chang, L.-W., & Duh, P.-D. (2005). Antioxidant Properties of Roasted Coffee Residues. In Journal of Agricultural and Food Chemistry (Vol. 53, Issue 7, pp. 2658–2663). American Chemical Society (ACS). https://doi.org/10.1021/jf0402429

37. ZIMMERMANN, L. (2005). HOW TO STUDY THE DIFFERENCE BETWEEN COLOR LIGHT AND COLOR PIGMENT IN THE CLASSROOM. In Periódico Tchê Química (Vol. 03, Issue 2, pp. 17–23). Dr. D. Scientific Consulting. https://doi.org/10.52571/ptq.v2.n03.2005.janeiro/3_pgs_17_23.pdf

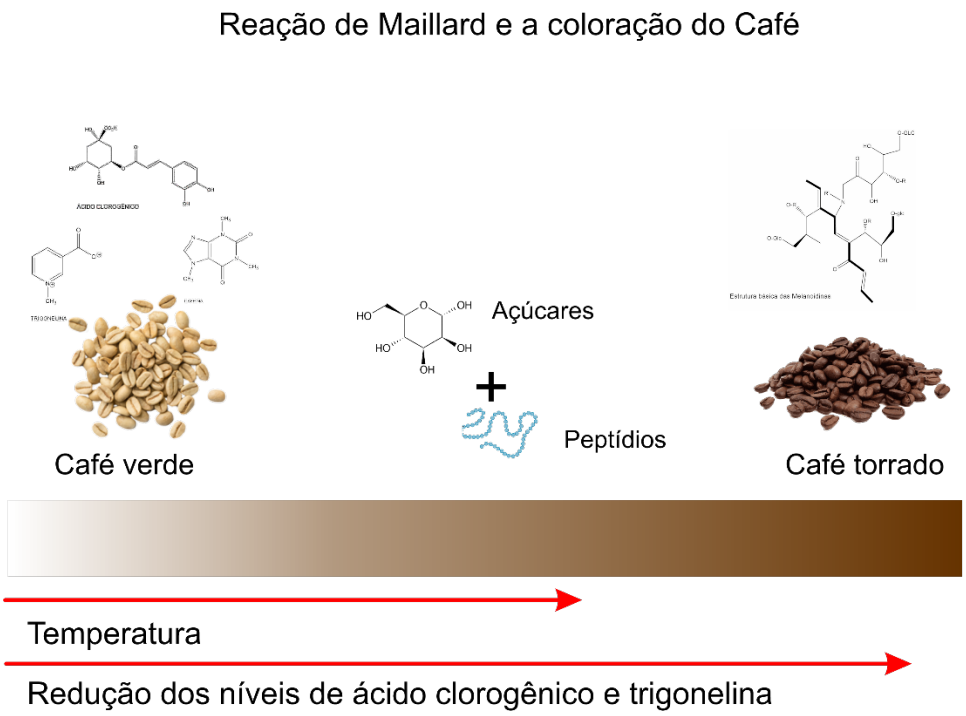

Figura 5. *Reação de Maillard representada na torra do café, de forma simplificada. Fonte: autores*

PERIÓDICO TCHÊ QUÍMICA
ARTIGO ORIGINAL

SÍNTESE, ESTUDO DE DOCAGEM E AVALIAÇÃO BIOLÓGICA DE DERIVADOS DA 4-AMINOANTIPIRINA-ISONIAZIDA COMO AGENTES HÍBRIDOS ANTIBACTERIANOS E ANALGÉSICOS

SYNTHESIS, DOCKING STUDY, AND BIOLOGICAL EVALUATION OF 4-AMINOANTIPYRINE-ISONIAZID DERIVATIVES AS A HYBRID ANTIBACTERIAL AND ANALGESIC AGENTS

تحضير ودراسة الالتحام والتقييم البيولوجي لمشتقات 4-امينو انتيبيرين-ايزونزايد كعوامل هجينة مضادة للبكتريا ومسكنة

MOHAMMAD, Abeer Essa[1]; MUHAMMAD-ALI, Munther Abduljaleel[2*]; JASIM, Ekhlas Qanber[3]

[1] University of Basrah, College of Pharmacy, Department of Pharmaceutical Chemistry. Basra, Iraq.

[2*] University of Basrah, College of Science, Department of Ecology. Basra, Iraq.

[3] University of Basrah, College of Science, Department of Pathological Analyses. Basra, Iraq.

** Corresponding author*
e-mail: munther.ali@uobasrah.edu.iq

Received 23 June 2022; received in revised form 26 August; 11 September 2022; accepted 02 October 2022

RESUMO

Introdução: 4-aminoantipirina é um dos derivados pirazolona, expôs uma grande variedade de atividades biológicas como compostos antimicrobianos, analgésicos, antivirais, anti-inflamatórios e anticancerígenos. Um dos derivados importantes é a pirazolona híbrida que inclui dois compostos orgânicos ou inorgânicos ligados para produzir novos agentes farmacêuticos que podem possuir atividade igual ou diferente dos medicamentos originais. **Objetivo:** O objetivo desta pesquisa foi sintetizar novos compostos derivados de 4-aminoantipirina e testar sua atividade biológica. **Métodos:** A síntese de derivados de 4-aminoantipirina, que contêm estruturalmente dois metades heterocíclicas, pirazolona com anéis de oxadiazol, triazol ou tetrazol. As estruturas dos compostos foram identificadas por espectroscopia de ^{1}H-NMR e FT-IR. Os compostos desenvolvidos foram *in vitro* para testar sua atividade analgésica e atividade antibacteriana contra cepas bacterianas de gram (+) e gram (-). **Resultados:** Os testes de avaliação antibacteriana mostraram que alguns compostos deram boa atividade e outros não apresentaram atividade antibacteriana. A atividade analgésica indicou que os compostos sintetizados tinham potência promissora. A energia de ligação livre (S) dos compostos com a proteína 6B73 foi de -4,90 a −8,76 kcal/mol, enquanto a energia livre (S) com a proteína 5C1M foi de −4,94 a −9,21 kcal/mol. **Discussão:** Entre os compostos testados, verificou-se que os compostos 1a, 4b e 5a apresentam atividade antibacteriana mais potente. A atividade analgésica mostrou que os compostos 1b, 4b e 5a apresentamram o melhor resutado usando métodos de placa quente em comparação com a droga padrão. Por outro lado, os compostos 1a, 4b e 5b deram boa atividade usando o método de contorção. **Conclusões:** Agentes analgésicos potentes, bons ou moderados e antibacterianos foram sintetizados usando reações químicas simples e de alto rendimento. As reações químicas incluem a síntese de agentes híbridos antibacterianos e analgésicos usando compostos de pirazolona.

Palavras-chave: *Pirazolona, azoles, antibacteriano, analgésico, acoplamento molecular*

ABSTRACT

Background: 4-aminoantipyrine is one of the pyrazolone derivatives, it has been exposed to a large range of biological activities as an antimicrobial, analgesic, antiviral, anti-inflammatory, and anticancer compound. One of the important derivatives is the hybrid pyrazolone which includes two organic or inorganic drugs attached to give new pharmaceutical agents which may be the same or different activity from the original drugs. **Aim:** This research aimed to synthesize novel compounds derived from 4-aminoantipyrine and test their biological activity. **Methods:** Synthesis of 4-aminoantipyrine derivatives, which contain structurally two heterocyclic moieties, pyrazolone with oxadiazole, triazole, or tetrazole rings. The structures of the compounds were identified by ^{1}H-NMR and FT-IR spectroscopy. The *in vitro*, developed compounds were screened for their analgesic activity and antibacterial

DOI: 10.52571/PTQ.v19.n42.2022.02_MUNTHER_pgs_12_28.pdf

activity against medically important gram (+) and gram (-) bacterial strains. **Results:** The antibacterial evaluation tests showed that some compounds gave good activity and others had no activity. The analgesic activity referred that the synthesized compounds had promising potency. The free binding energy (S) of the compounds with the protein 6B73 were −4.90 to −8.76 kcal/mol, whereas free energy (S) with the protein 5C1M gave −4.94 to −9.21 kcal/mol. **Discussion**: Among the tested compounds, it was found that compounds ***1a***, ***4b,*** and ***5a*** had more potent antibacterial activity. The analgesic activity showed that compounds ***1b***, ***4b***, and ***5a*** gave the best activity using hot plate methods compared with the standard drug. On the other hand, compounds ***1a***, ***4b***, and ***5b*** gave good activity using the writhing test method. **Conclusions:** Potent, good, or moderate analgesic and antibacterial agents were synthesized using simple and high-yield chemical reactions. The chemical reactions include the synthesis of hybrid antibacterial and analgesic agents using pyrazolone compounds.

Keywords: *Pyrazolone, azoles, antibacterial, analgesic, molecular docking*.

الخلاصة

الخلفية: يعتبر مركب 4-امينو انتيبارين أحد مشتقات البيرازولون ، وقد اكتشف له مجموعة كبيرة من الأنشطة البيولوجية كمضاد للميكروبات ، ومسكن ، ومضاد للفيروسات ، ومضاد للالتهابات ، ومضاد للسرطان. أحد المشتقات الهامة هو البيرازولون الهجين الذي يحتوي على عقارين عضويين أو غير عضويين مرتبطين لإعطاء عوامل صيدلانية جديدة والتي قد تكون نفس النشاط أو مختلفة عن الأدوية الأصلية. **الهدف:** الهدف من هذا البحث هو تصنيع مركبات جديدة مشتقة من -امينو انتيبارين واختبار نشاطها البيولوجي. **الطريقة:** تخليق مشتقات -امينو انتيبارين التي تحتوي تركيبيا على شقين غير متجانسين ، بيرازولون مع حلقات اوكسادايازول ، أو ترايازول ، أو تترازول. تم تحديد التركيب الكيميائي للمركبات بواسطة تحليل الرنين النووي المغناطيسي البروتوني ومطيافية الاشعة تحت الحمراء. في المختبر ، تم فحص المركبات المطورة لنشاطها المسكن ونشاطها المضاد للبكتيريا ضد صبغة الجرام (+) وضد صبغة الجرام (-) لبعض السلالات البكتيرية. **النتائج:** أظهرت اختبارات التقييم بمضادات البكتيريا أن بعض المركبات أعطت نشاطًا جيدًا والبعض الآخر ليس له أي نشاط. يشير النشاط المسكن إلى أن المركبات المحضرة لها فاعلية واعدة. كانت طاقة الارتباط الحر (S) للمركبات التي تحتوي على البروتين B736 من 4.90- إلى 8.76- كيلوجول/مول ، بينما كانت الطاقة الحرة (S) مع 5C1M هي 4.94- إلى 9.21- كيلوجول/مول. **المناقشة:** من بين المركبات المختبرة ، وجد أن المركبات ***a1*** و ***b4*** و ***a5*** لها نشاط مضاد للجراثيم أقوى. أظهر النشاط المسكن أن المركبات ***b1*** ، ***b4*** ، ***a5*** أعطت أفضل فعالية باستخدام طرق اللوح الساخن مقارنة بالعقار القياسي. من ناحية أخرى ، أعطت المركبات a1 و b4 و b5 نشاطًا جيدًا باستخدام طريقة اختبار الالتواء. **الاستنتاجات:** تم تصنيع عوامل مسكنة ومضادة للجراثيم قوية أو جيدة أو معتدلة باستخدام تفاعلات كيميائية بسيطة وعالية المردود. تشمل التفاعلات الكيميائية تخليق العوامل الهجينة المضادة للبكتيريا والمسكنات باستخدام مركبات البيرازولون.

الكلمات الدالة: *بايرازولون، ازولات، مضادات البكتريا، مسكنات الألم، الارساء الجزيئي.*

1. INTRODUCTION:

The increased biological activity of heterocyclic compounds and the fact that they allow for the creation of novel materials with distinctive features are two factors that contribute to the continual rise in interest in their synthesis. A biologically significant scaffold known as pyrazolone has been linked to numerous pharmacological activities, including antimicrobial (Verma *et al.*, 2021), anti-inflammatory (Mantzanidou *et al.,* 2021), analgesic (Bekhit *et al.,* 2022), antitubercular (Meta *et al.,* 2019), antioxidant (Silva *et al.,* 2018), and anticancer activities (Bennani *et al.,* 2020; Hassan *et al.,* 2021). Since they are members of a class of compounds with established medical chemistry applications, the synthesis of pyrazolone and its derivatives has attracted considerable interest from organic and medicinal chemists for many years.

Due to the widespread drug resistance, infectious diseases brought on by bacterial infections have emerged as a major public health issue. Bacterial and fungal infections play a role in morbidity and serious health issues produced globally (Ventola, 2015; Rayens & Norris, 2022). Millions of people experience bacterial illnesses yearly (Mukherjee *et al.,* 2019). Winder and Collins published the first study on the isoniazid (INH) mechanism of action in 1970 (Vilchèze & Jacobs, 2019). Isoniazid derivatives can potentially make bacterial strains resistant (Al-Khattaf *et al.,* 2021), and isoniazid hybrids have been the subject of numerous antimicrobial agent attempts (Pienaar *et al.,* 2018; Panda *et al.,* 2019; Dackouo & Arama, 2019).

The idea of hybrid compounds, in which two or more pharmacophores are covalently connected to form a single entity, is appealing in medicinal chemistry (Pawełczyk *et al.,* 2018). The two components of the hybrid molecule may either exert dual pharmacological action by acting on distinct targets or work in opposition to each other to balance out undesirable effects. It is hypothesized that adding lipophilic moieties to the INH structure may boost the ability of the drug to penetrate tubercle bacilli and increase its anti-TB efficacy (Szumilak *et al.,* 2021).

An INH-pyrrole hybrid exhibits bactericidal activity against drug-sensitive and drug-resistant strains (Johansen *et al.,* 2021). Since isatin (2,3-dioxoindole) provides a hydrophobic aromatic ring,

isatin-based compounds have remarkable anti-M. Tuberculosis capabilities and isatin-INH hybrids have drawn interest among the INH derivatives described thus far (Ding *et al.,* 2020; Abdel-Aziz *et al.,* 2017). Other research later showed that adding INH to isatin enhanced the antimycobacterial action of fresh compounds (Elsayed *et al.,* 2021).

The present study deals with synthesizing novel pyrazolone–isoniazid conjugates connected through sulfur linker using a molecular hybridization approach and investigating their biological properties against various microbial strains, including, *Staphylococcus aureus, Streptococcus, Escherichia coli*, and *Klebsiella pneumonia* mycobacteria and as analgesic agents.

2. MATERIALS AND METHODS:

The chemicals used were procured from the following companies, hydrazine hydrate, isonicotinic acid hydrazide, phenyl iso-thiocyanate, and sodium azide from Sigma-Aldrich Chemical Co. 4-aminoantipyrine, chloroacetyl chloride and 3-chloropropionyl chloride from Sunway Pharm (China). Absolute ethanol, dioxane, chloroform, and hydrochloric acid from Merck Ltd. Molar-Hintin agar from ALPHA (India). Uncorrected Barnstead electrothermal equipment in open capillaries was used to determine the physical characteristics of the produced compounds, particularly their melting point. Under UV light (λ = 254 nm), thin layer analytical chromatography on silica gel 60 F254 aluminum sheets measuring 20 × 20 cm (Merck) was used to track the progress of the reaction and check the purity of the produced chemicals. ^{1} H-NMR spectrum of the compounds, tetramethylsilane (TMS) served as an internal standard, and dimethyl sulfoxide (DMSO-d6) served as the solvent and using a 500 MHz INOVA (Switzerland) spectrometer. In the Chemistry Department of the College of Science at Basrah University, the FT-IR spectra of each tested compound were measured as KBr disks using an FT-IR 8400S SHIMADZU (Japan) instrument. Using a CHN elemental analyzer flash EA 1112 series, synthetic substances underwent elemental microanalysis (CHN) (Thermo Finnigan).

2.1. Synthesis of compounds

2.1.1 Synthesis of 2-chloro-N-(1,5-dimethyl-3-oxo-2-phenyl-2,3-dihydro-1H-pyrazol-4-yl)acetamide (1a) and 3-chloro-N-(1,5-dimethyl-3-oxo-2-phenyl-2,3-dihydro-1H-pyrazol-4-yl)propenamide (1b)

The compounds ***1a*** and ***1b*** were synthesized according to the procedure in our paper (Mohammad *et al.,* 2021).

In a 100 mL round-bottomed flask, 15ml of chloroform, 2.03 g, 0.01 mole of 4-aminoantipyrine, and 0.132 g, 0.01 mole of anhydrous potassium carbonate was added. To this mixture, 0.01 mole of chloroacetyl chloride or 3-chloropropionyl chloride was added dropwise with stirring for 20 minutes. The reaction mixture was refluxed in a water bath at 60 °C for 3 hr. Next, chloroform was flashed to give the viscous solution, which was washed with (5% w/v, 35 mL) aqueous solution of sodium bicarbonate, the precipitate formed was filtered and dried, then recrystallized with ethanol.

1a: Pale yellow crystals, 55% yield, m. p. 190-193 ^{o}C, IR (KBr): ν (cm^{-1}) = 3190 (N-H), 3043 (C-H, aromatic), 2928, 2874 (C-H, aliphatic), 1693, 1639 (C=O, amide), 1558, 1489 (C=C), 1315, 1296 (C-N). ^{1}H NMR (DMSO-d_6): δ = 9.47 (s, 1H, NH), 7.52 -7.31 (m, 5H, Ar-H), 4.24 (s, 2H, CH_2-Cl), 3.06 (s, 3H, N-CH_3), 2.13 (s, 3H, C-CH_3). Anal. Calc. (Found) for $C_{13}H_{14}ClN_3O_2$ (279.72): C, 55.82 (55.89), H, 5.04 (5.17), N, 15.02 (14.66).

1b: Pale yellow crystals, 80% yield, m. p. 210-211 ^{o}C, IR (KBr): ν (cm^{-1}) = 3190 (N-H), 3009 (C-H, aromatic), 2889 (C-H, aliphatic), 1685, 1647 (C=O, amide), 1531, 1489 (C=C), 1315, 1199 (C-N). ^{1}H NMR (DMSO-d_6): δ = 9.27 (s, 1H, NH), 7.53 -7.31 (m, 5H, Ar-H), 3.86 (t, 2H, *J* = 6.2 Hz, -CH_2-Cl), 2.73 (t, 2H, *J* = 6.2 Hz, -CH_2-), 3.05 (s, 3H, N-CH_3), 2.13 (s, 3H, C-CH_3). Anal. Calc. (Found) for $C_{14}H_{16}ClN_3O_2$ (293.75): C, 57.24 (57.62), H, 5.49 (5.13), N, 14.30 (14.70).

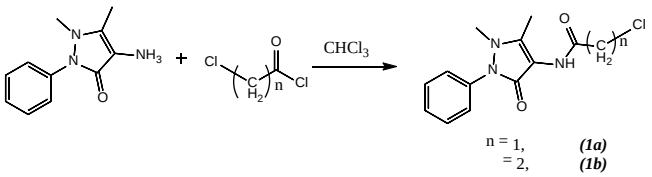

Scheme 1. *Synthesis of compounds* ***1a*** *and* ***1b***

2.1.2 Synthesis of 5-(pyridin-4-yl)-1,3,4-oxadiazole-2-thiol (2b)

In a mixture of 1.37g (0.1 moles) of isonicotinic acid hydrazide (INH) ***(2a)***, 0.9 mL (0.15 mole) of carbon disulfide, and 0.4g (0.1 moles) of sodium hydroxide (dissolved in the least amount of water) were added to a solution of 95% ethanol. The reaction mixture was heated at reflux for three hours until it no longer produced hydrogen sulfide.

The resulting mixture was diluted down and acidified with ice-cold diluted hydrochloric acid. The reaction mixture was filtered, water-washed, and recrystallized from ethanol for 30 minutes in an ice bath, as shown in Scheme 2 (Mohammed-Ali and Majeed, 2012).

***2a*:** White crystals, 69% yield, m. p. 199-201 °C. IR (KBr): ν (cm^{-1}) = 3032 (C-H, aromatic), 2684 (S-H), 1597 (C=N, oxadiazole ring), 1489 (C=C), 1267, 1149 (C-O-C). ^{1}H NMR (DMSO-d_6): δ (ppm) = 7.81 (d, 2H, pyridine-H_{ortho}), 8.81 (d, 2H, pyridine-H_{meta}).

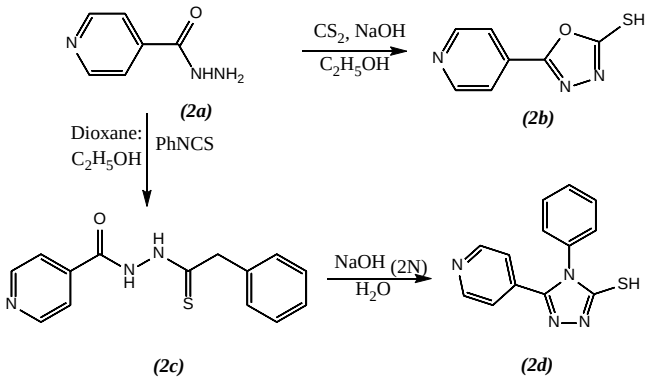

Scheme 2. Synthesis of compounds ***2b*** and ***2d***

2.1.3 Synthesis of triazole

*2.1.3.1 Synthesis of thiosemicarbazide (**2c**)*

At 60 °C, 1.19 mL (0.1 mole) of phenyl isothiocyanate was added to a mixture of 1.37g (0.1 mole) isonicotinic acid hydrazide **2a** in a cosolvent of dioxane:ethanol (4:1). The reaction mixture was agitated for 15 minutes at 60 °C and then for 1 hour at room temperature. The crystals were separated, filtered, and then dried at room temperature after being rinsed with cold ethanol, as shown in Scheme 2 (Alyahyaoy, 2019). Without additional purification, the products were utilized in the following phase.

*2.1.3.2 Synthesis of 4-phenyl-5-(pyridin-4-yl)-4H-1,2,4-triazole-3-thiol (**2d**)*

Thiosemicarbazide ***2c*** and sodium hydroxide (0.005 mole) were dissolved in 50 mL of water and heated over reflux for two hours. After filtering, a cold solution of 2 M HCl was added to the yellow solution to lower the pH level to 4. Crystals were separated, filtered, and water-washed (Dhaif et al., 2019). The end products were dried at room temperature after being recrystallized from methanol, as shown in Scheme 2.

2d: Pale yellow crystals, 64.7% yield, m. p. 290-292 °C. IR (KBr): ν (cm^{-1}) = 3066, 3093 (C-H, aromatic), 2688 (S-H), 1566 (C=N, triazole ring), 1550 (C=C), 1288 (C-N). ^{1}H NMR (DMSO-d_6): δ (ppm) = 7.23 (d, 2H, pyridine-H_{ortho}), 8.57 (d, 2H, pyridine-H_{meta}), 7.41-7.56 (m, 5H, Ar-H phenyl-triazole).

2.1.4 Synthesis of 1-Phenyl-1,2,3,4- tetrazole-5-thiol (3)

The following materials were combined and refluxed for 4 hours: 150 ml of water, 5.98 ml (0.05 mole) of phenyl isothiocyanate, and 4.87 g (0.075 mole) of sodium azide. The mixture was filtered off after cooling to remove the unreacted phenyl isothiocyanate, and the filtrate was then extracted with diethyl ether. Litmus paper was used to measure the pH of the aqueous layer, which was then treated with hydrochloric acid to a pH of about 3. The precipitate was a white solid. After being dried and recrystallized with ethanol, the filtered crystals underwent a water wash, as shown in Scheme 3 (Abdul-Nabi & Jasim, 2014; AL-Hakiem, 2020).

3: White crystals, 91% yield, m. p. 153-155 °C. IR (KBr): ν (cm^{-1}) = 3034 (C-H, aromatic), 2713 (S-H), 1589 (C=N, oxadiazole ring), 1500 (C=C), 1454 (N=N), 1215 (C-N).

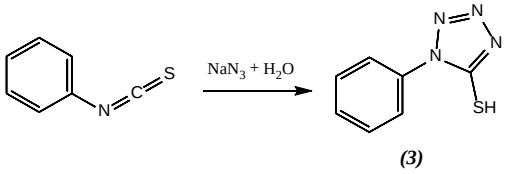

Scheme 3. Synthesis of compound ***3***

2.1.5 Synthesis of hybrid organic molecules 4a, 4b, 5a, and 5b

The compounds N-(1,5-dimethyl-3-oxo-2-phenyl-2,3-dihydro-1H-pyrazol-4-yl)-2-((4-phenyl-5-(pyridin-4-yl)-4H-1,2,4-triazol-3-yl)thio)acetamide ***4a***, N-(1,5-dimethyl-3-oxo-2-phenyl-2,3-dihydro-1H-pyrazol-4-yl)-3-((5-(pyridin-4-yl)-1,3,4-oxadiazol-2-yl)thio)propenamide ***4b***, N-(1,5-dimethyl-3-oxo-2-phenyl-2,3-dihydro-1H-pyrazol-4-yl)-2-((1-phenyl-1H-tetrazol-5-yl)thio)acetamide ***5a*** and N-(1,5-

dimethyl-3-oxo-2-phenyl-2,3-dihydro-1H-pyrazol-4-yl)-3-((1-phenyl-1H-tetrazol-5-yl)thio)propenamide ***5b*** were synthesized by the same procedure. (Othman *et al.,* 2019)

To a mixture containing 50 mL of absolute ethanol, 0.015 mole of the compounds ***2b***, ***2d,*** or ***3*** and 0.018 mole of ***1a*** or ***1b***, 0.02 mole of anhydrous sodium acetate were added. After being heated under reflux for three hours, the reaction mixture was allowed to cool and poured into 100 mL of ice-filled cold water. In order to recrystallize the solid, ethanol was collected and heated, as shown in Schemes 4 and 5.

4a: Off-white crystals, 68.8% yield, m. p. 224-225 °C. ν (cm^{-1}) = 3321 (N-H), 3039 (C-H, aromatic), 2931 (C-H, aliphatic), 1678, 1643 (C=O, amide), 1600 (C=N), 1539 (C=C), 1188, 1148 (C-O, C-N).^{1}H NMR (DMSO-d_6): δ (ppm) = 9.51 (s, 1H, NH), 7.51-7.62 (m, 5H, Ar-H phenyl-triazole), 7.30 (d, 2H, pyridine-H_{ortho}), 8.56 (d, 2H, pyridine-H_{meta}), 7.32-7.50 (m, 5H, Ar-H Phenyl-pyrazolone), 4.18 (s, 2H, -CH_2-S), 3.04 (s, 3H, N-CH_3), 2.11 (s, 3H, -CH_3). Anal. Calc. (Found) for $C_{26}H_{23}N_7O_2S$ (497.58): C, 62.76 (62.85), H, 4.66 (4.77), N, 19.71 (19.68).

4b: Off-white crystals, 69.1% yield, m. p. 210-211 °C. ν (cm^{-1}) = 3205 (N-H), 3032 (C-H, aromatic), 2889 (C-H, aliphatic), 1693, 1651 (C=O, amide), 1612 (C=N), 1531, 1452 (C=C), 1192, 1141 (C-N).^{1}H NMR (DMSO-d_6): δ (ppm) = 9.25 (s, 1H, NH), 7.82 (d, 2H, pyridine-H_{ortho}), 8.80 (d, 2H, pyridine-H_{meta}), 7.31-7.50 (m, 5H, Ar-H Phenyl-pyrazolone), 3.56 (t, 2H, -CH_2-S), 2.89 (t, 2H, -$\underline{CH_2}$-CH_2-S), 3.05 (s, 3H, N-CH_3), 2.13 (s, 3H, -CH_3). Anal. Calc. (Found) for $C_{21}H_{20}N_6O_3S$ (436.49): C, 57.79 (57.89), H, 4.52 (4.49), N, 19.25 (19.32).

5a: Pale yellow crystals, 66.2% yield, m. p. 110-113 °C. ν (cm^{-1}) = 3301 (N-H), 3027 (C-H, aromatic), 2989 (C-H, aliphatic), 1678, 1658 (C=O, amide), 1613 (C=N), 1589, 1535 (C=C), 1199, 1095 (C-N).^{1}H NMR (DMSO-d_6): δ (ppm) = 9.58 (s, 1H, NH), 7.67-7.73 (m, 5H, Ar-H phenyl-tetrazole), 7.31-7.53 (m, 5H, Ar-H Phenyl-pyrazolone), 4.36 (s, 2H, -CH_2-S), 3.05 (s, 3H, N-CH_3), 2.10 (s, 3H, -CH_3). Anal. Calc. (Found) for $C_{20}H_{19}N_7O_2S$ (421.48): C, 57.92 (57.84), H, 4.86 (4.80), N, 22.51 (22.46).

5b: Off-white crystals, 78.4% yield, m. p. 156-158 °C. ν (cm^{-1}) = 3178 (N-H), 3020 (C-H, aromatic), 2931 (C-H, aliphatic), 1681, 1647 (C=O, amide), 1620 (C=N), 1589, 1531 (C=C), 1203, 1145 (C-N). ^{1}H NMR (DMSO-d_6): δ (ppm) = 9.23 (s, 1H, NH), 7.65-7.67 (m, 5H, Ar-H phenyl-tetrazole), 7.31-7.52 (m, 5H, Ar-H Phenyl-pyrazolone), 3.67 (t, 2H, -CH_2-S), 2.86 (t, 2H, -$\underline{CH_2}$-CH_2-S), 3.04 (s, 3H, N-CH_3), 2.06 (s, 3H, -CH_3). Anal. Calc. (Found) for $C_{21}H_{21}N_7O_2S$ (435.51): C, 56.99 (57.11), H, 4.54 (4.52), N, 23.26 (23.16).

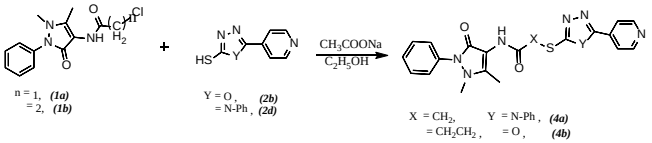

Scheme 4. Synthesis of compounds ***4a*** and ***4b***

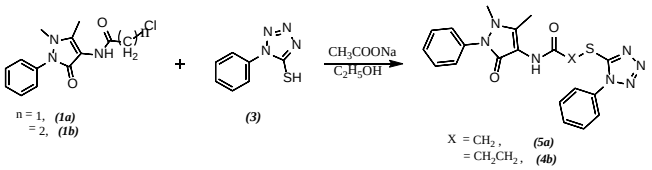

Scheme 5. Synthesis of compounds ***5a*** and ***5b***

2.2 Antibacterial Activity Evaluation

For evaluating in vitro antibacterial, Gram-positive bacteria (*S. aureus* and *Streptococcus*) and Gram-negative bacteria (*E. coli* and *Klebsiella pneumonia*) were used by disc diffusion method. Dimethyl sulfoxide (DMSO) was used to dissolve the compounds in solutions at concentrations of 1000, 500, 250, 125, and 50 g/ml. Mueller-Hinton Agar in the 20–30 ml volume was put into the 100 mm Petri plate. Whatman No. 4 (6 mm) diameter; impregnated with solutions of the chemicals under investigation. After that, the disc was placed on the medium's surface utilizing microorganisms. Twenty-four hours of incubation on Petri dishes at 37 °C. The antibacterial efficacy was calculated by measuring the diameter of the inhibitory zone in mm. (Mohammed & Mustafa, 2020; Fouad *et al.*, 2021).

2.3 Evaluation of Analgesic Activity

2.3.1 Writhing Test

Six albino mice were placed in each of the fourteen groups of albino mice. Animals that had been fasting overnight received the following care: Group 1 of mice was treated with (10 mL/kg) of vehicle (olive oil) and served as the control group, and Group 2 of mice was treated with 10 mg/kg of paracetamol and served as a standard group, while groups (3–14) were received 10 mg/kg of tested compounds. Every dosage of the compounds, paracetamol, and experimental drugs was administered orally via gastric gavage. To produce the nociception condition, mice in all groups received 10 mL/kg of a 1% v/v acetic acid solution intraperitoneally (i.p.) after 1 hour (pain).

The number of observed writhings in each mouse was tallied for 15 minutes, starting 5 minutes after the administration of acetic acid. The following method, Equation 1, was used to compute the percentage inhibition (I%) of writhing (abdominal constrictions), which was used to assess the analgesic potency:

$$Inhibition\%\ (I\%) = \left(\frac{N_c - N_t}{N_c}\right) x100 \qquad \text{(Eq. 1)}$$

Where N_c is the average of writhing numbers in the control group and N_t is the average of writhing numbers in the tested groups (Yimer *et al.*, 2020).

2.3.2 Hot Plate Test

Swiss albino mice of both sexes were divided into fourteen groups for this experiment, with six mice in each group. The mice were given the following care after an overnight fast: As a control group, group 1 of mice received 10 mL/kg of vehicle (olive oil), while group 2 of mice received 10 mg/kg of paracetamol as the standard group, and groups 3 through 14 of mice received 10 mg/kg of the test compounds orally. Mice were placed inside a glass cylinder on a well-controlled hot plate that was kept at a temperature of 55°C after an hour of all oral treatments. The time interval between the placement of the mice on the hot plate surface and the occurrence of fore or hind paw licking or jumping was noted as reaction time and was calculated using Equation 2.

$$Inhibition\%\ (I\%) = \left(\frac{T_t - T_c}{T_c}\right) x100 \qquad \text{(Eq. 2)}$$

Where T_t is the average reaction time in the tested group and Tc is the average reaction time in the control groups. To prevent paw injury, it has been considered that the cutoff period should not last more than 20 sec (Santenna *et al.*, 2019).

2.4 Docking studies

All compounds were projected using ChemDraw Software 2016. All water molecules and ligands were removed during molecular docking of the produced compounds ***1a***, ***1b***, ***2b***, ***2d***, ***3***, ***4a***, ***4b***, ***5a***, and ***5b*** using MOE 2015 v10. The crystal Structure of a nanobody-stabilized active state of the kappa-opioid receptor (protein ID: 6B73) and the crystal structure of the active mu-opioid receptor (proteins ID: 5C1M) were obtained from the RCSB protein data bank.

3. RESULTS AND DISCUSSION:

3.1. Results

In this study, it was synthesized some derivatives of 4-aminoantipyrine and tested for their antibacterial activity against selected bacteria, as well as their analgesic activities. Finally, we theoretically analyzed their properties regarding their molecular docking properties with selected protein sites. All the compounds were synthesized with good yield in pure form. Synthesized compounds were identified using melting point, and spectroscopic methods include FT-IR and ^{1}H-NMR techniques.

Synthesized compounds were evaluated for antibacterial and analgesic activities. The results of the antibacterial potential of compounds are presented in Table 1, and the results gave a clear view that the synthesized compounds exhibited different values of potency. We noted that compounds ***1a***, ***1b***, ***4b***, and ***5a*** gave an inhibition zone against all types of bacteria at the highest concentration (1000 µg/mL), whereas compound ***5b*** exhibited activity against three bacteria except Streptococcus, and finally, compound ***4a*** gave an activity against only Gram-negative bacteria.

The analgesic activity of the compounds ***1a***, ***1b***, ***4a***, ***4b***, ***5a***, and ***5b*** was evaluated in mice using the analgesia hot plate and writhing test methods compared with paracetamol as a standard drug. Table 2 shows the analgesic activity depending on the reaction time and inhibition% of the synthesized compounds and standard drugs by hot plate method, while Table shows the number of writhing and inhibition% of the synthesized compounds and standard drugs by the writhing method. Figure 1 shows the analgesic activity of the compounds using two methods.

Molecular docking analysis is the most effective way of determining how a target protein interacts with an inhibitory substance (Attique et al., 2019; Arjmand et al., 2022; Durhan et al., 2022). Docking investigations were performed using the software MOE (2015.10). The 3D crystallographic structure of the protein was downloaded from the Protein Data Bank website (www.rcsb.org) (PDB ID: 6B73 and ID: 5C1M). All compounds were represented by their 2D structures on ChemDraw Ultra 16.0.

The covalent docking of the synthesized compounds into the largest pocket of the kappa-opioid receptor (6B73) and mu-opioid receptor (5C1M) was simulated, and the docking scores

results are shown in Table 4. Tables 5 and 6 display the findings for just the substances that produced reliable molecular docking scores. The best simulation of the synthesized compounds with two types of protein was the final derivatives ***4a***, ***4b***, ***5a***, and ***5b***, which showed greater value S scores, as shown in Figures 1 and 2.

3.2. Discussions

3.2.1. Chemistry

Heating of isonicotinic acid hydrazide with carbon disulfide in the presence of an alcoholic alkaline medium gave sodium xanthate salt, which lost the hydrogen sulfide to form sodium oxadiazole ion, which was converted to oxadiazole thiol ***2b*** in an acidic medium. IR spectrum showed the medium absorption band at 2684 cm^{-1} attributed to the stretching vibration of the S-H bond (Hudson and Gerakines, 2018), and the medium band at 1597 cm^{-1} referred to the stretching vibration of C=N of the oxadiazole ring. In addition, the ^{1}H-NMR gave aromatic protons of the pyridine ring at 7.81 and 8.81 ppm, attributed to ortho and meta protons as doublet, respectively.

Two steps synthesized the triazole compound 2d, and the first included the synthesis of the intermediate thiosemicarbazide ***2c*** by mild heating of isonicotinic acid hydrazide and phenyl iso-thiocyanate in dioxane:ethanol cosolvent. In the second step, the white crystals of 2c, which separated, were subjected to cyclization in an aqueous alkaline medium. After treatment with an acidic solution, pale-yellow precipitation was formed. IR spectrum of ***2d*** gave a medium band at 2688 cm^{-1} which attributed to the stretching vibration of the S-H band, and the medium band at 1688 cm^{-1} referred to the stretching vibration of the C=N bond of the triazole ring (Salinas-Torres *et al.*, 2022). In addition, ^{1}H-NMR gave doublet signals aromatic pyridine protons at 7.23 and 8.57 ppm, another multiplet signal in the range 7.41-7.56 ppm related to protons of phenyl ring attached to triazole ring.

The synthesis of compound 1-phenyl-1,2,3,4- tetrazole-5-thiol ***3*** included cyclization of phenyl iso-thiocyanate with sodium azide in an aqueous solution to give white crystals with a good yield. The final product identified by IR spectroscopy gave a medium absorption band at 2713 cm^{-1} attributed to the stretching vibration of the S-H band and a strong band at 1454 cm^{-1} referred to as N=N stretching vibration.

The final compounds ***4a***, ***4b***, ***5a,*** and ***5b*** were synthesized by sulfur nucleophilic substitution (an attack by S^-) at the carbon atom attached to chloride of ***1a*** and ***1b***, and the mechanism of the reaction is according to SN2. The IR spectra of the products characterized by the lake of the S-H band and appearing in the medium-strong bands at the range 1678-1693 cm^{-1} and 1643-1658 cm^{-1} attributed to stretching vibration of carbonyl open and cyclic amide groups (Balan *et al.*, 2019). ^{1}H-NMR of all compounds showed the following signals, singlet signal at 9.23-9.58 ppm related to one proton of the H-N-C=O group, characteristic high field singlet signals at 3.04-3.05 and 2.06-2.13 ppm attributed to three protons of methyl groups attached to nitrogen and carbon atoms, respectively, of pyrazolone ring. The compounds ***4a*** and ***5a*** gave singlet signals at 4.18 and 4.36 ppm, respectively, related to two protons of methylene groups attached to the sulfur atom, while the compounds ***4b*** and ***5b*** gave triplet signals at 3.56 and 3.67 ppm attributed to methylene protons attached to sulfur atoms and coupled with another proton of methylene group with J=6.7 Hz.

3.2.2 Antibacterial activity

The compounds ***1a***, ***1b***, ***4a***, ***4b***, ***5a,*** and ***5b*** were tested for their antibacterial activity against Gram-negative bacteria (*Escherichia coli* and *Klebsiella pneumonia*) and Gram-positive bacteria (*Staphylococcus aureus* and *Streptococcus*) employing the filter paper disc diffusion method, and the inhibition zone diameter was measured after 24 hr. The preliminary results indicated that some compounds were active against the tested bacteria, as shown in Table 1.

Compound ***1a*** gave the best activity (17 mm) against *Streptococcus* at 1000 µg/mL as compared with other compounds, while mild activity as compared with standard drug (amoxicillin) at the same concentration. The compounds ***1a***, ***4b,*** and ***5a*** showed good activity against all bacterial strains under investigation at the highest concentration (1000 µg/mL). All compounds gave an inhibition zone in the range (7-9) mm against *Escherichia coli*. In contrast, some compounds gave an inhibition zone from no inhibition to 12 mm against *Klebsiella pneumonia* at the highest concentration. The compound ***4a*** gave weaker activity, which showed no inhibition against Gram-positive bacteria while giving inhibition zone 9 and 7 mm against *Escherichia coli* and *Klebsiella pneumonia*, respectively.

3.2.3. Analgesic activity

The results showed that compounds ***1b***, ***4b***, and ***5a*** gave the best activity (40%, 45%, and 51%, respectively) compared with other compounds. On the other hand, the synthesized compound ***4a*** gave moderate activity (32%) as compared with the standard drug.

The good activity of compounds ***4b*** and ***5a*** may be attributed to the chemical structure of the two types of compounds. It was observed that the presence of the compound fragment that contains the heterocyclic rings (oxadiazole and tetrazole) in these compounds gave better activity, which may be attributed to the presence of the heterocyclic rings that affect the physicochemical and pharmacokinetic properties of the entire compound (Hardjono *et al.*, 2017; Mazák *et al.*, 2019).

The results showed that compounds ***1a***, ***4b***, and ***5b*** gave good activity (68%, 52%, and 47%, respectively) compared with other compounds. On the other hand, the synthesized compounds ***1b*** and ***4a*** gave moderate activity (30% and 30%) as compared with the standard drug. Finally, it was noted that compound ***4b*** gave the best activity in every two methods as compared with the standard drug, as shown in Figure 1.

3.2.4. Molecular Docking Studies

The results showed that compounds favorable docking scores ranging from −4.90 to −8.76 kcal/mol and RMSD values in the range 1.05 to 2.31 Å with 6B73, whereas these compounds gave affinity in the range -4.94 to -9.20 kcal/mol and RMSD values 1.10 to 2.34 Å with the 5C1M protein. Compound ***5b*** gave the best affinity with 6B73 protein at -8.76 kcal/mol, whereas compound ***4b*** showed the best affinity with 5C1M protein (-9.20 kcal/mol).

According to Table 1, compound ***5b*** gave the highest docking scores of −8.76 kcal/mol and RMSD value 1.91 Å, which gave a good inhibitory potential of 47% in the writhing method. Compound ***5b*** docked with a binding affinity of −46.85 kcal/mol, which is the highest compared with the others, and interacted with LEU 212. Compound ***4a*** docked with a good binding affinity of −46.83 kcal/mol and interacted with LEU 212, LYS 227, and TYR 139. Compound ***4b*** docked with a binding affinity of −45.79 kcal/mol and interacted with CYS 210, GLN 115, and GLN 115.

Compound ***4b***, which docked with the highest binding affinity of -48.66 kcal/mol when compared to the other compounds and interacted with MET 151, LYS 303, and HIS 54, had the highest docking scores of -9.21 kcal/mol and RMSD value 1.34 Å, as shown in Table 2. With a binding affinity of about -46.52 kcal/mol, compound ***5b*** docked and interacted with LYS 233 and SER 53. With a binding affinity of about -46.21 kcal/mol, compound ***5a*** docked and interacted with HIS 54 and SER 53.

4. CONCLUSIONS:

The present study describes the synthesis of pyrazolone compounds ***4a***, ***4b***, ***5a***, and ***5b*** by reaction of 4-aminoantipyrine derivatives ***1a*** and ***1b*** and some synthesized heterocyclic compounds (oxadiazole; ***2b***, triazole; ***2d***, and tetrazole; ***3***). The results of the antimicrobial evaluation revealed that the activity of the compounds was between good and moderate. In contrast, the analgesic activity gave a clear view of the potency of some of the synthesized compounds as analgesic agents. Furthermore, according to the molecular docking studies, the final compounds (***4a***, ***4b***, ***5a***, and ***5b***) gave very good binding affinity coordinated with the largest site proteins (6B73 and 5C1M) compared with other synthesized compounds under investigation.

5. DECLARATIONS

5.1. Study Limitations

Identification of the synthesized compounds must done in private laboratories out of Iraq.

5.2. Funding source

This work was financially supported by the Authors.

5.3. Competing Interests

The authors declare no conflicts of interest.

6. HUMAN AND ANIMAL-RELATED STUDIES

6.1. Ethical Approval

All of the dealing procedures with animals described in this study were authorized by the Animal Ethics Committee, University of Basrah, Iraq (No. 2013/32).

7. REFERENCES:

1. Verma, R., Verma, S. K., Rakesh, K. P., Girish, Y. R., Ashrafizadeh, M., Kumar, K. S. S., & Rangappa, K. S. (2021). Pyrazole-based analogs as potential antibacterial agents against methicillin-resistance staphylococcus aureus (MRSA) and its SAR elucidation. *European journal of medicinal chemistry*, *212*, 113134. https://doi.org/10.1016/j.ejmech.2020.113134
2. Mantzanidou, M., Pontiki, E., & Hadjipavlou-Litina, D. (2021). Pyrazoles and pyrazolines as anti-inflammatory agents. *Molecules*, *26*(11), 3439. https://doi.org/10.3390/molecules26113439
3. Bekhit, A. A., Nasralla, S. N., El-Agroudy, E. J., Hamouda, N., Abd El-Fattah, A., Bekhit, S. A., ... & Ibrahim, T. M. (2022). Investigation of the anti-inflammatory and analgesic activities of promising pyrazole derivative. *European Journal of Pharmaceutical Sciences*, *168*, 106080. https://doi.org/10.1016/j.ejps.2021.106080
4. Meta, E., Brullo, C., Tonelli, M., Franzblau, S. G., Wang, Y., Ma, R., ... & Bruno, O. (2019). Pyrazole and imidazo [1, 2-b] pyrazole derivatives as new potential anti-tuberculosis agents. *Medicinal Chemistry*, *15*(1), 17-27. https://doi.org/10.2174/1573406414666180524084023
5. Silva, V. L., Elguero, J., & Silva, A. M. (2018). Current progress on antioxidants incorporating the pyrazole core. *European journal of medicinal chemistry*, *156*, 394-429. https://doi.org/10.1016/j.ejmech.2018.07.007
6. Bennani, F. E., Doudach, L., Cherrah, Y., Ramli, Y., Karrouchi, K., & Faouzi, M. E. A. (2020). Overview of recent developments of pyrazole derivatives as an anticancer agent in different cell line. *Bioorganic Chemistry*, *97*, 103470. https://doi.org/10.1016/j.bioorg.2019.103470
7. Hassan, A. S., Moustafa, G. O., Awad, H. M., Nossier, E. S., & Mady, M. F. (2021). Design, synthesis, anticancer evaluation, enzymatic assays, and a molecular modeling study of novel pyrazole–indole hybrids. *ACS omega*, *6*(18), 12361-12374. https://doi.org/10.1021/acsomega.1c01604
8. Ventola, C. L. (2015). The antibiotic resistance crisis: part 1: causes and threats. *Pharmacy and therapeutics*, *40*(4), 277.
9. Rayens, E., & Norris, K. A. (2022, January). Prevalence and healthcare burden of fungal infections in the United States, 2018. In *Open forum infectious diseases* (Vol. 9, No. 1, p. ofab593). US: Oxford University Press. https://doi.org/10.1093/ofid/ofab593
10. Mukherjee, S., Anderson, C. M., Mosci, R. E., Newton, D. W., Lephart, P., Salimnia, H., ... & Manning, S. D. (2019). Increasing frequencies of antibiotic resistant non-typhoidal Salmonella infections in Michigan and risk factors for disease. *Frontiers in medicine*, 250. https://doi.org/10.3389/fmed.2019.00250
11. Vilchèze, C., & Jacobs Jr, W. R. (2019). The isoniazid paradigm of killing, resistance, and persistence in Mycobacterium tuberculosis. *Journal of molecular biology*, *431*(18), 3450-3461. https://doi.org/10.1016/j.jmb.2019.02.016
12. Al-Khattaf, F. S., Mani, A., Hatamleh, A. A., & Akbar, I. (2021). Antimicrobial and cytotoxic activities of isoniazid connected menthone derivatives and their investigation of clinical pathogens causing infectious disease. *Journal of Infection and Public Health*, *14*(4), 533-542. https://doi.org/10.1016/j.jiph.2020.12.033
13. Pienaar, E., Linderman, J. J., & Kirschner, D. E. (2018). Emergence and selection of isoniazid and rifampin resistance in tuberculosis granulomas. *PLoS One*, *13*(5), e0196322. https://doi.org/10.1371/journal.pone.0196322
14. Panda, S. S., Girgis, A. S., Mishra, B. B., Elagawany, M., Devarapalli, V., Littlefield,

W. F., ... & Bokhtia, R. M. (2019). Synthesis, computational studies, antimycobacterial and antibacterial properties of pyrazinoic acid–isoniazid hybrid conjugates. *RSC advances*, *9*(35), 20450-20462. https://doi.org/10.1039/c9ra03380g
15. Dackouo, B., & Arama, D. P. (2019). Systematic Review of New Trends in Antitubercular Synthesis and Analysis. *Journal of Materials Science and Chemical Engineering*, *7*(01), 1. https://doi.org/10.4236/msce.2019.71001
16. Pawełczyk, A., Sowa-Kasprzak, K., Olender, D., & Zaprutko, L. (2018). Molecular consortia—Various structural and synthetic concepts for more effective therapeutics synthesis. *International journal of molecular sciences*, *19*(4), 1104. https://doi.org/10.3390/ijms19041104
17. Szumilak, M., Wiktorowska-Owczarek, A., & Stanczak, A. (2021). Hybrid drugs—a strategy for overcoming anticancer drug resistance? *Molecules*, *26*(9), 2601. https://doi.org/10.3390/molecules26092601
18. Johansen, M. D., Shalini, Kumar, S., Raynaud, C., Quan, D. H., Britton, W. J., ... & Kremer, L. (2021). Biological and biochemical evaluation of isatin-isoniazid hybrids as bactericidal candidates against mycobacterium tuberculosis. *Antimicrobial agents and chemotherapy*, *65*(8), e00011-21. https://doi.org/10.1128/AAC.00011-21
19. Ding, Z., Zhou, M., & Zeng, C. (2020). Recent advances in isatin hybrids as potential anticancer agents. *Archiv der Pharmazie*, *353*(3), 1900367. https://doi.org/10.1002/ardp.201900367
20. Abdel-Aziz, H. A., Eldehna, W. M., Keeton, A. B., Piazza, G. A., Kadi, A. A., Attwa, M. W., ... & Attia, M. I. (2017). Isatin-benzoazine molecular hybrids as potential antiproliferative agents: synthesis and in vitro pharmacological profiling. *Drug Design, Development and Therapy*, *11*, 2333. https://doi.org/10.2147/DDDT.S140164
21. Elsayed, Z. M., Eldehna, W. M., Abdel-Aziz, M. M., El Hassab, M. A., Elkaeed, E. B., Al-Warhi, T., ... & Mohammed, E. R. (2021). Development of novel isatin–nicotinohydrazide hybrids with potent activity against susceptible/resistant Mycobacterium tuberculosis and bronchitis causing–bacteria. *Journal of enzyme inhibition and medicinal chemistry*, *36*(1), 384-392. https://doi.org/10.1080/14756366.2020.1868450
22. Mohammad, A. E., Muhammad-Ali, M. A., Hameed, B. J., & Shaheed, D. Q. (2021). Design, synthesis, and characterization of some novel 4-aminoantipyrine derivatives and evaluation of their activity as analgesic agents. *Acta Poloniae Pharmaceutica*, *78*(5), 627-634. https://doi.org/10.32383/appdr/144130
23. Mohammed-Ali, M. A., & Majeed, N. N. (2012). Synthesis, characterization and study of antibacterial and antifungal activities of some 1, 3, 4-oxadiazole compounds. *J. Chem. Pharm. Res*, *4*, 315-321.
24. Alyahyaoy, H. A. (2019). Synthesis, characterization and antibacterial evaluation of new 1, 2, 4-triazole-3-thiol derivatives. *International Journal of Green Pharmacy (IJGP)*, *13*(3). https://doi.org/10.22377/ijgp.v13i3.2600
25. Dhaif, H. K., Jasim, E. Q., Muhajjar, Z. A., & Shanta, A. A. (2019). Corrosion Inhibition of Mild-Steel in 0.5 M HCl using some prepared 1, 2, 3-Triazoles Derivatives. *Mediterranean Journal of Chemistry*, *9*(4), 290-304. https://doi.org/10.13171/mjc9419111010655hkd
26. Abdul-Nabi, A. S., & Jasim, E. Q. (2014). Synthesis, Characterization and study of some tetrazole compounds as new corrosion inhibitors for C-steel in 0.5 M HCl solution. *International Journal of Engineering Research*, *3*(10), 613-617.
27. AL-Hakiem MM. (2020). Synthesis, Characterization and Biological Evaluation of Some Sulfa Drug Derivatives. *MSc Thesis, University of Basrah*.
28. Othman, A. A., Kihel, M., & Amara, S. (2019). 1, 3, 4-Oxadiazole, 1, 3, 4-thiadiazole and 1, 2, 4-triazole derivatives as potential antibacterial agents. *Arabian Journal of Chemistry*, *12*(7), 1660-1675. https://doi.org/10.1016/j.arabjc.2014.09.003
29. Mohammed, E. T., & Mustafa, Y. F. (2020). Coumarins from Red Delicious apple seeds: Extraction, phytochemical analysis, and evaluation as antimicrobial agents. *Systematic Reviews in Pharmacy*, *11*(2), 64-70. DOI: https://doi.org/10.5530/srp.2020.2.11
30. Fouad, S. A., El-Gendey, M. S., Ahmed, E. M., Hessein, S. A., Ammar, Y. A., & Zaki,

Y. H. (2021). Convenient Synthesis of Some New Thiophene, Pyrazole, and Thiazole Derivatives Bearing Biologically Active Sulfonyl Guanidine Moiety. *Polycyclic Aromatic Compounds*, 1-19. https://doi.org/10.1080/10406638.2021.1988999

31. Yimer, T., Birru, E. M., Adugna, M., Geta, M., & Emiru, Y. K. (2020). Evaluation of analgesic and anti-inflammatory activities of 80% methanol root extract of Echinops kebericho M.(Asteraceae). *Journal of Inflammation Research*, *13*, 647. https://doi.org/10.2147/JIR.S267154
32. Santenna, C., Kumar, S., Balakrishnan, S., Jhaj, R., & Ahmed, S. N. (2019). A comparative experimental study of analgesic activity of a novel non-steroidal anti-inflammatory molecule–zaltoprofen, and a standard drug–piroxicam, using murine models. *Journal of Experimental Pharmacology*, *11*, 85. https://doi.org/10.2147/JEP.S212988
33. Attique, S. A., Hassan, M., Usman, M., Atif, R. M., Mahboob, S., Al-Ghanim, K. A., ... & Nawaz, M. Z. (2019). A molecular docking approach to evaluate the pharmacological properties of natural and synthetic treatment candidates for use against hypertension. *International journal of environmental research and public health*, *16*(6), 923. https://doi.org/10.3390/ijerph16060923
34. Arjmand, B., Hamidpour, S. K., Alavi-Moghadam, S., Yavari, H., Shahbazbadr, A., Tavirani, M. R., ... & Larijani, B. (2022). Molecular Docking as a Therapeutic Approach for Targeting Cancer Stem Cell Metabolic Processes. *Frontiers in pharmacology*, *13*. https://doi.org/10.3389/fphar.2022.768556
35. Durhan, B., Yalçın, E., Çavuşoğlu, K., & Acar, A. (2022). Molecular docking assisted biological functions and phytochemical screening of Amaranthus lividus L. extract. *Scientific reports*, *12*(1), 1-16. https://doi.org/10.1038/s41598-022-08421-8
36. Hudson, R. L., & Gerakines, P. A. (2018). Infrared spectra and interstellar sulfur: New laboratory results for H2S and four malodorous thiol ices. *The Astrophysical Journal*, *867*(2), 138. https://doi.org/10.3847/1538-4357/aae52a
37. Salinas-Torres, A., Portilla, J., Rojas, H., Becerra, D., & Castillo, J. C. (2022). Synthesis, Spectroscopic Analysis, and In Vitro Anticancer Evaluation of 2-(Phenylsulfonyl)-2H-1, 2, 3-triazole. *Molbank*, *2022*(2), M1387. https://doi.org/10.3390/M1387
38. Balan, V., Mihai, C. T., Cojocaru, F. D., Uritu, C. M., Dodi, G., Botezat, D., & Gardikiotis, I. (2019). Vibrational spectroscopy fingerprinting in medicine: from molecular to clinical practice. *Materials*, *12*(18), 2884. ttps://doi.org/10.3390/ma12182884
39. Hardjono, S., Siswandono, S., & Andayani, R. (2017). Evaluation of N-benzoylthiourea derivatives as possible analgesic agents by predicting their physicochemical and pharmacokinetic properties, toxicity, and analgesic activity. *Indonesian Journal of Biotechnology*, *22*(2), 76-85. https://doi.org/10.22146/ijbiotech.27171
40. Mazák, K., Noszál, B., & Hosztafi, S. (2019). Advances in the physicochemical profiling of opioid compounds of therapeutic interest. *ChemistryOpen*, *8*(7), 879-887. https://doi.org/10.1002/open.201900115

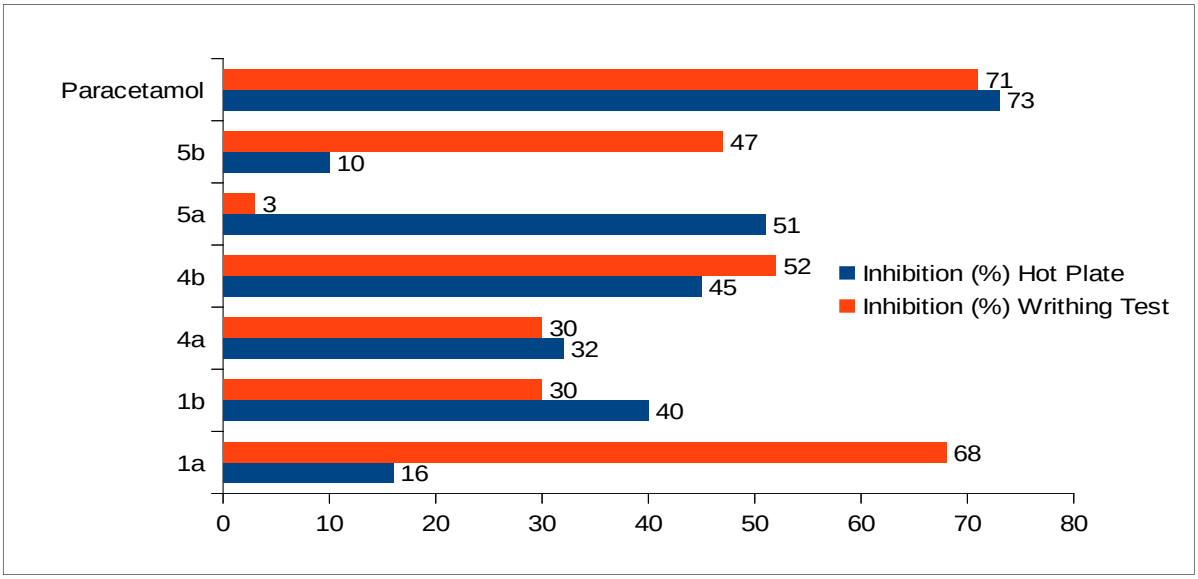

Figure 1. *Analgesic activity of the compounds using hot plate and writhing test methods*

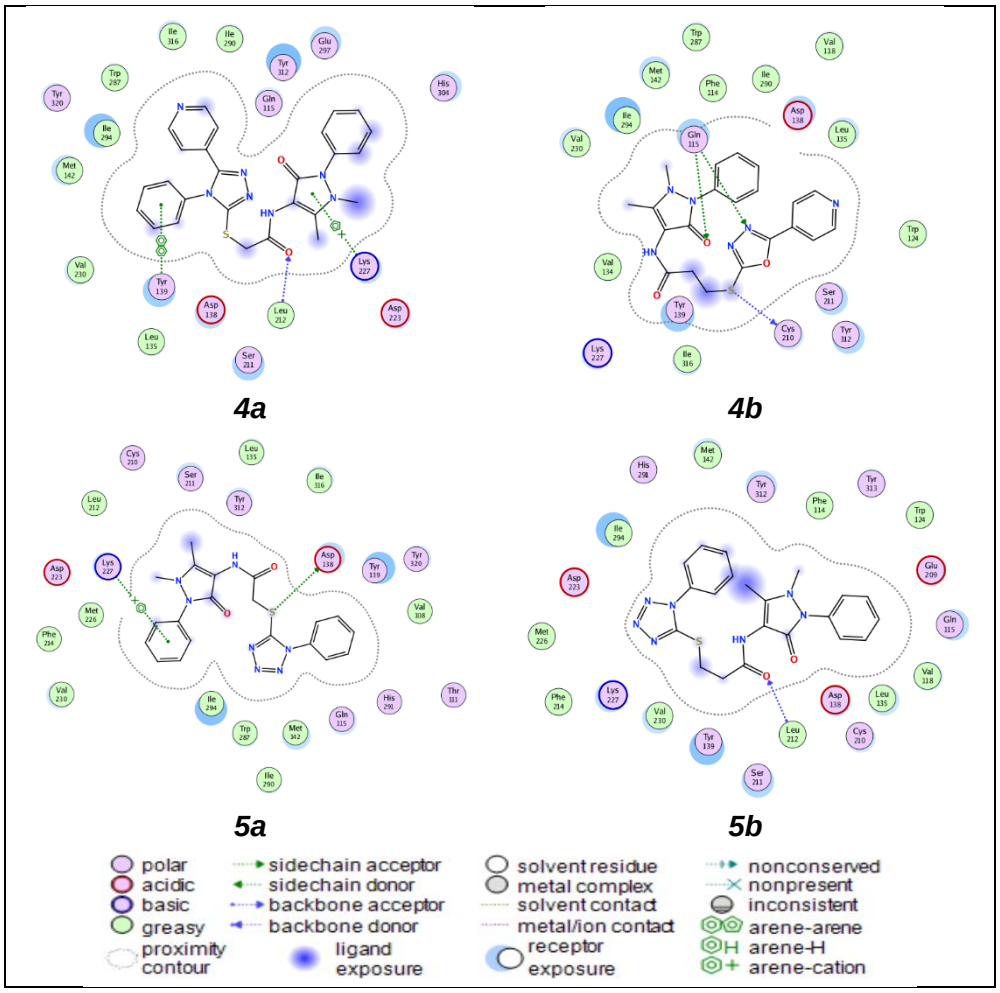

Figure 2. *2D binding affinity of the compounds with 6B73*

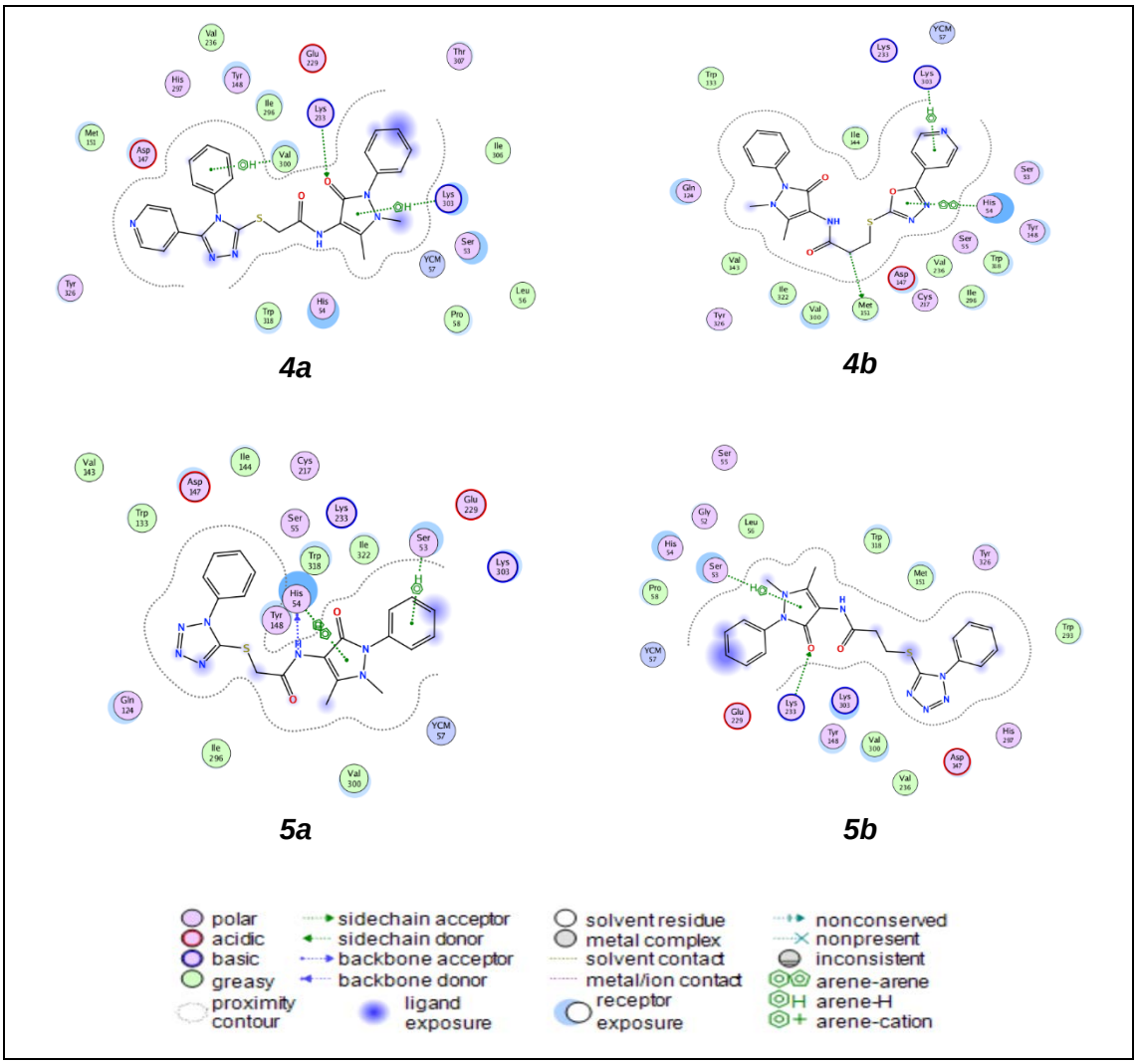

Figure 3. *2D binding affinity of the compounds with 5C1M*

Table 1. *Inhibition zone of the synthesized compounds against the tested bacteria at different concentrations*

Compound	Conc. (µg/ml)	Inhibition zone (mm)			
		S. aureus	***Streptococcus***	***E.coli***	***Klebsiella pneumonia***
1a	1000	10	17	9	8
	500	10	15	7	8
	250	8	15	7	NI
	125	7	10	NI	NI
	50	7	8	NI	NI
1b	1000	10	10	7	NI
	500	9	7	7	NI
	250	7	7	NI	NI
	125	NI	NI	NI	NI
	50	NI	NI	NI	NI
4b	1000	10	9	8	8
	500	9	9	8	7
	250	7	7	7	7
	125	7	NI	NI	NI
	50	NI	NI	NI	NI
4a	1000	NI	NI	9	7
	500	NI	NI	7	NI
	250	NI	NI	7	NI
	125	NI	NI	NI	NI
	50	NI	NI	NI	NI
5a	1000	11	9	9	12
	500	8	7	7	9
	250	7	NI	7	7
	125	NI	NI	NI	NI
	50	NI	NI	NI	NI
5b	1000	10	NI	9	10
	500	9	NI	9	9
	250	7	NI	8	7
	125	7	NI	NI	7
	50	NI	NI	NI	NI
Amoxicillin	1000	17	15	40	35
	500	14	12	36	30
	250	14	12	31	28
	125	12	10	29	22
	50	9	9	25	20

NI: No Inhibition

Table 2. *Evaluation of analgesic activity by the hot plate method*

Group	Reaction Time (Seconds)	Inhibition (%)
Standard	13.41 ± 1.84 ***	73
Control	3.62 ± 0.74	
1a	4.35 ± 0.95	16
1b	6.08 ± 1.02 *	40
4a	5.33 ± 0.81	32
4b	6.63 ± 0.73 *	45
5a	7.36 ± 1.14 **	51
5b	4.09 ± 0.86	10

*Each value is mean ±S.D. for six mice, *p <0.05, **p <0.01, ***p <0.001 compared with normal control. Data were analyzed by using one-way ANOVA followed by a T-test*

Table 3. *Evaluation of analgesic activity by the writhing method*

Group	Number of Writhing	Inhibition (%)
Standard	12.36 ± 3.25 ***	71
Control	42.36 ± 4.47	
1a	13.95 ± 2.58 ***	68
1b	29.65 ± 5.24	30
4a	29.79 ± 4.21	30
4b	20.41 ± 3.62 **	52
5a	41.60 ± 7.08	3
5b	22.31 ± 3.69 *	47

*Each value is mean ±S.D. for six mice, *p <0.05, **p <0.01, ***p <0.001 compared with normal control. Data were analyzed by using one-way ANOVA followed by a T-test*

Table 4: *Docking scores of synthesized compounds covalently bound to the active site of 6B73 protein and 5C1M protein*

Compd.	Docking affinity (kcal/mol)			
	6B73	RMSD Å	5C1M	RMSD Å
1a	-6.89	1.05	-6.29	1.20
1b	-6.73	1.18	-6.56	1.98
2b	-4.90	1.17	-5.04	2.13
2d	-5.86	1.59	-5.54	1.10
3	-5.18	1.13	-4.94	1.39
4a	-8.48	1.77	-9.00	2.34
4b	-8.01	2.31	-9.21	1.34
5a	-8.00	2.11	-8.94	1.48
5b	-8.76	1.91	-8.86	2.13

Table 5. *Molecular docking score, RMSD, and binding affinity for the compounds showed valid molecular docking scores with 6B73*

Compd	S Score kcal/mol	RMSD Å	Bonds between Atoms of Compounds and Residues of Active Site of 6B73						
			Compd Atoms	Receptor Atoms	Receptor Residues	Interaction	d (Å)	E (kcal/mol)	Total E (kcal/mol)
1a	-6.89	1.05	Cl 33	O	HIS 291	H-donor	3.04	-0.1	-29.62
			O 25	CA	HIS 291	H-acceptor	3.29	-1.2	
1b	-6.73	1.18	O 25	CA	LYS 227	H-acceptor	3.45	-0.7	-27.51
			Cl 36	NZ	LYS 227	H-acceptor	3.95	-0.8	
			C 29	5-ring	HIS 291	H-pi	3.90	-2.4	
2b	-4.90	1.17	-	-	-	-	-	-	-23.28
2d	-5.86	1.59	S 16	OD1	ASP 138	H-donor	3.76	-1.2	-24.60
3	-5.18	1.13	S 1	SD	MET 142	H-donor	4.04	-1.0	-24.47
			5-ring	CZ3	TRP 287	pi-H	3.95	-0.8	
4a	-8.48	1.77	O 32	N	LEU 212	H-acceptor	3.22	-2.7	-46.83
			5-ring	NZ	LYS 227	pi-cation	3.64	-0.8	
			6-ring	6-ring	TYR 139	pi-pi	3.82	0	
4b	-8.01	2.31	S 38	O	CYS 210	H-donor	4.00	-0.4	-45.79
			O 3	NE2	GLN 115	H-acceptor	3.02	-2.3	
			N 34	NE2	GLN 115	H-acceptor	3.06	-1.4	
5a	-8.00	2.11	S 33	OD2	ASP 138	H-donor	4.10	-0.5	-36.34
			6-ring	NZ	LYS 227	pi-cation	4.25	-1.2	
5b	-8.76	1.91	O 32	N	LEU 212	H-acceptor	2.98	-1.7	-46.85

Table 6. *Molecular docking score, RMSD, and binding affinity for the compounds showed valid molecular docking scores with 5C1M*

Compd	S Score kcal/mol	RMSD Å	Bonds between Atoms of Compounds and Residues of Active Site of 5C1M						
			Compd Atoms	Receptor Atoms	Receptor Residues	Interaction	d (Å)	E (kcal/mol)	Total E (kcal/mol)
1a	-6.29	1.20	N 22	SD	MET 151	H-donor	4.40	-1.4	-30.44
			C 26	SD	MET 151	H-donor	3.80	-0.8	
1b	-6.56	1.98	C 33	5-ring	HIS 297	H-pi	3.60	-0.7	-29.17
			5-ring	5-ring	HIS 54	pi-pi	3.92	0	
2b	-5.04	2.13	S 16	O	HIS 54	H-donor	3.63	-3.2	-22.10
			5-ring	5-ring	HIS 54	pi-pi	3.66	0	
2d	-5.54	1.10	N 12	SD	MET 151	H-donor	3.71	-0.5	-22.43
			C 1	5-ring	HIS 297	H-pi	4.12	-1.0	
			5-ring	6-ring	TYR 148	pi-pi	3.48	0	
3	-4.94	1.39	S 1	O	ASP 147	H-donor	3.68	-0.7	-21.48
4a	-9.00	2.34	O 3	CE	LYS 233	H-acceptor	3.13	-0.9	-45.89
			6-ring	CG2	VAL 300	pi-H	4.40	-0.7	
			5-ring	CD	LYS 303	pi-H	4.00	-0.9	
4b	-9.21	1.34	C 29	SD	MET 151	H-donor	3.89	-0.8	-48.66
			6-ring	CE	LYS 303	pi-H	4.64	-0.6	
			5-ring	5-ring	HIS 54	pi-pi	3.66	0	
5a	-8.94	1.48	N 26	O	HIS 54	H-donor	3.11	-2.3	-46.21
			6-ring	CB	SER 53	pi-H	3.95	-1.0	
			5-ring	CA	HIS 54	pi-H	3.95	-1.2	
			5-ring	5-ring	HIS 54	pi-pi	3.97	0	
5b	-8.86	2.13	O 3	CB	LYS 233	H-acceptor	3.27	-1.1	-46.52
			5-ring	CE	SER 53	pi-H	4.01	-0.6	

PERIÓDICO TCHÊ QUÍMICA
ARTIGO ORIGINAL

EFEITO DO CACTO AMAZÔNICO (*Cereus jamacaru*) COMO COAGULANTE NATURAL PARA A REMOÇÃO DA TURBIDEZ DE ÁGUAS SUPERFICIAIS

EFFECT OF AMAZON CACTUS (*Cereus jamacaru*) AS A NATURAL COAGULANT FOR THE REMOVAL OF TURBIDITY FROM SURFACE WATER

RISS, Jordana Souza Paula[1,3*]; FARIAS, Leovergildo Rodrigues[1]; SOUZA, Verônica Paula[2]; ARAÚJO, Glécio Ísavo[1]; VITAL, Marcos José Salgado[5].

[1] Instituto Federal de Roraima, Departamento de Ensino. Brasil.

[2] Universidade Estadual de Roraima, Programa de Mestrado em Educação. Brasil.

[3] Universidade Federal de Roraima, Programa de Pós-graduação em Recursos Naturais - PRONAT. Brasil.

** Corresponding author*
e-mail: jordana.riss83@gmail.com

Received 12 September 2022; received in revised form 28 September 2022; accepted 06 October 2022

RESUMO

Introdução: O Brasil sofre com a falta de saneamento básico e esse fato se intensifica na região Amazônica quando pensamos nas populações vivendo em áreas de difícil acesso. A aplicação de coagulantes naturais surge como uma alternativa promissora, apresenta metodologia simples, de baixo custo, de fácil reprodução e acessível, promovendo a saúde e melhorias ambientais. O uso de coagulantes químicos pode acarretar malefícios ao ambiente e à saúde humana. **Objetivo:** Portanto, o objetivo desse estudo foi avaliar o efeito de coagulação de uma espécie de cacto amazônico aplicado ao tratamento de água para consumo humano. **Métodos:** Para o estudo, coletou-se cerca de 500 gramas da parte aérea do *Cereus jamacaru* às margens da BR 174 na região do lavrado de Roraima. No laboratório, foram retirados os espinhos, o material vegetal foi lavado, cortados a uma espessura de um centímetro, secos em estufa a 60 °C por 36 horas, triturados em liquidificador e peneirados até a obtenção de um pó, o qual foi testado como coagulante natural. A água utilizada no estudo foi coletada do Rio Branco no município de Boa Vista-RR e caracterizada quanto a sua turbidez inicial. **Resultados:** A dosagem de 0,2g do coagulante natural de cacto apresentou significativa redução na turbidez da água de estudo, deixando-a dentro dos padrões de potabilidade estabelecidos para as água subterrâneas. **Discussão:** A coagulação no contexto sanitário é evidenciada em razão da remoção de partículas microscópicas associadas aos microrganismos patogênicos, normalmente encontrados nas águas brutas e com velocidade de sedimentação muito reduzida. Substituir substâncias químicas poluidoras por coagulantes naturais no tratamento da água para consumo humano contribui para a qualidade de vida. **Conclusão:** O cacto amazônico *Cereus jamacaru* demonstrou eficácia de coagulação para a análise do parâmetro turbidez da água para consume humano.

Palavras-chave: *Qualidade da água, Saúde humana, Biocoagulante*

ABSTRACT

Background: Brazil suffers from a lack of basic sanitation in many regions, intensified in the Amazon region due to its difficult access. The application of natural coagulants is a promising alternative since it eliminates the use of chemicals, is a simple, low-cost method that is easy to reproduce, and is accessible to any community, thus promoting health and environmental improvements. On the other hand, the use of chemical coagulants can cause harm to the environment and human health. **Aim:** Therefore, the objective of this study was to evaluate the coagulation effect of a species of Amazonian cactus applied in the treatment of water for human consumption. **Methods:** For the study, about 500 grams of the aerial part of the *Cereus jamacaru* was collected on the banks of the BR 174 in the region of Roraima. The spines were removed in the laboratory, the plant material was washed, cut to a thickness, dried in an oven at 60 °C for 36 hours, then ground and sieved until obtaining a powder, which was tested as a natural coagulant. The water used in the study was collected from the Branco River in Boa Vista, Roraima, and characterized its initial turbidity. **Results:** The dosage of 0.2g of the natural cactus coagulant showed a significant reduction in the turbidity of the study water, leaving it within the potability standards established for groundwater. **Discussion**: Coagulation in the sanitary context is evidenced by the removal of

DOI: 10.52571/PTQ.v19.n42.2022.03_RISS_pgs_29_36.pdf

microscopic particles associated with pathogenic microorganisms, normally found in raw water and with very low sedimentation speed. Replacing polluting chemical substances with natural coagulants in the treatment of water for human consumption contributes to the quality of life. **Conclusion:** The Amazonian cactus *Cereus jamacaru* demonstrated coagulation efficiency for analyzing the turbidity parameter of water for human consumption.

Keywords: *Quality water, Human health, Biocoagulant*

1. INTRODUCTION:

According to the National Information System on Basic Sanitation, 39.4 million Brazilians do not have access to treated water (BRASIL, 2018). The problem of lack of basic sanitation intensifies in the Amazon region of Brazil, principally due to its difficult access areas. In addition, economic viability and the complexity of the operation may make it impossible to implement specific water treatment methods in some locations (MELLO, 2018). To supply good quality water to the population for their daily activities, water intended for supply goes through a treatment process in water treatment plants (ETA). The conventional and most commonly used treatment in Brazilian ETAs consists of four stages: coagulation and flocculation, decantation, filtration, and finally, chlorination and fluoridation. Coagulation stands out as a process involving the application of chemicals that allow the removal of dissolved compounds in the water and the destabilization of colloidal suspensions and solids that cannot be removed by sedimentation or filtration. Closely linked to coagulation is flocculation, during which particles destabilized by the coagulant coalesce and form flakes amenable to decantation (LIMA JUNIOR, 2018; RICHTER, 2009).

Following the principles of green chemistry proposed in the 90s, Lima Junior and Abreu (2018) state that the development of coagulants and flocculants, based on biodegradable natural raw materials abundant in nature, called natural coagulants or biocoagulants, has been gaining more and more space in research focused on environmental technologies since natural coagulants follow the concept of eco-friendly material, those designed to cause the least harm to nature. Therefore, studies with cacti that can be used for water treatment have received great attention due to their chemical composition since they have nutrients with coagulation potential (ZARA; THOMAZINI; LENZ, 2012). Furthermore, during water treatment, the accumulation of residues of non-biodegradable metal hydroxides generated during coagulation and flocculation processes, the high concentration of sludge that presents ecotoxic potential (OLADOJA *et al*., 2017), and the relationship with pathologies that affect the central nervous system, such as dementia and Alzheimer's and Parkinson's diseases, are some of the results of the application of chemical coagulants to the treatment of water for human consumption (CHUA *et al*., 2019; FERMINO *et al*., 2017; WALTON, 2013). Such hazards make studies with natural coagulants advantageous as there is a high availability of raw materials, are often renewable, have low corrosiveness on the water distribution system, and there is a decrease of up to five times in the volume of sludge generated in the water treatment process. In addition, they do not present risks to human and animal health, and there is a significant reduction in costs and dangers in the treatment processes (TEIXEIRA *et al*., 2017).

Mandacaru (*C. jamacaru*) is a cactus native to Brazil, abundant in the northeast region of the country (ZARA; THOMAZINI; LENZ, 2012) and found in the Roraima field (OLIVEIRA, 2016; PASSOS, 2019). According to Cavalcante (2013), some metabolic and structural adaptations are necessary, so that species of the cactus family can survive in different environments, including adverse ones. Studies with cactus intended for water treatment have received significant attention due to their chemical and structural composition since they contain nutrients, proteins, amylose, malic acid, resin, vitamins, and cellulose (ZARA; THOMAZINI; LENZ, 2012). However, research on the application of cactus in water treatment is still scarce, and it is worth mentioning that no records were found about this application with species from the Amazon region of Brazil.

This study was developed in the context of the Brazilian Amazon and considered the environmental, spatial, temporal, and mainly social conjuncture. The state of Roraima is located in the northwest of the northern region of Brazil and is predominated by rainforest vegetation; however, in the central-eastern region, there is a huge strip of farmland known as "lavrado", a local name given to the savanna region. The farmland of Roraima is highly important for conserving biodiversity and water resources; therefore, the cactus *Cereus jamacaru* De Candolle (popularly

known as Mandacaru) was studied for treating water. Furthermore, due to its polymers, which have coagulating and flocculating action, it is believed that the cactus is not only effective but also safer in the treatment of water, thus promoting lower impacts on the environment and human health. Therefore, the objective of this study was to evaluate the coagulation effect of a species of Amazonian cactus applied to water treatment for human consumption.

2. MATERIALS AND METHODS:

Raw water samples from the Branco River were collected near the extraction point used by the Water and Sewage Company of Roraima (CAER), located in the city of Boa Vista, state of Roraima, Brazil, under geographic coordinates 760511 E, 312928 N. The collection was carried out in March 2021 in a period of drought in the State of Roraima. 12 liters of water were collected, stored in amber glasses, placed in a styrofoam box containing ice for cooling and transported to the laboratory of the Federal University of Roraima. Coagulation assays were performed on the same day of collection. Water characterization before and after treatment was performed by measuring turbidity (Akso TU430) based on the 20th Standard Methods for the Examination of Water and Wastewater (APHA; AWWA; WEF, 2017).

2.1. Preparation of the natural coagulant

The natural coagulant (NC) was prepared with 500 grams (g) of the aerial part of *C. jamacaru*, which was collected in the agricultural region of Roraima. First, the spines of the plant material were removed and discarded, and then the cactus was washed under running water, cut into pieces of about 1 centimeter (cm), and placed on trays (Figure 1a). These were then placed in an oven at 60 ºC for drying (MILLER *et al*., 2008; OTHMANI *et al*., 2020).

After drying, the cactus pieces were ground in a household blender and sieved to provide a powder (Figure 1b) with particles of about 300 micrometers (µm) in diameter. This powder was stored in a sealed container, dated and identified, and kept in a refrigerator until the tests were performed using the jar test equipment.

2.2. Coagulation test

The coagulation assay was performed using jar test equipment (Afakit AT-700) with six jars with a blade speed regulated for two mixing regimes: fast (150 rpm for three minutes); slow (60 rpm for 17 minutes); plus a sedimentation time of 30 minutes with the equipment turned off (Table 1). In the jars, 400 milliliters (mL) of raw water were used according to the adapted methodology of Zara *et al*. (2012).

The dosages of the natural coagulant of cactus and the aluminum sulfate (control) were determined according to values obtained in the literature and in the pre-assays of this study. They were 0.032 g of aluminum sulfate (Zara *et al*., 2012) and 0.01, 0.02, 0.04, 0.05, 0.1, 0.2, 0.3, 0.4 and 0.5 g of natural cactus coagulant (ORTIZ; ASTUDILLO; MARTÍNEZ, 2013; FEDALA *et al*., 2015), which were applied directly to the 400 mL of water contained in individual jars. At the end of the coagulation assay, samples of the treated water were collected from each jar with a 20 mL graduated pipette, and a new turbidity measurement was performed.

Table 1. *Stages and rotation speeds and duration for each step of the coagulation assay.*

Stages	Rotation/Duration
Rapid mixing	150 rpm/3 minutes
Slow mixing	60 rpm/17 minutes
Sedimentation	0/30 minutes

3. RESULTS AND DISCUSSION:

3.1. Results

The raw water used in the coagulation test showed initial turbidity of 23 turbidity units (NTUs). After this test, a new turbidity measurement was performed (Table 2). The potability standard for human consumption water is established by Ordinance No. 888, of May 4, 2021, by the Brazilian Ministry of Health (BRASIL, 2021) and has a maximum limit of 5 NTUs established as a standard in the turbidity parameter of the distribution network.

The decreased efficacy of turbidity removal with increased dosage of the natural coagulant (Figure 2) demonstrated in this study corroborates the results of Pichler *et al*. (2012), who used the mucilage of cacti *Opuntia ficus-indica* in water treatment and observed that, by increasing the dose of mucilage, after sedimentation of the flakes, the turbidity of the supernatant also increased.

3.2. Discussion

Although the use of natural coagulants is a sustainable alternative for treating water for human consumption, the application of forms, such as powders, mucilage, or unpurified extracts, directly in the water to be treated leads to an increase in organic matter, thus leaving the water more turbid.

Choy *et al*. (2014) attribute the increase in organic matter to the presence of lipids, biomolecules that do not participate in the coagulation process. Although it was not possible to perform quantification tests of organic matter, this effect can be observed when verifying the initial turbidity of 23 NTUs of the water used in this study with the highest coagulant dosage of 0.5 g of cactus powder that presented the lowest efficiency for removal and left the water with a greenish appearance. However, it is possible to improve the treated water quality using filters, considering that the flakes formed by biomolecules are usually large and easily retained and do not require more advanced filtration systems (PICHLER *et al*., 2012).

Unlike some studies, which demonstrated that the higher the turbidity of the water to be treated, the better the efficiency of natural coagulants, the effect observed in the present study was satisfactory for the sample of water with low turbidity (23 NTUs). In a comparative study with aluminum sulfate, Pichler, Young, and Alcantar (2012) obtained excellent results with the cactus of the genus *Opuntia* by demonstrating that the same turbidity removal efficiency could be obtained with the cactus using a dosage 300 times lower than that of the chemical coagulant.

Pritchard *et al*. (2010) used a natural coagulant based on *Moringa oleifera* seed to treat water with a turbidity of 40 NTUs and 200 NTUs, and the removal efficiency at the end of treatment was 50% and 90%, respectively. A possible justification for this behavior lies in the fact that both *Moringa oleifera* and cacti are considered polyelectrolytes, i.e., they are flocculating polymers with different ionic charges that act in the formation of flakes and assist in coagulation.

For Baghvand *et al*. (2010), low turbidity waters have a small amount of colloidal matter, i.e., this lower concentration of colloids suspended in water limits the contact rate between particles and flocculating polymers, thus hindering the coagulation process and consequently the performance of the coagulant. Therefore, an alternative for treating low turbidity waters is the addition of synthetic turbidity in order to create the formation of heavier flakes, which settle more easily.

4. CONCLUSIONS:

The Amazonian cactus *C. jamacaru* demonstrated coagulation efficacy in the analysis of the turbidity of the sampled water. Replacing polluting chemicals with natural coagulants in water treatment for human consumption contributes to the quality of life by helping communities that do not have access to clean water and protecting the environment. It is possible to suggest the execution of new studies that seek to perform other tests of the physicochemical parameters and the zeta potential to guarantee the effectiveness and safety of cactus application as a natural coagulant for the treatment of water for human consumption.

5. DECLARATIONS

5.1. Study Limitations

The study is limited to the sample size and the period of the collection of the samples.

5.2. Acknowledgements

We thank the Postgraduate Program in Natural Resources at the Federal University of Roraima and the Novo Paraíso Campus of the Federal Institute of Roraima, for supporting the research.

5.3. Funding source

The authors funded this research.

5.4. Competing Interests

There are no potential conflict of interest in this publication.

5.5. Open Access

6. REFERENCES:

1. American public health association, american works association, water environment federation. (2017). Standard Methods for the Examination of Water and Wastewater. Denver, CO.

2. Baghvand, A., Zand, A. D., Mehrdadi, N.& Karbassi, A. (2010) Optimizing coagulation process for low to high turbidity waters using aluminum and iron salts. American Journal of Environmental Sciences,5 (6): 442-448.

3. BRASIL. Ministério da Saúde. Portaria nº888, de 04 de maio de 2021. Consolidação das normas sobre as ações e os serviços de saúde do Sistema Único de Saúde. Diário Oficial da União, Brasília, DF. 2021. Disponível em: <http://www.saude.gov.br>. Acesso em: 15 mai. 2022.

4. Chua, S.C, Malek, M. A., Chong, F. K., Sujarwo, W., HO, Y.C. Red Lentil (Lens culinaris) extract as a novel natural coagulant for turbidity reduction: an evaluation, characterization and performance optimization study. Water, [S.l], v. 11, n. 8, aug.2019.

5. Choy, S. Y., nagendra, K. M. P., Wu, T. Y., Raghunandan, M. E.& Ramanan, R. N. (2014). Utilization of plant-based natural coagulants as future alternatives towards sustainable water clarification. Journal of Environmental Sciences, 11 (26): 2178-2189.

6. Fedala, N., Lounici, H., Drouiche, N., Mameri, N. & Drouiche, M. (2015). Physical parameters affecting coagulation of turbid water with Opuntia ficus-indica cactus. Ecological Engineering, (77): 33-36.

7. Fermino, L. S., Pedrangelo, A. C. S., Silva, P. K. M., Azevedo, R. E. C., Yamaguchi, N. U., Ribeiro, R. M.. Water treatment with conventional and alternative coagulants. Chemical Engineering Transactions, Milano, vol. 57, p. 1189-1194, mar. 2017.

8. Lima Júnior, R. N. & Abreu, F. O. M. S. (2018). Produtos Naturais Utilizados como Coagulantes e Floculantes para Tratamento de Águas: Uma Revisão sobre Benefícios e Potencialidades. Revista Virtual de Química, 3 (10): 709-735.

9. Mello, C. (2018) Trabalho, tecnologia e solidariedade. Florianópolis: Insular.

10. Miller, S. M., Fugate, E. J., Craver, V. O., Smith, J. A., & Zimmerman, J. B. (2008). Toward understanding the efficacy and mechanism of Opuntia spp. as a natural coagulant for potential application in water treatment. Environmental science & technology, 42(12), 4274–4279. https://doi.org/10.1021/es7025054

11. Oladoja, N. A., Saliu, T. D., Ololade, I. A., Anthony, E. T. & Bello, G. A. (2017). A new indigenous green option for turbidity removal from aqueous system. Separation and Purification Technology, (186): 166-174.

12. Ortiz, A. V., Astudillo, I. C. & Martínez, G. J. (2013). Caracterización de la Opuntia ficus-indica para su uso como coagulante natural. Revista Colombiana de Biotecnología, 1 (15):137-144.

13. Othmani, B., Gamelas, J., Rasteiro, M. G., & Khadhraoui, M. (2020). Characterization of Two Cactus Formulation-Based Flocculants and Investigation on Their Flocculating Ability for Cationic and Anionic Dyes Removal. Polymers, 12(9), 1964. https://doi.org/10.3390/polym12091964.

14. Pichler, T., Young, K. & Alcantar, N. (2012). Eliminating turbidity in drinking water using the mucilage of a common cactus. Water Science & Technology: Water Supply, 2 (12):179-186.

15. Pritchard, M., Craven, T., Mkandawire, T., Edmondson, A. S. & O'Neill, J. G. (2010).

A study of the parameters affecting the effectiveness of Moringa oleifera in drinking water purification. Physics and Chemistry of the Earth, Parts A/B/C, 13-14 (35): 791-797.

16. Richter, Carlos A. (2009). Água: métodos e tecnologia de tratamento. São Paulo: Edgard Blucher.

17. Teixeira, M. R., Camacho, F. P.; Sousa, V. S. & Bergamasco, R. (2017). Green technologies for cyanobacteria and natural organic matter water treatment using natural based products. Journal of Cleaner Production, (162): 484-490.

18. Walton, J. R. (2013). Aluminum's involvement in the progression of Alzheimer's disease. Journal of Alzheimer's Disease, 35 (1): 7- 43.

19. Zara, R. F, Thomazini, M. H.& Lenz, G. F. (2012). Estudo da eficiência de polímero natural extraído do cacto mandacaru (Cereus jamacaru) como auxiliar nos processos de coagulação e floculação no tratamento de água. Revista de estudos ambientais 2 (14):75-83.

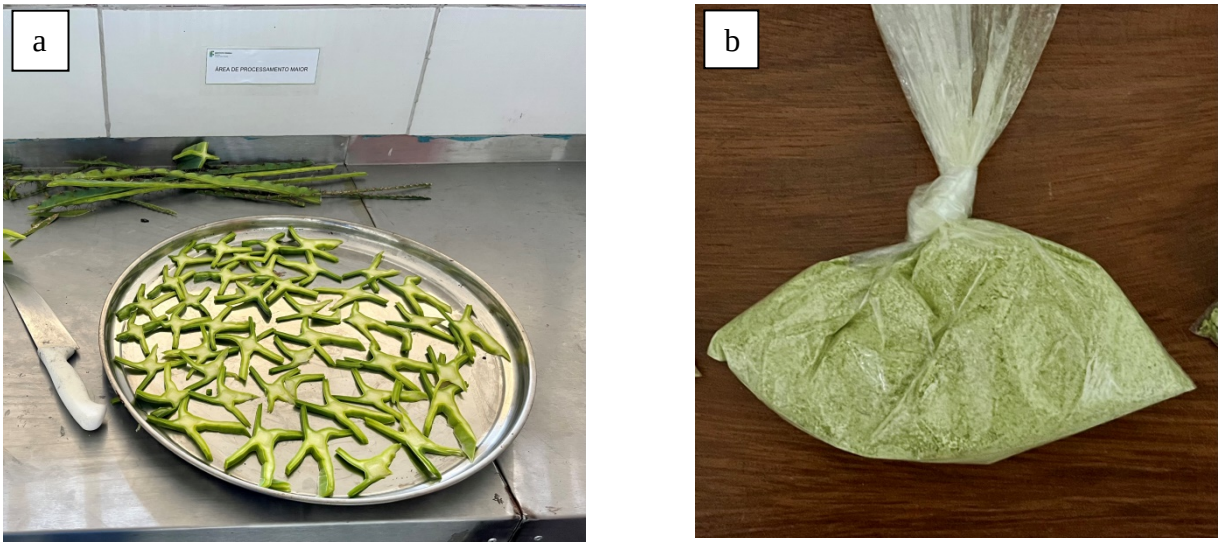

Figure 1. *a.Plant material processing. b. Coagulant powder.* ***Source:*** *the authors*

Table 2. *Turbidity removal values for each dosage and coagulants used.*

Initial turbidity of water sample (NTUs)	Dosage of coagulants (g)	Turbidity after application of coagulants (NTUs)
23	0.032 g aluminum sulphate (control)	2.5
	0.01 g of cactus NC	5.24
	0.02 g of cactus NC	4.91
	0.04 g of cactus NC	4.5
	0.05 g of cactus NC	4.43
	0.1 g of cactus NC	3.49
	0.2 g of cactus NC	2.49
	0.3 g of cactus NC	2.80
	0.4 g of cactus NC	3.99
	0.5 g of cactus NC	7

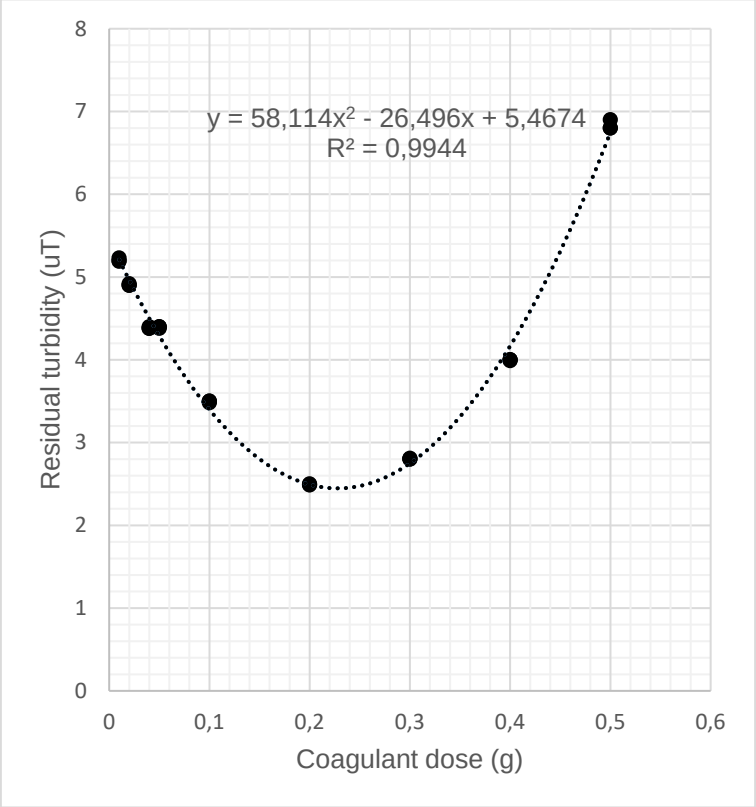

Figure 2. *Removal of turbidity vs. the dosage of coagulants.* ***Source:*** *the authors*

PERIÓDICO TCHÊ QUÍMICA
ARTIGO ORIGINAL

SOROPREVALÊNCIA DE ANTICORPOS IGG COVID-19 NA CIDADE DE SHAHREKORD, IRÃ

SEROPREVALENCE OF COVID-19 IGG ANTIBODIES IN SHAHREKORD COUNTY, IRAN

شیوع سرمی آنتی بادی های IgG کووید 19 در شهرستان شهرکرد، ایران

ASADI-SAMANI, Majid[1]; MOGHNI, Mandana[2]; KHEIRI, Soleiman[3]; MORADI, Mohammad-Taghi[4]*; KHORRAMI, Zahra[5]

[1] Cellular and Molecular Research Center, Basic Health Sciences Institute, Shahrekord University of Medical Sciences, Shahrekord. Iran.

[2] Department of Pathology, Shahrekord University of Medical Sciences, Shahrekord. Iran.

[3] Modeling in Health Research Center, Shahrekord University of Medical Sciences, Shahrekord. Iran.

[4] Medical Plants Research Center, Basic Health Sciences Institute, Shahrekord University of Medical Sciences, Shahrekord. Iran.

[5] Social Determinants of Health Research Center, Shahrekord University of Medical Sciences, Shahrekord. Iran.

** Corresponding author*
e-mail: mtmoradi65@gmail.com

Received 11 August 2022; received in revised form 21 September 2022; accepted 03 October 2022

RESUMO

Introdução: A estimativa da soroprevalência de anticorpos covid-19 pode ser usada para prever com mais precisão a epidemia, estimar a vulnerabilidade da comunidade, obter informações sobre a progressão da doença e gerenciar o tratamento da doença. **Objetivos:** O presente estudo foi desenhado para avaliar a soroprevalência de anticorpos IgG contra o vírus COVID-19 na população urbana do município de Shahrekord (Irã). **Methods:** Neste estudo analítico-descritivo, foram identificadas 690 pessoas residentes no município de Shahrekord encaminhadas a laboratórios de diagnóstico médico entre Outubro e Dezembro de 2020, e os níveis séricos de IgG foram medidos através do teste ELISA. O teste estatistico Qui-quadrado e o teste de Spearman, executados no SPSS-20, foram utilizados para investigar a relação entre as variáveis. **Results:** Das 690 amostras, 190 foram positivas para anticorpos IgG contra COVID-19. A frequência de anticorpos positivos foi de 27,5% [IC 95%: 23,1-30 (26,9% em homens e 28% em mulheres)]. Não houve relação significativa entre a soroprevalência de COVID-19 e sexo, ocupação, estado civil e IMC (P > 0,05). A soroprevalência de COVID-19 foi significativamente maior em indivíduos com histórico de contato com pessoa infectada, indivíduos com sintomas de COVID-19 durante a pandemia, indivíduos com histórico de diagnóstico definitivo por PCR e indivíduos com idade superior a 60 anos (P < 0,05). **Discussões:** Com base nos resultados, a soroprevalência de anticorpos contra COVID-19 na população estudada foi de 27,5% e superior à prevalência da doença baseada em testes de triagem molecular.. **Conclusão:** A determinação da prevalência de anticorpos IgG contra COVID-19 na comunidade para ajudar na previsão mais precisa da epidemia pode ser utilizada no gerenciamento da doença.

Palavras-chave: *Coronavírus, COVID-19, Epidemiologia, Anticorpos, Sistema imunológico.*

ABSTRACT

Background: Estimation of seroprevalence of COVID-19 antibodies can be used to predict the epidemic more accurately and estimate the vulnerability of the community, gain information on disease progression, and manage disease treatment. **Aims:** The present study was designed to evaluate the seroprevalence of IgG antibodies against the COVID-19 virus in the urban population of Shahrekord county (Iran). **Methods:** In this descriptive-analytical study, 690 people living in Shahrekord county referred to medical diagnostic laboratories in the county between October to December 2020 were identified, and their serum IgG levels were measured using ELISA. Chi-square and Spearman's test in SPSS 20 were used to investigate the relationship between variables.

DOI: 10.52571/PTQ.v19.n42.2022.04_MORADI_pgs_37_45.pdf

Results: Out of 690 samples, 190 were positive for IgG antibodies against COVID-19. The frequency of positive antibodies was 27.5% [CI 95%: 23.1-30 (26.9% in men and 28% in women)]. There was no significant relationship between the seroprevalence of COVID-19 and gender, occupation, marital status, and BMI (P>0.05). Seroprevalence of COVID-19 was significantly higher in individuals with a history of contact with an infected person, individuals with COVID-19 symptoms during the pandemic, individuals with a history of definitive diagnosis based on PCR, and individuals aged over 60 years (P<0.05). **Discussion:** Based on the results, the seroprevalence of antibodies against COVID-19 in the study population was 27.5% and more than the prevalence of the disease based on molecular screening tests. **Conclusion:** Determination of IgG antibodies prevalence against COVID-19 in the community to help in more accurate prediction of the epidemic can be used in managing the disease.

Keywords: *Coronavirus, COVID-19, Epidemiology, Antibodies, Immune system.*

چکیده

زمینه: *تخمین شیوع سرمی آنتی‌بادی‌های کووید-19 می‌تواند برای پیش‌بینی دقیق‌تر اپیدمی و تخمین آسیب‌پذیری جامعه، کسب اطلاعات در مورد پیشرفت بیماری و مدیریت درمان بیماری استفاده شود.* ***هدف:*** *مطالعه حاضر به منظور ارزیابی شیوع سرمی آنتی بادی های IgG علیه ویروس کووید-19 در جمعیت شهری شهرستان شهرکرد طراحی و اجرا شد.* ***روش کار:*** *در این مطالعه توصیفی-تحلیلی، تعداد 690 نفر از افراد ساکن در شهرستان شهرکرد که در فاصله مهر تا آذرماه سال 1399 به آزمایشگاه‌های تشخیص پزشکی شهرستان مراجعه کرده بودند، شناسایی و سطح سرمی IgG آنها با روش الایزا اندازه‌گیری شد. برای بررسی رابطه بین متغیرها از آزمون کای اسکوئر و اسپیرمن درنرم افزار SPSS- 20 استفاده شد.* ***یافته ها:*** *از 690 نمونه آزمایش شده، 190 نفر از نظر آنتی بادی IgG علیه کووید-19 مثبت بودند. میزان فراوانی آنتی بادی های مثبت 27.5 درصد (CI 95%: 23.1-30%)، در مردان 26.9 درصد و در زنان 28 درصد بود. بین شیوع سرمی کووید-19 با جنسیت، شغل، وضعیت تاهل و BMI رابطه معنی داری وجود نداشت (P>0.05). شیوع سرمی کووید-19 به طور معناداری در افراد با سابقه تماس با فرد آلوده، افراد دارای علائم کووید-19 در طی پاندمی، افراد با سابقه تشخیص قطعی بر اساس تست PCR و افراد بالای 60 سال بیشتر بود (P<0.05).* ***بحث:*** *بر اساس نتایج، شیوع سرمی آنتی بادی های ضد کووید-19 در جمعیت مورد مطالعه 27.5 درصد و بیشتر از شیوع بیماری بر اساس تست های غربالگری مولکولی بود.* ***نتیجه‌گیری:*** *تعیین میزان شیوع آنتی‌بادی‌های IgG علیه کووید-19 در جامعه می‌تواند برای پیش بینی دقیق تر اپیدمی و مدیریت بیماری استفاده شود.*

واژگان کلیدی: ویروس کرونا، کووید-19، اپیدمیولوژی، آنتی بادی ها، سیستم ایمنی.

1. INTRODUCTION:

Despite advances in the prevention and treatment of diseases, the emergence of viral diseases continues and is considered a serious public health issue. In the past 20 years, we have seen viral epidemics such as SARS-CoV in 2002-2003, H1N1 flu in 2009, and then MERS-CoV in 2012. Recently, in December 2019, an unknown epidemic was reported in Wuhan, China, with an unexplained infection of the lower respiratory tract (Wu *et al*., 2021; Alsamman and Zayed, 2020). The new virus was initially called nCoV-2019. Subsequently, the International Committee on Taxonomy of Viruses (ICTV) named the virus SARS-CoV-2 due to 80% similarity of its nucleotides to SARS's, which is a member of the coronaviridae family. As with the causative agent of SARS this virus belongs to the βCoV2 group and is therefore considered as a positive-stranded RNA virus coated with a helical nucleocapsid (Lupia *et al*., 2020). Approximately 30 types of coronaviruses have been identified in humans, mammals, and birds. So far, it has been established that seven types of viruses have caused infections in humans: alpha and beta. The genomes of these viruses encode four structural proteins, namely, nucleocapsid (N), membrane (M), envelope (E), and spike (S) (Walls *et al*., 2020; Ahmed *et al*., 2020). The human immune system produces two types of antibodies, namely IgM and IgG, against the virus. The presence of IgM antibodies against this virus indicates the acute phase of the disease, and the presence of IgG antibodies, as a stable response against this disease, indicates that immunity against this disease has developed (Bryant *et al*., 2020; Stadlbauer *et al*., 2020; Farnsworth and Anderson; 2020).

The high potential of this virus for human-to-human transmission on the one hand, and international travel, on the other hand, has increased the incidence of the disease in different countries. Besides this, many carriers are asymptomatic, which indicates the need for prevention and screening of patients to control the devastating effects of the disease. Reports suggest that 25-50% of people infected with the virus may never have symptoms, and some may only have mild illnesses (Rodriguez-Morales *et al*., 2020). However, to date, no accurate information has been reported on the number of asymptomatic patients, the rate of improvement in the immune system, or the likelihood of recurrence of COVID-19.

Tests based on the presence of antibodies in the serum of COVID-19 patients can identify people who have been exposed to the virus and help to gain insight into how the disease has spread and even become fatal, and understand the immune system's response rate to the disease and the likelihood of its recurrence appropriately. In addition, these tests are useful for identifying individuals who have exhibited a complete immune response to disease after recovery (Haveri *et al*., 2020; Xu *et al*., 2020; Infantino *et al*., 2020). In these experiments, the presence of antibodies is evaluated. Since the antigens and antibodies produced against the virus are substantially more stable than the virus RNA, they are less sensitive during sample transfer and storage. Therefore false negative tests are comparatively less likely.

This study aimed to determine the seroprevalence of IgG antibodies against COVID-19 in Shahrekord county and to compare the prevalence of the disease based on the serology and molecular tests in the community.

2. MATERIALS AND METHODS:

2.1. Study design and data collection

This descriptive-analytical study was performed cross-sectional between September and November 2020 in indigenous people referred to (public and private) medical diagnostic laboratories in Shahrekord for reasons other than COVID-19. The protocol of the study was approved by the Ethics Committee of Shahrekord University of Medical Sciences (IR.SKUMS.REC.1399.073), and informed consent to participate in the study was obtained from all participants, and the principles of data confidentiality were carefully observed by investigators. Based on the number of positive cases, available reports, and the statistical consultant's opinion, the sample size was considered at least 600 people during the study, and blood samples were taken from 690 patients, and their information was also collected.

Sampling was performed randomly and systematically. To this end, one out of every three who were referred to medical diagnostic laboratories in Shahrekord was randomly selected until the required sample size was achieved.

Complementary data were collected using a checklist of sociodemographic characteristics based on the information accessible through the Sib system of the Ministry’s Vice Chancellor for Health. This information included age, gender, occupation, marital status, history of molecular COVID-19 test, symptoms since the pandemic onset, history of hospitalization due to COVID-19, history of contact with an infected person, weight, and height.

2.2. Detection of SARS-CoV-2 IgG antibodies

Blood samples were transferred to the Virology Laboratory of Shahrekord University of Medical Sciences for serum isolation. The serum of the patients was centrifuged for 15 minutes at 3000 rpm and kept in the freezer at -20 °C until the experiments. This study evaluated the serum level of IgG antibodies against COVID-19 using an ELISA kit (Pishtaz Teb).

To evaluate the level of IgG antibodies in serum samples isolated from patients' blood cells, serum samples, and all materials and reagents were first brought to room temperature. IgG kit controls were ready to use and did not require dilution. However, serum samples were diluted at 1:101 using a sample dilution solution. Two wells for blank, two wells for negative control (containing phosphate buffer solution and 0.05% protective substance and negative human serum for IgG antibody against SARS-CoV-2), and then positive control (containing buffer solution, containing protein as stabilizer and 0.05% protective substance and inactivated human serum, containing IgG antibody against SARS-CoV-2) was poured in duplicate, and other wells were used for samples. One hundred µl of positive control, 100 µl of negative control, and 100 µl of diluted samples were introduced into the corresponding wells of the ELISA kit covered with N antigens (N-coating, one of the most abundant antigens of virus) of SARS-CoV-2. The wells were then covered with a special plate label and left at 37 °C for 30 minutes. Afterward, the contents of the wells were emptied, and the wells were washed five times with a ready-to-use washing solution. Then, 100 µl of ready-to-use conjugated enzyme solution (containing human anti-IgG antibody solution bound to horseradish peroxidase) was added to the wells except for the blank wall. The wells were covered again with a special plate label and left at 37 °C for 30 minutes. Next, the contents of the wells were emptied, and the wells were washed five times with a ready-to-use washing solution. After washing, 100 µl of ready-to-use dye solution (containing tetramethylbenzidine and oxygenated water) was poured into all wells, and the wells were left at room temperature in the dark for 15 minutes. In this step, 100 µl of stopper solution (containing 1

normal hydrochloric acid) was added to each well to stop the enzymatic reactions and turn the blue color into yellow. Finally, the optical absorbance of the wells was read by an ELISA reader using a 450 nm filter up to half an hour after adding the stopper solution, and a 630 nm filter was used as a reference filter.

To calculate the results, the cut-off value was obtained by Equation 1:

Cut off value = Average optical absorbance of negative control + 0.15 (Eq. 01)

Then, the index value was calculated by dividing the sample's optical absorbance by the cut-off value to determine the positive and negative results. According to Equation 1, values higher than 1.1 and those lower than 0.9 negatives are considered positive. Therefore, samples with an index value of 0.9-1.1 were considered suspicious and retested using fresh serum or plasma after some time.

It should be noted that based on the information mentioned in the kit instructions, the sensitivity of the kit for measuring IgG antibodies against SARS-CoV-2 is 94.1%, and its specificity is 98.3%.

2.3. Statistical analysis

Qualitative variables were described using frequency and percentage, and quantitative variables were described using mean and standard deviation. The relationship between variables was assessed using Chi-square and Spearman's correlation tests. The analysis was done by SPSS 23 and significantly defined as $P<0.05$.

3. RESULTS AND DISCUSSION:

3.1. Results

Of the 690 studied individuals, 301 (43.6%) were male. The mean age of participants was 45.3±19.5 years (range; 5 months-92 years). Overall, 190 were positive for COVID-19-specific IgG. The prevalence of positive antibodies in our participants was 27.5% [CI 95%: 23.1-30 (26.9% in men and 28% in women)] (Table 1). Among the participants in the study, PCR test using nasal swabs was reported positive in 110 patients (15.9%) up to the time of sampling. There was no significant relationship between the seroprevalence of COVID-19 and gender, occupation, marital status, and BMI ($P>0.05$). However, the seroprevalence of COVID-19 (positive antibody) was significantly higher in people with a history of contact with an infected person, people with COVID symptoms during the pandemic, people with a history of definitive diagnosis based on PCR, and people over 50 years of age ($P<0.05$) (Table 1).

Of patients with positive antibodies, 23.6% had a history of hospitalization due to COVID-19. The mean antibody titer in patients with a positive antibody with a history of hospitalization was 10.95±6.35, and in patients with a positive antibody without a history of hospitalization, 9.5±6.1 ($P=0.199$).

In individuals with positive antibodies, Spearman's correlation coefficient showed a statistically significant relationship between age and IgG antibody titer, so with increasing age, the amount of antibody titer increased ($r=0.187$, $P<0.01$).

The mean BMI was 26.5±5.17 kg/m² in individuals with positive antibodies and 26.2±4.9 kg/m² in negative-antibody subjects ($P>0.05$).

3.2. Discussion

The outbreak of coronavirus has become a major concern across the world. Studies have shown that the prevalence of the disease has not been accurately reported due to the mild form of the disease, which causes many people with COVID-19 to be unaware of their disease or their molecular test results to be false-negative, necessitating serology-based procedures for a more acceptable estimate of the disease. For example, a report from the Chinese Center for Disease Control and Prevention, including 445,500 people, stated that the disease was mild in 81% of patients, with only 14% having a severe form of the illness and 5% having a critical form; asymptomatic infections have also been reported, indicating the high number of asymptomatic patients and the need for serological tests (Wang *et al*., 2020). In another study on the prevalence of COVID-19 on a cruise ship, in which almost all passengers and crew were screened for the virus, approximately 17% of the participants had a positive report. However, about half of the 619 confirmed cases were asymptomatic at the time of diagnosis (Mizumoto *et al*., 2020). Besides this, a study of the seroprevalence of antibodies in Santa Clara, California, showed that the infection caused by the virus was much wider than the number of cases confirmed using clinical findings and

molecular tests (Bendavid *et al*., 2020). Also, a study (2020) on the serological characteristics of SARS-CoV-2 infection from the time of exposure to the onset of symptoms showed the need for tests based on the evaluation of antibodies against the coronavirus (Lou *et al*., 2020). In this regard, several teams around the world have begun testing population samples for SARS-CoV-2 antibodies, whose initial findings show uncertainty about the exact prevalence of the disease in the current situation (Stadlbauer *et al*., 2020, Haveri *et al*., 2020; Xu *et al*., 2020; Infantino *et al*., 2020).

In the present study, which was conducted to investigate the seroprevalence of IgG antibodies against COVID-19 in the urban population of Shahrekord County, the seroprevalence of COVID-19 was 27.5%, which is higher than the prevalence of the disease based on molecular evaluations (15.9%). In a study (2020) on the seroprevalence of anti-SARS-CoV-2 IgG antibodies in the general Indian population, the serum level of IgG antibodies was determined by ELISA, and the results indicated a low seroprevalence in India so that by mid-May 2020, less than 1% (0.73%) of the population had been exposed to infection. The low prevalence of antibody levels in most regions of India indicates that India is in the first phase of the epidemic, and most of the population is still susceptible to the disease (Murhekar *et al*., 2020). In Iran, only one study, conducted from March to 20 May 2020, examined the prevalence of antibodies against SARS-CoV-2 in 18 cities from 17 provinces using ELISA. The study included 9,181 people, including 5,372 ones from high-risk populations (including front-line physicians and nurses, non-front-line health workers, pharmacy staff, taxi drivers, bank employees, and cashiers in supermarkets and chain stores) and 3,530 individuals from the general population (including those registered in the Iranian electronic health system or health care centers). That study showed a 17.1% and 20% prevalence of SARS-CoV-2 specific antibodies in the general and high-risk populations. According to these results, it can be estimated that the prevalence of SARS-CoV-2 specific antibodies is higher than the number of cases confirmed by PCR tests in the reports. The reason for the difference in the prevalence reported in the study conducted in Iran and that in the present study could be the time of the study, causing more people to be exposed to the virus and the prevalence to increase. Also, in the study conducted in Iran, after estimating population-based prevalence, the cities of Rasht, Qom, Gorgan, and Babol, with seroprevalence of 72.6%, 58.5%, 43.9%, and 22.4%, respectively, had the highest prevalence (Poustchi *et al*., 2021). The difference in prevalence in different areas can be due to reasons such as weather conditions and differences in the concentration and movement of people in public places, as well as the characteristics of mass communication among people.

In the present study, a statistically significant relationship was observed between age and IgG antibody titer, so the amount of antibody titer increased with increasing age. Reports from some countries have suggested the role of age as a risk factor for disease severity (Jiang *et al*., 2020; Hossain *et al*., 2021). Studies have also shown that the rate of inflammation is higher in older people, and with increased inflammation in the body, the rate of systemic response of the immune system increases, and consequently, the level of antibodies in the blood will increase (Hotamisligil *et al*., 2006; Gonzalez-Quintela *et al*., 2008), being, in fact, one of the reasons for the relationship between aging and increased antibody titer in the present study. In addition to age, in the current study, the seroprevalence of COVID-19 was significantly higher in individuals with a history of contact with an infected person, individuals with COVID symptoms during the pandemic, and individuals with a history of definitive diagnosis based on PCR. These results are all in line with the higher risk of the disease and a higher likelihood of immune response in such individuals and confirm the need to follow health protocols and social distancing to reduce its incidence (Hossain *et al*., 2021).

4. CONCLUSIONS:

In the present study, the seroprevalence of IgG antibodies against COVID-19 in the urban population of Shahrekord county was 27.5%, higher than the prevalence of the disease based on molecular screening tests. Therefore, serological tests can be suggested for a more accurate prediction of the epidemic and for better management of the prevention and treatment of the disease.

5. DECLARATIONS

5.1. Study Limitations

Since the study is cross-sectional, the study is limited to a time of evaluation.

5.2. Acknowledgements

We would like to thank the Vice Chancellor for Research and Technology of the University, all

our dear colleagues in different departments, and the participants in the study who assisted in conducting this study.

5.3. Funding source

We want to thank the Vice Chancellor for Research and Technology of the University, all our dear colleagues in different departments, and the participants in the study who assisted in conducting this study.

5.4. Competing Interests

There were no conflicts of interest in conducting this research.

6. HUMAN AND ANIMAL-RELATED STUDIES

6.1. Ethical Approval

The protocol of this research has been approved by the Ethical Committee of Shahrekord University of Medical Sciences (ethics code: IR.SKUMS.REC.1399.073).

7. REFERENCES:

1. Wu, Z., Harrich, D., Li, Z., Hu, D., & Li, D. (2020). The unique features of SARS-CoV-2 transmission: Comparison with SARS-CoV, MERS-CoV and 2009 H1N1 pandemic influenza virus. In Reviews in Medical Virology (Vol. 31, Issue 2). Wiley. https://doi.org/10.1002/rmv.2171

2. Alsamman, A. M., & Zayed, H. (2020). The transcriptomic profiling of SARS-CoV-2 compared to SARS, MERS, EBOV, and H1N1. In M. Schindler (Ed.), PLOS ONE (Vol. 15, Issue 12, p. e0243270). Public Library of Science (PLoS). https://doi.org/10.1371/journal.pone.0243270

3. Lupia, T., Scabini, S., Mornese Pinna, S., Di Perri, G., De Rosa, F. G., & Corcione, S. (2020). 2019 novel coronavirus (2019-nCoV) outbreak: A new challenge. In Journal of Global Antimicrobial Resistance (Vol. 21, pp. 22–27). Elsevier BV. https://doi.org/10.1016/j.jgar.2020.02.021

4. Walls, A. C., Park, Y. -J., Tortorici, M. A., Wall, A., McGuire, A. T., & Veesler, D. (2020). Structure, Function, and Antigenicity of the SARS-CoV-2 Spike Glycoprotein. In Cell (Vol. 181, Issue 2, pp. 281-292.e6). Elsevier BV. https://doi.org/10.1016/j.cell.2020.02.058

5. Ahmed, S. F., Quadeer, A. A., & McKay, M. R. (2020). Preliminary Identification of Potential Vaccine Targets for the COVID-19 Coronavirus (SARS-CoV-2) Based on SARS-CoV Immunological Studies. In Viruses (Vol. 12, Issue 3, p. 254). MDPI AG. https://doi.org/10.3390/v12030254

6. Bryant, J. E., Azman, A. S., Ferrari, M. J., Arnold, B. F., Boni, M. F., Boum, Y., Hayford, K., Luquero, F. J., Mina, M. J., Rodriguez-Barraquer, I., Wu, J. T., Wade, D., Vernet, G., & Leung, D. T. (2020). Serology for SARS-CoV-2: Apprehensions, opportunities, and the path forward. In Science Immunology (Vol. 5, Issue 47). American Association for the Advancement of Science (AAAS). https://doi.org/10.1126/sciimmunol.abc6347

7. Stadlbauer, D., Amanat, F., Chromikova, V., Jiang, K., Strohmeier, S., Arunkumar, G. A., Tan, J., Bhavsar, D., Capuano, C., Kirkpatrick, E., Meade, P., Brito, R. N., Teo, C., McMahon, M., Simon, V., & Krammer, F. (2020). SARS-CoV-2 Seroconversion in Humans: A Detailed Protocol for a Serological Assay, Antigen Production, and Test Setup. In Current Protocols in Microbiology (Vol. 57, Issue 1). Wiley. https://doi.org/10.1002/cpmc.100.

8. Farnsworth, C. W., & Anderson, N. W. (2020). SARS-CoV-2 Serology: Much Hype, Little Data. In Clinical Chemistry (Vol. 66, Issue 7, pp. 875–877). Oxford University Press (OUP). https://doi.org/10.1093/clinchem/hvaa107

9. Rodriguez-Morales, A. J., Cardona-Ospina, J. A., Gutiérrez-Ocampo, E.,

Villamizar-Peña, R., Holguin-Rivera, Y., Escalera-Antezana, J. P., Alvarado-Arnez, L. E., Bonilla-Aldana, D. K., Franco-Paredes, C., Henao-Martinez, A. F., Paniz-Mondolfi, A., Lagos-Grisales, G. J., Ramírez-Vallejo, E., Suárez, J. A., Zambrano, L. I., Villamil-Gómez, W. E., Balbin-Ramon, G. J., Rabaan, A. A., Harapan, H., … Sah, R. (2020). Clinical, laboratory and imaging features of COVID-19: A systematic review and meta-analysis. In Travel Medicine and Infectious Disease (Vol. 34, p. 101623). Elsevier BV. https://doi.org/10.1016/j.tmaid.2020.101623.

10. Haveri, A., Smura, T., Kuivanen, S., Österlund, P., Hepojoki, J., Ikonen, N., Pitkäpaasi, M., Blomqvist, S., Rönkkö, E., Kantele, A., Strandin, T., Kallio-Kokko, H., Mannonen, L., Lappalainen, M., Broas, M., Jiang, M., Siira, L., Salminen, M., Puumalainen, T., … Savolainen-Kopra, C. (2020). Serological and molecular findings during SARS-CoV-2 infection: the first case study in Finland, January to February 2020. In Eurosurveillance (Vol. 25, Issue 11). European Centre for Disease Control and Prevention (ECDC). https://doi.org/10.2807/1560-7917.es.2020.25.11.2000266.

11. Xu, Y., Xiao, M., Liu, X., Xu, S., Du, T., Xu, J., Yang, Q., Xu, Y., Han, Y., Li, T., Zhu, H., & Wang, M. (2020). Significance of serology testing to assist timely diagnosis of SARS-CoV-2 infections: implication from a family cluster. In Emerging Microbes Infections (Vol. 9, Issue 1, pp. 924–927). Informa UK Limited. https://doi.org/10.1080/22221751.2020.1752610.

12. Infantino, M., Damiani, A., Gobbi, F.L., Grossi, V., Lari, B., Macchia, D., *et al*., (2020). Serological assays for SARS-CoV-2 infectious disease: benefits, limitations, and perspectives. In Israel Medical Association (Vol. 22, Issue 4, pp. 203-210).

13. Wang, D., Hu, B., Hu, C., Zhu, F., Liu, X., Zhang, J., Wang, B., Xiang, H., Cheng, Z., Xiong, Y., Zhao, Y., Li, Y., Wang, X., & Peng, Z. (2020). Clinical Characteristics of 138 Hospitalized Patients With 2019 Novel Coronavirus–Infected Pneumonia in Wuhan, China. In JAMA (Vol. 323, Issue 11, p. 1061). American Medical Association (AMA). https://doi.org/10.1001/jama.2020.1585.

14. Mizumoto, K., Kagaya, K., Zarebski, A., & Chowell, G. (2020). Estimating the asymptomatic proportion of coronavirus disease 2019 (COVID-19) cases on board the Diamond Princess cruise ship, Yokohama, Japan, 2020. In Eurosurveillance (Vol. 25, Issue 10). European Centre for Disease Control and Prevention (ECDC). https://doi.org/10.2807/1560-7917.es.2020.25.10.2000180.

15. Bendavid, E., Mulaney, B., Sood, N., Shah, S., Bromley-Dulfano, R., Lai, C., Weissberg, Z., Saavedra-Walker, R., Tedrow, J., Bogan, A., Kupiec, T., Eichner, D., Gupta, R., Ioannidis, J. P. A., & Bhattacharya, J. (2021). COVID-19 antibody seroprevalence in Santa Clara County, California. In International Journal of Epidemiology (Vol. 50, Issue 2, pp. 410–419). Oxford University Press (OUP). https://doi.org/10.1093/ije/dyab010.

16. Lou, B., Li, T.-D., Zheng, S.-F., Su, Y.-Y., Li, Z.-Y., Liu, W., Yu, F., Ge, S.-X., Zou, Q.-D., Yuan, Q., Lin, S., Hong, C.-M., Yao, X.-Y., Zhang, X.-J., Wu, D.-H., Zhou, G.-L., Hou, W.-H., Li, T.-T., Zhang, Y.-L., … Chen, Y. (2020). Serology characteristics of SARS-CoV-2 infection after exposure and post-symptom onset. In European Respiratory Journal (Vol. 56, Issue 2, p. 2000763). European Respiratory Society (ERS). https://doi.org/10.1183/13993003.00763-2020.

17. Murhekar, M., Bhatnagar, T., Selvaraju, S., Rade, K., Saravanakumar, V., Vivian Thangaraj, J., Kumar, M., Shah, N., Sabarinathan, R., Turuk, A., Anand, P., Asthana, S., Balachandar, R., Bangar, S., Bansal, A., Bhat, J., Chakraborty, D., Rangaraju, C., Chopra, V., … Bhargava, B. (2020). Prevalence of SARS-CoV-2 infection in India: Findings from the national serosurvey, May-June 2020. In Indian Journal of Medical Research (Vol. 152, Issue 1, p. 48). Medknow. https://doi.org/10.4103/ijmr.ijmr_3290_20.

18. Poustchi, H., Darvishian, M., Mohammadi, Z., Shayanrad, A., Delavari, A., Bahadorimonfared, A., Eslami, S., Javanmard, S. H., Shakiba, E., Somi, M. H., Emami, A., Saki, N., Hormati, A., Ansari-Moghaddam, A., Saeedi, M., Ghasemi-Kebria, F., Mohebbi, I., Mansour-Ghanaei, F., Karami, M., … Malekzadeh, R. (2021). SARS-CoV-2 antibody seroprevalence in the general population and high-risk occupational groups across 18 cities in Iran: a population-based cross-sectional study. In The Lancet Infectious Diseases (Vol. 21, Issue 4, pp. 473–481). Elsevier BV. https://doi.org/10.1016/s1473-3099(20)30858-6.

19. Jiang, F., Deng, L., Zhang, L., Cai, Y., Cheung, C. W., & Xia, Z. (2020). Review of the Clinical Characteristics of Coronavirus Disease 2019 (COVID-19). In Journal of General Internal Medicine (Vol. 35, Issue 5, pp. 1545–1549). Springer Science and Business Media LLC. https://doi.org/10.1007/s11606-020-05762-w.

20. Hossain, A., Nasrullah, S. M., Tasnim, Z., Hasan, Md. K., & Hasan, Md. M. (2021). Seroprevalence of SARS-CoV-2 IgG antibodies among health care workers prior to vaccine administration in Europe, the USA and East Asia: A systematic review and meta-analysis. In EClinicalMedicine (Vol. 33, p. 100770). Elsevier BV. https://doi.org/10.1016/j.eclinm.2021.100770.

21. Hotamisligil, G. S. (2006). Inflammation and metabolic disorders. In Nature (Vol. 444, Issue 7121, pp. 860–867). Springer Science and Business Media LLC. https://doi.org/10.1038/nature05485.

22. Gonzalez-Quintela, A., Alende, R., Gude, F., Campos, J., Rey, J., Meijide, L. M., Fernandez-Merino, C., & Vidal, C. (2007). Serum levels of immunoglobulins (IgG, IgA, IgM) in a general adult population and their relationship with alcohol consumption, smoking and common metabolic abnormalities. In Clinical and Experimental Immunology (Vol. 151, Issue 1, pp. 42–50). Oxford University Press (OUP). https://doi.org/10.1111/j.1365-2249.2007.03545.x.

Table 1. *Demographic characteristics of study participants*

Variables	Total number	Number of positive serology cases (%)	OR (95% CI) based on the univariable model	Significance level (P value)
Age groups				
Under 20 yr	45	13(28.9)	0.637 (0.306-1.328)	0.025
20-29 yr	93	18(19.4)	0.376 (0.202-0.702)	
30-39 yr	95	27(28.4)	0.623 (0.353-1.099)	
40-49 yr	106	29(37.9)	0.591 (0.340-1.027)	
50-59 yr	87	33(37.9)	0.959 (0.549-1.674)	
Over 60 yr	131	51(38.9)	1.0 [Reference]	
Gender				
Male	301	81(26.9)	0.946 (0.675-1.325)	0.764
Female	389	109(28)	1.0 [Reference]	
Marital status				
Single	64	13(20.3)	0.583 (0.198-1.71)	0.223
Married	344	114(33.1)	1.133 (0.453-2.832)	
Widow/widower-divorced	49	17(34.7)	1.214 (0.418-3.524)	
Under 15 yr	23	7(30.4)	1.0 [Reference]	
Occupation				
Housewife	176	53(30.1)	1.077 (0.323-3.589)	0.552
Student	51	11(21.6)	0.688 (0.18-2.62)	
Laborer	24	10(41.7)	1.786 (0.434-7.353)	
Civil servant	113	40(35.4)	1.37 (0.404-4.649)	
Jobless	36	10(27.8)	0.962 (0.244-3.783)	
Self-employed	68	24(35.3)	1.364 (0.386-4.816)	
Under 6 yr	14	4(28/6)	1.0 [Reference]	
History of definitive diagnosis by PCR				
Yes	110	71(64.5)	5.882 (3.728-9.279)	<0.001
No	385	91(23.6)	1.0 [Reference]	
Having symptoms during the pandemic				
Yes	169	95(56.2)	4.963 (3.308-7.445)	<0.01
No	326	67(20.6)	1.0 [Reference]	
History of contact with an infected person				
Yes	99	61(61.6)	4.736 (2.977-7.533)	<0.001
No	395	100(25.3)	1.0 [Reference]	
Working outside the home				
Yes	205	74(36.1)	1.441 (0.979-2.122)	0.064
No	277	78(28.2)	1.0 [Reference]	

PERIÓDICO TCHÊ QUÍMICA
ARTIGO ORIGINAL

ESTUDOS *IN SILICO* DE DITERPENOS EXTRAÍDOS DA *Paubrasilia echinata* Lam. E DERIVADOS FRENTE A INTEGRASE E TRANSCRIPTASE REVERSA DO HIV-1

IN SILICO STUDIES OF DITERPENES EXTRACTED FROM *Paubrasilia echinata* Lam. AND DERIVATIVES AGAINST HIV-1 INTEGRASE AND REVERSE TRANSCRIPTASE

SILVA, Fábia Martins[1]; RAMOS, Clécio Sousa[1]; SCOTTI, Luciana[2,3]; MONTEIRO, Alex France Messias[1,2*]

[1]Programa de Pós-Graduação em Química, Departamento de Química, Universidade Federal Rural de Pernambuco. Brasil.

[2]Programa de Pós-Graduação em Produtos Naturais e Sintéticos Bioativos, Centro de Ciências da Saúde, Universidade Federal da Paraíba. Brasil.

[3]Gestão de Ensino e Pesquisa, Hospital Universitário, Universidade Federal da Paraíba. Brasil.

*Autor correspondente
e-mail: *alexfrancem@gmail.com*

Received 22 June 2022; received in revised form 23 October 2022; accepted 30 October 2022

RESUMO

Introdução: O HIV é um retrovírus cuja multiplicação viral está associada a três enzimas. A transcriptase reversa, responsável por sintetizar o DNA vital com base em seu RNA; a integrase, responsável por integrar o DNA viral ao DNA humano; e uma protease responsável pela clivagem do código genético em unidade menores e funcional. Muitos grupos de pesquisas pelo mundo estão motivados na proposta de novos bioativos contra o HIV. **Objetivos:** Propor diterpenos naturais ou produtos sintéticos da espécie de planta Pau-Brasil frente ao vírus HIV por meio de técnicas *in silico*. **Métodos:** Foram utilizados diterpenos encontrados no extrato etanólico do Pau-Brasil (*Paubrasilia echinata* Lam.), assim como alguns produtos dos mesmos que foram avaliados por meios computacionais. O trabalho foi desenvolvido através de uma triagem hibrida (*ligand based e structure based*) para uma possível atividade biológica desses fitoconstituintes frente às enzimas principais da multiplicação do HIV-1. **Resultados:** Os ensaios computacionais apontaram que os compostos ALX04 e ALX07 apresentaram possível atividade frente as proteínas HIV-integrase e transcriptase reversa, respectivamente. Nenhum composto foi ativo simultaneamente frente as duas enzimas (HIV-integrase e transcriptase reversa), e todos os demais compostos demonstraram-se inativos. **Discussão:** Foram utilizados os diterpenos encontrados no extrato etanólico do Pau-Brasil (*Paubrasilia echinata* Lam.), assim como alguns derivados, onde foram avaliados através dos métodos computacionais. O trabalho foi desenvolvido por meio de uma seleção híbrida (e baseada e estruturada) realizada para apontar uma atividade viável observável. aos modelos de predição testadas. **Conclusões:** Os ensaios computacionais apontaram os diterpenos ALX04 e ALX07 apresentaram promissora atividade retroviral.

Palavras-chave: *Docking molecular, HIV-1, simulação in silico, Pau-Brasil,* toxidade*.*

ABSTRACT

Introduction: HIV, whose viral multiplication is associated with three enzymes. Reverse transcriptase is responsible for synthesizing vital DNA based on its RNA; integrase is responsible for integrating viral DNA into human DNA; and protease is responsible for cleaving the genetic code into smaller, functional units. Many research groups around the world are motivated by the proposal of a new bioactive against HIV. **Objectives:** To propose natural diterpenes or synthetic products from the Pau-Brasil plant species against HIV through *in silico* techniques. **Methods:** Diterpenes found in the ethanolic extract of Pau-Brasil (*Paubrasilia echinata* Lam.) were used, as well as some of their products that were known by computational means. The work was developed through a hybrid screening (ligand-based and structure-based) for a possible biological activity of these phytoconstituents against the main enzymes of HIV-1 multiplication. **Results:** Computational assays showed that the compounds ALX04 and ALX07 showed possible activity against HIV-integrase and reverse transcriptase proteins, respectively. No compound was simultaneously active against the two enzymes (HIV-integrase and reverse transcriptase), and all other compounds proved inactive. **Discussion**: Diterpenes found in the ethanolic extract of Pau-Brasil (*Paubrasilia echinata* Lam.) were used, and some results were obtained through

DOI: 10.52571/PTQ.v19.n42.2022.05_MESSIAS_pgs_46_59.pdf

computational methods. The work was developed to achieve a viable observable activity to the tested prediction models. **Conclusions:** Computational assays showed that the diterpenes ALX04 and ALX07 had promising assays of retroviral activity.

Keywords: *Molecular docking, HIV-1, in silico simulation, Pau-Brasil, toxicity*.

1. INTRODUÇÃO

1.1 Vírus de imunodeficiência humana

A AIDS (*Acquired Immunodeficiency Syndrome*) é considerada um problema de saúde pública, que acomete pessoas do mundo todo, independentemente de classe social, gênero, raça e outros. Está associada a prática sexual e comportamentos de risco como o compartilhamento de seringas para usuários de drogas injetáveis, contato direto com sangue contaminado e transmissão vertical de mãe para filho. (Machado-Zaldívar *et al*., 2021; van den Broek, 2021)

A grande maioria dos casos de infecção dão-se pela relação sexual sem o uso do preservativo, sendo o mais eficaz método profilático da doença recomendado pelos órgãos de saúde. A conscientização de hábitos sexualmente seguros e que propiciam menor exposição ao vírus do HIV (*Human Immunodeficiency Virus*) é realizada através de campanhas educativas destinadas a todas as idades. (Presanis *et al*., 2021; Stone *et al*., 2021)

Segundo a WHO (*World Health Organization),* a faixa de vulnerabilidade está entre 15 a 49 anos, e milhões de pessoas morrem anualmente vítimas de complicações decorrentes a infecção pelo HIV. É verídica a informação de que a AIDS propriamente dita não é capaz de provocar diretamente a morte do infectado, porém, ocorre a diminuição das células imunológicas devido a infecção pelos retrovírus, assim diminui gradativamente a capacidade de defesa dos anticorpos contra os microrganismos invasores causada pela AIDS. Há relatos que com todos esses problemas acarretados pelo vírus, o indivíduo pode vir a óbito decorrentes de ações infecciosas secundárias como a pneumonia, tuberculose, meningite e outras doenças. (Melo *et al*., 2021)

De acordo com a WHO, 2021 muitas pessoas vivem com o HIV, segundo dados, a população infectada em 2021 foi cerca de 38,4 milhões, dos quais 19,7 milhões foram mulheres. Segundo o boletim epidemiológico, houveram 1,5 milhões de novos casos de infecção no mundo. Em crianças abaixo de 15 anos de idade corresponde a cerca de 1,7 milhões do total, com 160mil novos casos desde o ano passado, conforme mostrado na Figura 1. (Giroir, 2020; Jiang *et al*., 2020)

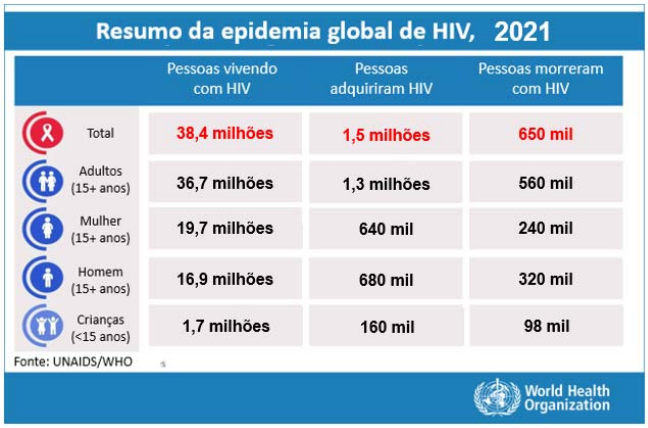

Figura 1. *Dados estatísticos do HIV - UNAIDS/WHO.*

1.2. Quimioinformática

No desenvolvimento de novos fármacos é possível contar com o auxílio da quimioinformática, com o planejamento racional de novos bioativos. Através das ferramentas *in silico* os cientistas são capazes de predizer uma determinada atividade biológica, analisando vários parâmetros estruturais, com base em moléculas cujas atividades já foram testadas. (Brian, 2021; Monica *et al*., 2021)

Estudos de QSAR (*Quantitative Structure-Activity Relationship*) e outros métodos computacionais reduzem custos vinculados as pesquisas, e preveem possíveis resultados satisfatórios, contudo, os métodos *in silico* possuem suas margens de erros inerentes dos processos, mas estes podem ser reduzidos através de cuidadosas validações que vão se aprimorando ao longo da aplicabilidade das ferramentas de química computacional. (Bhole *et al*., 2021; Ding *et al*., 2021)

1.3. *Paubrasilia echinata* Lam.

O gênero *Caesalpinia* pertence à família *Fabaceae*. No mesmo encontra-se aproximadamente 100 espécies de plantas que estão distribuídas geograficamente em todo o mundo em regiões subtropicais e tropicais (Lichtenberg *et al*., 2022; Mescia *et al*., 2022; Xavier *et al*., 2022).

O Pau-Brasil, assim popularmente

conhecido (*Paubrasilia echinata* Lam.), foi a primeira espécie de árvore brasileira encontrada historicamente pelos portugueses e comercializadas por causa que nela encontram-se corantes que eram usados para a fabricação de tintura para roupas (Carvalho *et al*., n.d.; Correia Soeiro *et al*., 2022).

O presente trabalho teve como objetivo propor a utilização de diterpenos naturais ou produtos sintéticos da espécie de planta Pau-Brasil, frente ao vírus HIV, por meio de técnicas *in silico*, visando impedir a replicação do vírus.

2. MATERIÁIS E MÉTODOS

2.1 Materiais

Todos as análises computacionais foram realizadas no sistema operacional Microsoft Windows 8.1, assim como programa de editor de texto Microsoft Word e criador de planilhas e tratamentos estatísticos o programa Microsoft Excel ambos do pacote Microsoft Office 365.

Para obtenção das estruturas 2D das moléculas estudadas foi utilizado o programa MarvinSketch v22.9 da Chemaxon, e para otimização e obtenção das estruturas 3D foi o programa HyperChem ™ v7.5.

Cinco moléculas (Tabela 1) foram usadas como controles, estas moléculas correspondem a estruturas químicas de fármacos que são comumente usadas no tratamento anti-HIV:

Tabela 1. *Controles usados na pesquisa.*

ID	Inibição	Nome	Sigla	%Abs
C01	IN	Raltegravir	RAL	57.24
C02	IN	Dolutegravir	DTG	74.78
C03	TR	Lamivudina	3TC	69.86
C04	TR	Zidovudina	AZT	72.83
C05	TR	Efavirenz	EFZ	95.78

Os compostos ALX01-ALX07 (Tabela 2) são diterpenos isolados a partir do extrato etanólico dos caules da *Paubrasilia echinata* e derivados inspirados pela pesquisa publicada em 2011 (Cota *et al*., 2011), conforme mostradas na Tabela 2.

Tabela 2. *Relação dos compostos diterpenos testados.*

ID	Structure
ALX01	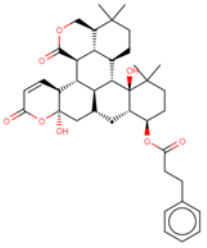
ALX02	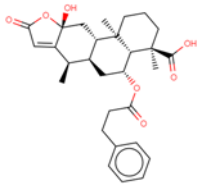
ALX03	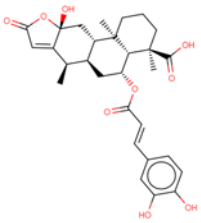
ALX04	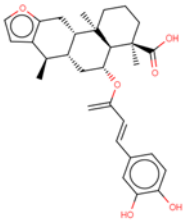
ALX05	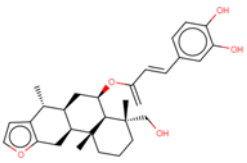
ALX06	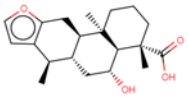
ALX07	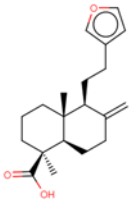

Para a construção dos modelos de predição foi usado o software KNIME Analytics Platform 3.7, utilizando o classificador *RandomForest* e o preditor *Weka* 3.7 para elaborar um workflow baseada em uma floresta de árvores de decisão randômica para as predições realizadas. (Leite *et al*., 2021; Silverio, 2021).

Os descritores moleculares foram obtidos através do programa Dragon 5, com 1310 descritores moleculares calculados.

Para o cálculo da área de superfície topológica polar (TPSA), violações da regra de Lipinski foi utilizado o programa gratuito Drug Likeness Tool - DruLiTo para windows [http://www.niper.gov.in/pi_dev_tools/DruLiToWeb/DruLiTo_index.html] (Umar et al., 2021)

Para os riscos de citotoxidade as estruturas foram importadas para o programa gratuito OSIRIS DataWarrior v5.5.0, avaliando quatro parâmetros toxicológicos: carcinogênese (CAR), mutagênese (MUT), irritabilidade do tecido (IRR) e efeito tóxico no sistema reprodutor (ESR).

Os metabólitos hepáticos foram obtidos importando os códigos *smiles* das moléculas testadas para o servidor online GLORY (*Generator of the Structures of Likely Cytochrome P450 Metabolites Based on Predicted Sites of Metabolism*) (de Bruyn Kops *et al*., 2019; Stork *et al*., 2019), assim, obtendo os metabólitos mais abundantes no processo.

Para o estudo do acoplamento molecular as moléculas foram importadas as moléculas estudadas aprovadas nas etapas anteriores, estas moléculas interagiram no sitio ativo dos receptores PDB ID 1QS4 integrase (IN) e PDB ID 2RF2 transcriptase reversa (TR).

Para esse estudo de ancoragem foi usado o programa Molegro Virtual Docker 6.0, levando em consideração o algoritmo *MolDock Score* para avaliação da eficiência de interação.

2.3 Métodos

Foi realizada inicialmente uma triagem virtual híbrida que consiste em uma abordagem baseada no ligante juntamente com a proteica de forma combinada. Assim é possível obter as moléculas com melhores perfis farmacológicos *in silico*, analisando a biodisponibilidade, a absorção, os riscos de citotoxidade, a interação ligante-receptor a estabilidade no sítio ativo e a predição da atividade biológica.

A triagem virtual consiste na classificação de substâncias com base nas características que melhor explicam a atividade biológica a ser observada, estas características podem estar vinculada a um grupo funcional da molécula ou a uma ligação de hidrogênio que possa ser útil e servir para nortear análogos com atividade promissora a partir das melhorias realizadas nessas características.

Esta abordagem é conhecida como planejamento racional de fármacos, muito usada em pesquisas na área de química de fármacos, contribuindo ainda, para a diminuição do tempo de bancada, desperdício de solventes na síntese de novos bioativos. (Tibúrcio, 2022)

Tanto os compostos testados quantos os controles foram desenhados para obtenção da estrutura 2D, em seguida foram importados para o Hyper para obtenção da sua estrutura 3D otimizada. A otimização das suas estruturas químicas, foram realizadas através do método da mecânica molecular (MM+) e semiempírico (AM1) para obtenção de suas estruturas químicas tridimensionais. (Moura, 2021)

As moléculas para a construção dos modelos de predição foram extraídas do banco de dados de estruturas químicas ChEMBL Database utilizando a palavra chave "*Human Immunodeficiency Virus*", obtendo os conjuntos de moléculas CHEMBL3471 para integrase e CHEMBL247 para transcriptase reversa do HIV-1.

A acuragem das planilhas obtidas conforme mencionado acima, foi feita removendo-se todas as moléculas repetidas, pelo critério de moléculas com massa molecular superior a 800 g/mol, células vazias, conversão das atividades (IC_{50}) para molar, remoção de solventes, remoção de sais e estruturas com erros de valência.

2.3.1 Modelos de predição – atividade biológica, permeabilidade e absorção intestinal

Foram desenvolvidos cinco modelos, um para predizer a possível atividade biológica frente a enzima protease, um frente a integrase, um frente a transcriptase reversa, um para a absorção intestinal (HIA) e outro para a permeabilidade no intestino (CACO-2). (Bencheikh *et al*., 2022; Forrestall *et al*., 2021)

Esses modelos geraram dados para a discussão da sua capacidade preditiva, além da validação interna cruzada, foram calculados os coeficientes de correlação de Matthews (MCC) para avaliar a qualidade de todos os modelos. (Albertini, 2022; Monteiro, 2021)

2.3.2 Taxa de absorção oral, riscos de citotoxidade e violações a regra de Lipinski

A taxa de absorção oral (%Abs) foi calculada com base na área de superfície topológica polar de cada uma das estruturas avaliadas, utilizando a Equação 1 (Ahsan *et al*., 2016; Gonzalez *et al*., 2018; Tuncbilek *et al*., 2018):

$$\%Abs = 109 - (0.345 \times TPSA) \quad \text{(Eq.1)}$$

Ao utilizar a taxa de absorção como parâmetro de exclusão na triagem virtual, apenas são considerados as moléculas que apresentam %Abs igual ou superior a menor taxa dentre os fármacos usados como controle.

Avaliando os riscos de toxidade foram considerados as estruturas sem riscos em nenhum dos quatro parâmetros toxicológicos estudados (CAR, MUT, IRR, ESR). (Sánchez-Suárez *et al*., 2022; Sander *et al*., 2015).

2.3.3 Predição dos metabólitos hepáticos

Após a obtenção dos metabólitos hepáticos, essas estruturas tiveram seus descritores moleculares calculados, e foram analisados os riscos de toxidades dos metabólitos de alto *score*, qualquer molécula ALX01-ALX09 que apresentasse metabólitos com score acima de 50%, e com alto risco de toxidade em algum parâmetro foram desconsiderados das análises posteriores, ao longo o desenvolvimento computacional desse estudo.

2.3.4 Simulação de docking molecular

As moléculas foram submetidas ao Molegro para obtenção das suas energias de interação do complexo ligante-receptor na ancoragem molecular, para cada molécula que foi aprovada ao longo da triagem até esta etapa, frente a integrase e a transcriptase reversa do HIV-1.

Além do *docking,* foi realizado o *redocking* com o ligante complexado junto a proteína com as mesmas condições computacionais que o *docking* original, fazendo com que seja possível a estimativa do RMSD (*Root Mean Square Deviation*), que é o valor do desvio entre os mesmos átomos do ligante complexado junto a proteína e o mesmo ligante importado, com ele é possível validar o protocolo usado para o acoplamento, quanto mais baixo o RMSD melhor a precisão do encaixe molecular realizado, comumente adotados valores menores que 2Å (Santos, 2021).

3. RESULTADOS E DISCUSSÃO

3.1 Resultados

Os compostos ALX01 a ALX07 foram submetidos a um modelo de predição de atividade biológica frente a proteína integrase do HIV-1, conforme os dados da Tabela 3.

Tabela 3. *Resultados da predição da atividade inibitória frente a IN.*

ID	Domínio	ATV	%ATV
ALX01	Não confiável	Inativo	46.42
ALX02	Confiável	Inativo	33.35
ALX03	Confiável	Inativo	46.91
ALX04	Confiável	Ativo	52.42
ALX05	Confiável	Inativo	46.83
ALX06	Confiável	Inativo	32.82
ALX07	Confiável	Inativo	42.15

ATV = Predição de atividade; %ATV = Probabilidade de possível atividade.

Também foram avaliadas as possíveis atividades frente a enzima transcriptase reversa, conforme mostrada na Tabela 4 abaixo:

Tabela 4. *Resultados da predição da atividade inibitória frente a TR.*

ID	Domínio	ATV	%ATV
ALX01	Não confiável	Inativo	15.50
ALX02	Confiável	Inativo	23.00
ALX03	Confiável	Inativo	20.00
ALX04	Confiável	Inativo	37.00
ALX05	Confiável	Inativo	40.50
ALX06	Confiável	Inativo	43.00
ALX07	Confiável	Ativo	55.00

Foram calculados os dados importantes para a avaliação da confiabilidade do modelo de predição de atividade anti-HIV, esses dados estão discriminados na Tabela 5:

Tabela 5. *Dados estatísticos dos modelos criados*.

	IN		TR	
	Teste	**Cross**	**Teste**	**Cross**
SENS	0.83	0.80	0.87	0.86
ESPEC	0.86	0.81	0.89	0.85
MCC	0.69	0.62	0.76	0.71
Acurácia	0.84	0.81	0.88	0.85
Curva ROC	91.97	87.64	96.71	93.99

Teste = grupo de teste do modelo de predição; Cross = grupo de validação cruzada.

Após a atividade predita, também foram obtidas as probabilidades da permeabilidade intestinal (CACO-2) e a absorção intestinal (HIA), através de modelos de predição no KNIME, com parâmetros semelhantes aos das predições das atividades. Os dados podem ser vistos na Tabela 6.

Tabela 6. *Resultados dos modelos de CACO-2 e HIA.*

CACO-2			
ID	**Domínio**	**ATV**	**%ATV**
ALX04	Confiável	Permeável	80.00
ALX07			93.00
HIA			
ALX04	Confiável	Absorvível	83.50
ALX07			94.00

Os dados estatísticos, com relação a confiabilidade dos modelos gerados são apresentados na Tabela 7.

Tabela 7. *Dados estatísticos comparativos dos modelos de CACO-2 e HIA.*

CACO-2		
	Teste	**Cross**
SENS	0.97	0.97
ESP	0.68	0.56
MCC	0.67	0.61
Acurácia	0.83	0.88
Curva ROC	87.27	87.22
HIA		
SENS	0.90	0.96
ESP	0.65	0.70
MCC	0.57	0.50
Acurácia	0.90	0.85
Curva ROC	89.06	90.94

SENS = sensibilidade; ESP = especificidade e MCC = coeficiente de correlação de Matthews.

Após as predições foram obtidos os dados computacionais referentes aos parâmetros toxicológicos, conforme Tabela 8:

Tabela 8. *Resultados da predição dos riscos de toxidade.*

ID	**MUT**	**CAR**	**ESR**	**IRR**	**TOX**
ALX04	Não	Não	Não	Não	Não
ALX07	Não	Baixo	Não	Não	Sim

MUT = Mutagenicidade; CAR = carcinogenicidade; ESR = efeito tóxico no sistema reprodutor; IRR = irritabilidade do tecido e TOX = toxidade total.

Já os dados da taxa de absorção por via oral (%Abs) e violações a regra de Lipinski (LIP) são mostrados na Tabela 9.

Tabela 9. *Resultados da taxa de absorção oral e violações a regra de Lipinski.*

ID	**%Abs**	**LIP**
ALX04	74.46	1
ALX07	91.60	0

Tomando como base apenas as estruturas de cada molécula testada (*ligand based*), é pertinente apresentar os dados *structure based*, iniciando pela simulação de *docking* molecular, as

energias de interação ligante-receptor podem ser vistas na Tabela 10 a seguir:

Tabela 10. *Dados do docking molecular para IN e TR.*

Composto	$ENERGIA_{IN}$	$ENERGIA_{TR}$
	kcal/mol	
ALX04	-99.65	-
Dolutegravir	-66.85	-
$Ligante_{IN}$	-76.33	-
Raltegravir	-50.21	-
ALX07	-	-107.98
Efavirenz	-	-131.20
Lamivudina	-	-84.23
$Ligante_{TR}$	-	-145.28
Zidovudina	-	-100.98
RMSD	**0.16**	**0.41**

Iniciando a triagem com base na estrutura do receptor, conforme pode ser visto na Tabela 10, os dois diterpenos testados apresentaram afinidades consideráveis com os receptores testados, o composto ALX04 apresentou $Energia_{IN}$ = -99.65 kcal/mol, uma energia inferior ao ligante complexado junto a proteína escolhida.

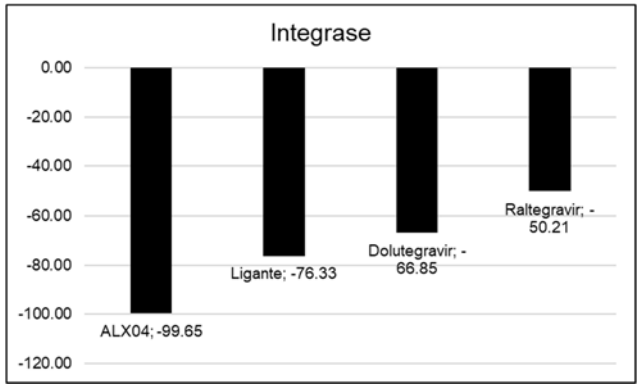

Figura 2. *Gráfico das energias ligante-receptor da IN.*

Na Figura 2, o diterpeno ALX04 apresentou energia mais baixa, não apenas com o ligante, mas também aos controles positivos considerados dolutegravir (-66.85 kcal/mol) e raltegravir (-50.21 kcal/mol).

Já para TR os resultados também foram promissores, onde o composto ALX07 apresentou energia de interação ligante-receptor $Energia_{TR}$ de -107.98 kcal/mol, valor menor que os controles zidovudina (-100.98 kcal/mol) e lamivudina (-84.23 kcal/mol), conforme a Figura 3.

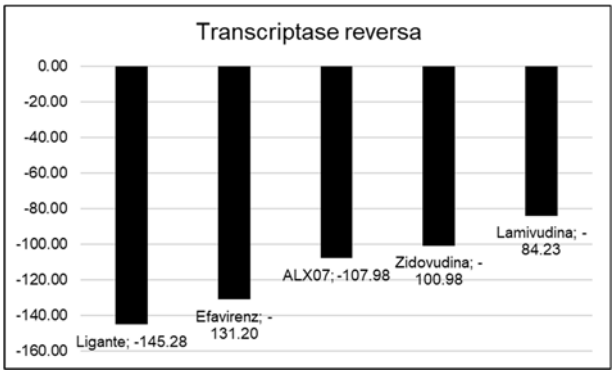

Figura 3. *Gráfico das energias ligante-receptor da TR.*

Na Tabela 11 são mostradas as interações encontradas no estudo de docking molecular dos dois diterpenos estudados:

Tabela 11. Relação das interações com os resíduos de aminoácidos de IN e TR.

	TR			
	H	**Estérica**		
Ligante		2Lys101	His235	Leu234
ALX07	Lys103 Pro236	Leu100 Val179 2Lys101	Tyr318 Tyr188 2Val106	His235 Lys103 Pro236
Efavirez	2Lys101	His235 Gly190	Val106	Val179
Lamivudina	Lys101 Pro236	Tyr188	Lys101	2Tyr181
Zidovudina	Val179 Lys101 Lys103	2Tyr188 His235	Tyr181 Pro236	2Lys101
	IN			
Ligante	Lys159 2Thr66 Asn155 2Lys156 2Glu152	2Glu152	Lys159	
ALX04	Thr66 Cys65 Glu92 His67 Asp64 Asp116	2Asn155 4Glu152 His67	Lys156 2Asp64 Cys65	Thr66 Ile151 Gln148
Raltegravir	2Lys156 2Asn155 Thr66	2Glu152 Asn155	Asp64 Ile151	
Dolutegravir	Asn155 2Gln148 Asp64	2Thr66 2Asp64 3Glu152	3Lys159 Asp116 Ile151	Asn155 Lys156

Os dois compostos (ALX04 e ALX07) foram importados ao programa online Glory, para a predição de seus metabólitos hepáticos, assim como a predição das abundâncias de cada

espécie no processo metabólico. Com isso, os metabólitos mais expressivos tiveram suas toxidades avaliadas de acordo com os dados obtidos no OSIRIS, conforme mostrados na Tabela 12.

Tabela 12. *Tabela contendo os metabólicos hepáticos dos diterpenos ALX04 e ALX07.*

ID_{Comp}	$\%_{Abundância}$	Tox	Estrutura
ALX04	100.00	Não	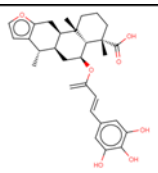
	74.34		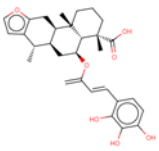
	69.06		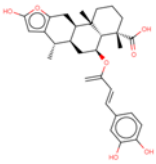
ALX07	100.00	Baixa CAR	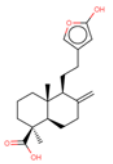
	80.54		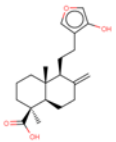
	75.11		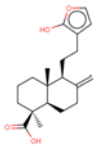
	69.23		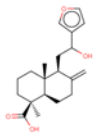

3.2. Discussões

De acordo com os resultados obtidos nos dois modelos (integrase e transcriptase reversa), apenas o composto ALX04 apresentou atividade frente a integrase com 52.42% de provável atividade. Já para TR, apenas o composto ALX07 apresentou atividade, com probabilidade de 55% de acordo com o modelo criado, segundo os dados das Tabelas 3 e 4.

Avaliando os dados estatísticos (Tabela 5) com relação a sensibilidade dos modelos apresentados, ou seja, a capacidade que o modelo apresenta de acertar a predição das moléculas ativas, em ambos os modelos foi entre 80-87% entre o grupo de teste e a validação interna cruzada de cada modelo. Além disso, o mesmo acontece com a especificidade, que corresponde ao acerto dos inativos, sendo os modelos sensível e específico, ou seja, capaz de acertar a partir de 80% a predição de ativos e inativos.

Outro dado estatístico que vale mencionar acerca dos outros modelos, é que a taxa total de acerto além de ficar também acima de 80% (acurácia), como consequência a performance do modelo está variando entre 87.64-93.99% de acordo com a curva ROC. Ainda mais, o coeficiente de correlação de Matthews exprime a qualidade das informações, com valores acima de 0.5 então os modelos podem ser considerados preditivos, com boa confiabilidade.

Avaliando a possível absorção e permeabilidade no intestino expressos na Tabela 6, os compostos testados apresentaram bons resultados para predição de CACO-2 e HIA, indicando uma tendência a apresentarem boa biodisponibilidade e resposta biológica, contribuindo para a proposição das moléculas como possíveis retrovirais.

Através dos dados da Tabela 7, os modelos de CACO-2 e HIA apresentam boa capacidade de acerto tanto para positivos quanto negativos (sensibilidade e especificidade acima de 60%), sendo os modelos mais sensíveis, ou seja, com melhor capacidade de predizer verdadeiros positivos, como também boa qualidade na predição global (MCC > 50%), podem considerar os resultados confiáveis.

O composto com probabilidade de inibição da IN (ALX04) não apresentou riscos de toxidade em nenhum dos 4 parâmetros avaliados (Tabela 8). Em contra partida, o composto ALX07, com possibilidade de inibição da TR, apresentou baixo risco de carcinogênese.

Contudo, os efeitos tóxicos de muitos retrovirais são amplamente conhecidos e relatados em diversos estudos, por isso a molécula ALX07 mesmo tendo apresentado baixo risco citotóxico, será considerada para o restante das análises teóricas deste estudo. (dos Santos Silva *et al*., 2022; Gonçalves *et al*., 2022)

Discutindo outro parâmetro ADMET, conforme mostrado na Tabela 1, a menor taxa de absorção verificada entre os controles positivos foi para o raltegravir (57.24%). Sendo assim, as duas moléculas (ALX04 e ALX07) cuja taxa de

absorção fora calculada apresentaram resultados superiores a menor taxa observada entre os controles considerados, com %Abs entre 74-92% é possível esperar a possível administração por via oral destes bioativos, melhorando a viabilidade e biodisponibilidade do possível medicamento.

Além da viabilidade, para análise da possível biodisponibilidade é necessário levar em consideração outros parâmetros farmacodinâmicos e cinéticos, além dos econômicos e logísticos envolvidos. Uma propriedade útil que foi calculada nesse estudo são as violações a regra de Lipinski, na qual aponta que um bioativo promissor deve violar apenas uma regra, condição vista nos dois compostos estudados nesta etapa.

No docking molecular foi observado que os compostos estudados apresentaram afinidade significativa com o respectivo receptor, o composto ALX04 apresentou energia do complexo ligante-receptor mais baixa, indicando que esse complexo possui melhor afinidade que o ligante complexo e os controles testados, podendo indicar que o composto apresente ação inibitória no sitio ativo.

Semelhante aconteceu com o composto ALX07, que apresentou bons resultados de interação, inclusive frente ao AZT, que dentre os controles frente a RT é o mais usado em pesquisas na proposição de retrovirais para HIV-1.

Analisando a Tabela 11 é possível perceber que, existem várias interações comuns entre os compostos submetidos, para o ancoramento molecular do composto ALX04 também foi observado interações semelhantes, conforme mostrado, com o inibidor e o raltegravir com o resíduo Thr66 numa interação de hidrogênio, e algumas estéricas como Glu152, Asp64, Asn155, Lys156 e Ile151.

Já o composto ALX07 apresentou interações de hidrogênios comuns com os controles lamivudina (Pro236) e zidovudina (Lys103), e estéricas com todos os inibidores de IN usados como controle, incluindo com o ligante (Lys101 e His235).

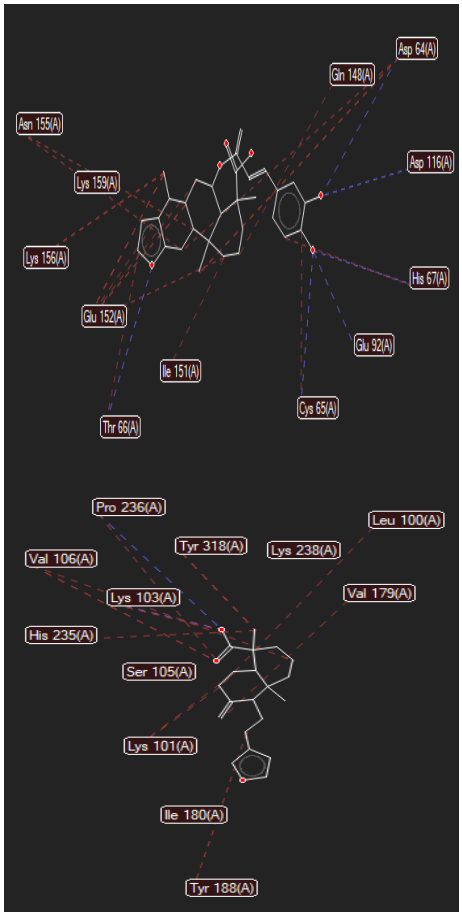

Figura 4. Esquema gráfico das interações entre ALX04 e o inibidor complexado junto a IN.

As interações tanto de hidrogênio quanto estéricas podem ser vistas da Figura 4, é possível perceber que o maior número de interações do ALX04 está nos oxigênios aromáticos e em suas vizinhanças. No composto ALX07 é visto uma concentração maior de interações com o éster ligado a dois anéis não aromáticos, mostrado na Figura 5:

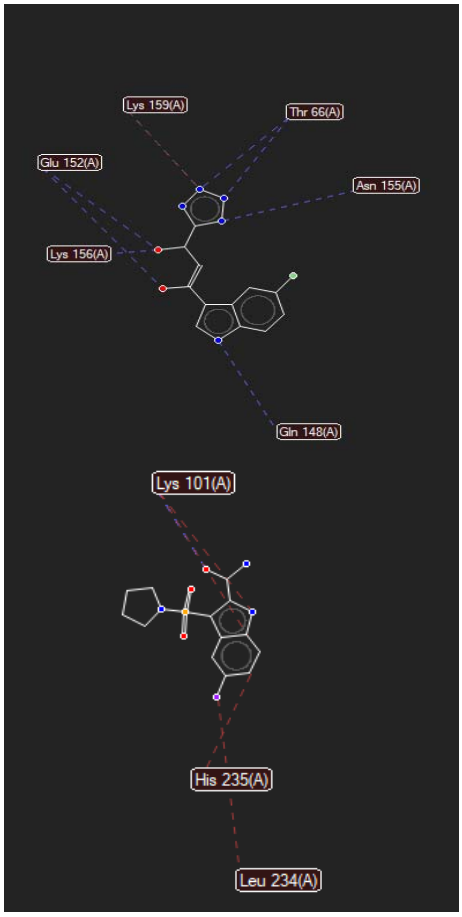

Figura 5. Esquema gráfico das interações entre ALX07 e inibidor complexo junto a TR.

Para a molécula ALX04 é possível perceber que os anéis condensados se mantiveram após processo metabólico, modificando a posição dos substituintes do anel aromático do éter conjugado, outra observação foi a acerca desses metabólitos é que o éster alifático ligado a cadeia de anéis condensado se manteve nos metabólitos de maior abundância.

As observações acima, levam a acreditar que o processo metabólico hepático simulado, não modificou o possível grupo farmacofórico das duas moléculas testadas, tendo em vista que, os contribuintes observados no *docking* molecular mantiveram-se sem alterações significativas, como também não influenciou negativamente na predição dos riscos de toxidade das moléculas precursoras.

Para a transcriptase reversa o ligante apresentou interações próximas aos anéis aromáticos conjugados, incluindo o nitrogênio do anel indólico e não na amida como esperada com base nas interações observadas no composto ALX07.

Contudo, a existência de anéis aromáticos com átomos capazes de promover ligações de hidrogênio como o nitrogênio e oxigênio, assim como funções alifáticas vizinhas contendo esses átomos, apresentaram importância nos acoplamentos moleculares observados.

Semelhantemente aconteceu com o composto ALX07, onde os metabólitos abundantes diferem-se estruturalmente de seus precursores basicamente pela posição da hidroxila ligada ao anel aromático de cinco membros. Ou seja, a estrutura cíclica da molécula também pode ser considerada o grupo farmacofórico, pois está diretamente associada ao acoplamento molecular, conforme mostrado na simulação de *docking* com a TR.

Os demais diterpenos extraídos do Pau-Brasil, não apresentaram atividades frente a nenhuma das principais proteínas do HIV, as proteínas responsáveis pela multiplicação retroviral, contudo juntamente com elas foram testadas moléculas sem a carbonila que se ligam aos anéis condensados, estes apresentaram resultados promissores.

4. CONCLUSÕES

Dentre os nove compostos testados inicialmente, apenas 2 apresentaram atividades promissores, no qual o composto ALX04 apresentou possível atividade frente a integrase e o composto ALX07 para a transcriptase reversa.

Sugere-se, portanto, que os diterpenos modificados podem apresentar atividade inibitória para a integrase e os naturais para transcriptase reversa.

Estudos biológicos devem ser considerados em pesquisas posteriores, para validar todo o estudo apresentado nesta pesquisa, contudo pesquisas como esta impulsionam cientistas que trabalham com o planejamento e/ou desenvolvimento de retrovirais.

5. DECLARAÇÕES

5.1. Limitações do estudo

O estudo é limitado aos compostos simulados, aos softwares utilizados e as simulações realizadas.

5.2. Acknowledgements

CNPQ, CAPES e FACEPE

5.3. Fonte de financiamento

CNPQ, CAPES e FACEPE

5.4. Competing Interests

Nenhum conflito de interesses

5.5. Open Access

6. REFERÊNCIAS

1. Ahsan, M. J., Amir, M., Bakht, M. A., Samy, J. G., Hasan, M. Z., & Nomani, M. S. (2016). Synthesis and antimicrobial activity of N1-(3-chloro-4-fluorophenyl)-N4-substituted semicarbazone derivatives. *Arabian Journal of Chemistry*, *9*, S861–S866.
2. Albertini, T. T. (2022). *Aplicação de redes neurais artificias para a predição da atividade biológica de compostos visando contribuição para a farmacologia: revisão bibliográfica*.
3. Bencheikh, B., Cheriet, M., Djemil, R., & Khatmi, D. (2022). In Silico Study of Selected Natural Products as SARS-CoV-2 MPro Binder: Molecular Docking and Molecular Dynamics Simulation. *Polycyclic Aromatic Compounds*, 1–13.
4. Bhole, R. P., Bonde, C. G., Bonde, S. C., Chikhale, R. V, & Wavhale, R. D. (2021). Pharmacophore model and atom-based 3D quantitative structure activity relationship (QSAR) of human immunodeficiency virus-1 (HIV-1) capsid assembly inhibitors. *Journal of Biomolecular Structure and Dynamics*, *39*(2), 718–727.
5. Brian, W. (2021). *Bioinformatics and machine learning in prevention, detection and treatment of HIV/AIDS*. Brac University.
6. Carvalho, J. C. S., Silveira, E. R., & Matos, T. M. (n.d.). Perspectivas na pesquisa de Plantas Medicinais Brasileiras. *Laboratório de Anatomia Vegetal*, 194.
7. Correia Soeiro, M. de N., Vergoten, G., & Bailly, C. (2022). Molecular docking of brazilin and its analogs to barrier-to-autointegration factor 1 (BAF1). *Annals of the New York Academy of Sciences*.
8. Cota, B. B., Siqueira, E. P., Zani, C. L., & Oliveira, D. M. (2011). New diterpenes of Caesalpinia echinata Lam. *34 Annual Meeting of the Brazilian Chemical Society - Chemistry for a Better World*. http://inis.iaea.org/search/search.aspx?orig_q=RN:43081146
9. de Bruyn Kops, C., Stork, C., Šícho, M., Kochev, N., Svozil, D., Jeliazkova, N., & Kirchmair, J. (2019). GLORY: Generator of the Structures of Likely Cytochrome P450 Metabolites Based on Predicted Sites of Metabolism. *Frontiers in Chemistry*, *7*. https://doi.org/10.3389/fchem.2019.00402
10. Ding, X., Kang, D., Sun, L., Zhan, P., & Liu, X. (2021). Combination of 2D and 3D-QSAR Studies on DAPY and DANA Derivatives as Potent HIV-1 NNRTIs. *Journal of Molecular Structure*, 131603.
11. dos Santos Silva, R. R., Roma, R. R., da Silva Chagas, F. D., & Freitas, A. L. P. (2022). MAPPING OF PATENTS RELATED TO PROTEASE INHIBITORS AND HIV. *Revista INGI-Indicação Geográfica e Inovação*, *6*(2), 1636–1645.
12. Forrestall, K. L., Burley, D. E., Cash, M. K., Pottie, I. R., & Darvesh, S. (2021). 2-Pyridone natural products as inhibitors of SARS-CoV-2 main protease. *Chemico-Biological Interactions*, *335*, 109348.
13. Giroir, B. P. (2020). The time is now to end the HIV epidemic. *American Journal of Public Health*, *110*(1), 22–24.
14. Gonçalves, B. C., de Araujo Lima, N., Franchi, M. G., Batista, A. P., Maria, L. A. A., dos Santos, R. F., Soares, B. C., Vicco, L. R., do Vale Senedese, M. S., & Pereira, C. D. (2022). FATORES QUE INFLUENCIAM A ADESÃO DA TERAPIA ANTIRRETROVIRAL (TARV). *RECIMA21-Revista Científica Multidisciplinar-ISSN*

2675-6218, *3*(4), e341341–e341341.

15. Gonzalez, M. M., Cabrerizo, F. M., Baiker, A., Erra-Balsells, R., Osterman, A., Nitschko, H., & Vizoso-Pinto, M. G. (2018). β-Carboline derivatives as novel antivirals for herpes simplex virus. *International Journal of Antimicrobial Agents*, *52*(4), 459–468.
16. Jiang, H., Zhou, Y., & Tang, W. (2020). Maintaining HIV care during the COVID-19 pandemic. *The Lancet HIV*, *7*(5), e308–e309.
17. Leite, D. R. A., de Moraes, R. M., & Lopes, L. W. (2021). Método de Aprendizagem de Máquina para Classificação da intensidade do desvio vocal utilizando Random Forest. *Journal of Health Informatics*, *12*.
18. Lichtenberg, S., Huber-Sannwald, E., Reyes-Agüero, J. A., Anhuf, D., & Nehren, U. (2022). Pau-brasil and string instrument bows telecouple nature, art, and heritage. *Ecology and Society*, *27*(1).
19. Machado-Zaldívar, L. Y., Blanco-de Armas, M., Dubed-Echevarría, M., Díaz-Torres, H. M., López-Rizo, L. S., Pérez-Guevara, M. T., Lantero-Abreu, M. I., & Rodríguez-Acosta, M. (2021). Pretreatment HIV Drug-resistance Surveillance as a Tool for Monitoring and Control of the HIV/AIDS Epidemic in Cuba. *MEDICC Review*, *23*(2).
20. Melo, G. C. de, Carvalho, A. C. A., Moreira, A. da S., & Paixão, J. T. dos S. (2021). Tempo de sobrevida e distância para acesso a tratamento especializado por pessoas vivendo com HIV/Aids no estado de Alagoas, Brasil. *Revista Brasileira de Epidemiologia*, *24*.
21. Mescia, T. B., Louro, R. P., Barbedo, C. J., Carbonero, E. R., Figueiredo-Ribeiro, R. de C. L., & Braga, M. R. (2022). Changes in cell wall composition and ultrastructure related to desiccation during the seed maturation of Paubrasilia echinata (brazilwood). *Protoplasma*, 1–15.
22. Monica, G. La, Lauria, A., Bono, A., & Martorana, A. (2021). Off-Target-Based Design of Selective HIV-1 PROTEASE Inhibitors. *International Journal of Molecular Sciences*, *22*(11), 6070.
23. Monteiro, A. F. M. (2021). *Triagem virtual híbrida, predições admet e modelagem molecular de compostos 2-aminotiofenos frente ao HIV-1*.
24. Moura, É. P. de. (2021). *Estudo in silico de flavonoides e compostos análogos pertencentes à família Asteraceae contra a doença de Alzheimer*.
25. Presanis, A. M., Harris, R. J., Kirwan, P. D., Miltz, A., Croxford, S., Heinsbroek, E., Jackson, C. H., Mohammed, H., Brown, A. E., & Delpech, V. C. (2021). Trends in undiagnosed HIV prevalence in England and implications for eliminating HIV transmission by 2030: an evidence synthesis model. *The Lancet Public Health*, *6*(10), e739–e751.
26. Sánchez-Suárez, J., Villamil, L., Díaz, L., & Coy-Barrera, E. (2022). Uncovering Streptomyces-Derived Compounds as Cosmeceuticals for the Development of Improved Skin Photoprotection Products: An In Silico Approach to Explore Multi-Targeted Agents. *Scientia Pharmaceutica*, *90*(3), 48.
27. Sander, T., Freyss, J., Von Korff, M., & Rufener, C. (2015). DataWarrior: An open-source program for chemistry aware data visualization and analysis. *Journal of Chemical Information and Modeling*, *55*(2), 460–473. https://doi.org/10.1021/ci500588j
28. Santos, A. K. F. de S. (2021). *Avaliação comparativa da atividade antinociceptiva e mecanismo de ação decorrente da administração de 3, 4, 5-trimetoxicinamato de metila (M-TMCA) e 3, 4, 5-trimetoxicinamato de butila (B-TMCA) em camundongos*.
29. Silverio, P. S. de S. N. (2021). *3D-QSARpy: Combinando estratégias de seleção de atributos e técnicas de aprendizado de máquina para construir modelos QSAR 3D*.
30. Stone, J., Mukandavire, C., Boily, M., Fraser, H., Mishra, S., Schwartz, S., Rao, A., Looker, K. J., Quaife, M., & Terris-Prestholt, F. (2021). Estimating the contribution of key populations towards HIV transmission in South Africa. *Journal of the International AIDS Society*, *24*(1), e25650.
31. Stork, C., Embruch, G., Šícho, M., de Bruyn Kops, C., Chen, Y., Svozil, D., & Kirchmair, J. (2019). NERDD: a web portal providing access to in silico tools for drug

discovery. *Bioinformatics*. https://doi.org/10.1093/bioinformatics/btz695

32. Tibúrcio, R. da S. (2022). *Planejamento, síntese e avaliação do potencial de novos2-aminoselenofenos como candidatos a fármacos leishmanicidas*.
33. Tuncbilek, M., Kucukdumlu, A., Guven, E. B., Altiparmak, D., & Cetin-Atalay, R. (2018). Synthesis of novel 6-substituted amino-9-(β-d-ribofuranosyl) purine analogs and their bioactivities on human epithelial cancer cells. *Bioorganic & Medicinal Chemistry Letters*, *28*(3), 235–239.
34. Umar, H. I., Saliu, T. P., Josiah, S. S., Ajayi, A., & Danjuma, J. B. (2021). In silico studies of bioactive compounds from selected African plants with inhibitory activity against nitric oxide synthase and arginase implicated in asthma. *Egyptian Journal of Medical Human Genetics*, *22*(1), 1–16.
35. van den Broek, N. (2021). Mini commentary on BJOG-20-1962. R1 'Slower response to treatment of iron deficiency anemia in HIV-infected pregnant women: a prospective cohort study'Anaemia in pregnancy remains a global health problem. *Authorea Preprints*.
36. Xavier, Y. K. da S., Sobral, M. de A., Lima, G. M. de S., Silva, T. D. da, Ferreira, A. M. M. S., Souza, F. A. de, Souza, I. A. de, & Maia, C. S. (2022). Caracterização fitoquímica e atividade antifúngica do extrato etanólico obtido da mistura de sementes e vagens de Caesalpinia echinata Lam / Phytochemical characterization and antifungal activity of the ethanolic extract obtained from the seed and pod mix. *Brazilian Applied Science Review*, *6*(2), 375–390. https://doi.org/10.34115/basrv6n2-003

Tabela 11. *Relação das interações com os resíduos de aminoácidos de IN e TR.*

		TR		
	H		**Estérica**	
Ligante		2Lys101	His235	Leu234
ALX07	Lys103 Pro236	Leu100 Val179 2Lys101	Tyr318 Tyr188 2Val106	His235 Lys103 Pro236
Efavirez	2Lys101	His235 Gly190	Val106	Val179
Lamivudina	Lys101 Pro236	Tyr188	Lys101	2Tyr181
Zidovudina	Val179 Lys101 Lys103	2Tyr188 His235	Tyr181 Pro236	2Lys101
		IN		
Ligante	Lys159 2Thr66 Asn155 2Lys156 2Glu152	2Glu152	Lys159	
ALX04	Thr66 Cys65 Glu92 His67 Asp64 Asp116	2Asn155 4Glu152 His67	Lys156 2Asp64 Cys65	Thr66 Ile151 Gln148
Raltegravir	2Lys156 2Asn155 Thr66	2Glu152 Asn155	Asp64 Ile151	
Dolutegravir	Asn155 2Gln148 Asp64	2Thr66 2Asp64 3Glu152	3Lys159 Asp116 Ile151	Asn155 Lys156

PERIÓDICO TCHÊ QUÍMICA
ARTIGO ORIGINAL

AVALIAÇÃO DA INCERTEZA DE MEDIÇÃO DE MÉTODO ANALÍTICO PARA DETERMINAÇÃO QUANTITATIVA DE ÁCIDOS URSÓLICO E OLEANÓLICO NO PROCESSAMENTO DE MAÇÃS DE RESÍDUOS AGROINDUSTRIAIS

MEASUREMENT UNCERTAINTY EVALUATION OF ANALYTICAL METHOD FOR QUANTITATIVE DETERMINATION OF URSOLIC AND OLEANOLIC ACIDS IN APPLE PROCESSING AGROINDUSTRIAL WASTE MATERIAL

ვაშლის გადამუშავების აგროინდუსტრიულ ნარჩენ მასალაში ურსოლისა და ოლეანოლის მჟავების რაოდენობრივი განსაზღვრის ანალიზის მეთოდის გაზომვის განუსაზღვრელობის შეფასება

RUBASHVILI, Imeda[1]*; TSITSAGI, Mzia[1]; EBRALIDZE, Ketevan[1];

[1]Ivane Javakhishvili Tbilisi State University, Petre Melikishvili Institute of Physical and Organic Chemistry. Georgia.

** Corresponding author*
e-mail: rubashvili@yahoo.fr

Received 20 September 2022; received in revised form 30 October 2022; accepted 07 November 2022

RESUMO

Introdução: O bagaço de maçã representa uma fonte de barata e rica em compostos bioativos com propriedades valiosas - ácido ursólico (UA) e ácido oleanólico (OA). Devido à ampla gama de aplicações nas indústrias farmacêutica e nutracêutica, esses compostos possuem alto valor comercial, e possuir um método analítico adequado com incerteza de medição é de grande importância e praticidade. **Objetivo:** O objetivo do presente trabalho foi estimar detalhadamente a incerteza de medição para o método de HPLC validado combinado com o procedimento de extração para a determinação de ácido ursólico e ácido oleanólico do bagaço da maçã. **Métodos:** A análise cromatográfica foi realizada utilizando o sistema LC-20AD Prominence Shimadzu e a extração assistida por ultrassom foi realizada utilizando o banho ultrassônico DW-5200DTS para obter e determinar a concentração de ácido ursólico e ácido oleanólico em bagaço de maçã. O processo de avaliação da incerteza de medição foi realizado pelo diagrama de Ishikawa e uma combinação das abordagens *bottom-up* e *top-down*. **Resultados:** O teor de ácido ursólico e ácido oleanólico (mg/g) em bagaço de maçã com o valor da incerteza expandida foi calculado, determinado em é 7,06 ± 0,647 mg/g (k=1,96; P=95%) e 4,70 ± 0,422 mg/g (k=1,96; P=95%), respectivamente. Foram observadas seis fontes de todos os contribuintes de incertezas que afetaram a medição. **Discussão:** O valor da incerteza padrão do tipo A foi 3 vezes menor do que a incerteza padrão do tipo B para ambos os analitos. Os resultados mostram que a incerteza padrão do tipo B é um dos principais contribuintes, e o valor da incerteza expandida do método validado não mudará de teste para teste nas mesmas condições laboratóriais. **Conclusões:** A metodologia descrita neste trabalho apresenta os detalhes e aspectos práticos da abordagem híbrida usando os dados de validação do método e propõe instruções passo a passo para avaliar a incerteza de medição do método quantitativo.

Palavras-chave: *Incerteza de Medição, HPLC, Ácido Ursólico, Ácido Oleanólico*

ABSTRACT

Background: Apple pomace represents a low-cost and rich source of bioactive compounds with valuable properties - ursolic acid (UA) and oleanolic acid (OA). Due to the wide range of applications in pharmaceutical and nutraceutical industries, these compounds have a high commercial value, and possessing a suitable analytical method with measurement uncertainty is of great significance and practicability. **Aim:** The purpose of the present work was to estimate detailed measurement uncertainty for the validated HPLC method combined with the extraction procedure for the determination of UA and OA in apple pomace. **Methods:** The chromatographic analysis using LC-20AD Prominence Shimadzu System and ultrasound-assisted extraction using the ultrasonic bath DW-5200DTS were performed to obtain and determine UA and OA in apple pomace. The process of measurement uncertainty evaluation was performed by the Ishikawa diagram and a combination

DOI: 10.52571/PTQ.v19.n42.2022_06_RUBASHVILI_pgs_60_74.pdf

of bottom-up and top-down approaches. **Results:** The content of UA and OA (mg/g) in apple pomace with the value of the expanded uncertainty was calculated, which is 7.06 ± 0.647 mg/g (k=1.96; P=95%) and 4.70 ± 0.422 mg/g (k=1.96; P=95%), respectively. Six sources of all the contributors of uncertainties were observed that affected the measurement. **Discussion**: The A-type standard uncertainty value was 3 times less than the B-type standard uncertainty for both analytes. The results show that B-type standard uncertainty is a major contributor, and the value of the expanded uncertainty of the validated method will not change from test to test in the same laboratory conditions. **Conclusions:** The methodology described in this work explains well the details and practical aspects of the hybrid approach using the method validation data and proposes step-by-step instructions to evaluate the measurement uncertainty of the quantitative method.

Keywords: *Measurement Uncertainty, HPLC, Ursolic Acid, Oleanolic Acid*

რეზიუმე

შესავალი: ვაშლის ნარჩენი წარმოადგენს ძვირფასი თვისებების მქონე ბიოლოგიურად აქტიური ნივთიერებების - ურსოლისა და ოლეანოლის მჟავების იაფფასიან და მდიდარ წყაროს. ფარმაცევტულ და ნუტრაცევტულ ინდუსტრიაში მათი ფართო გამოყენების გამო აღნიშნულ ნივთიერებებს მაღალი კომერციული მნიშვნელობა გააჩნიათ და სათანადო ანალიზური მეთოდის ფლობას გაზომვის განუსაზღვრელობით დიდი პრაქტიკული მნიშვნელობა გააჩნია. **მიზანი:** წარმოდგენილი ნაშრომის მიზანს წარმოადგენს ვაშლის ნარჩენში ურსოლისა და ოლეანოლის მჟავების ექსტრაქციის პროცედურასთან შეუღლებული მაღალეფექტური სითხური ქრომატოგრაფიული ვალიდირებული მეთოდის გაზომვის განუსაზღვრელობის დეტალური შეფასება. **მეთოდები:** ქრომატოგრაფიული ანალიზი და ულტრაბგერითი ექსტრაქცია განხორციელდა LC-20AD Prominence Shimadzu სისტემისა და ულტრაბგერითი აბაზანის DW-5200DTS გამოყენებით. გაზომვის განუსაზღვრელობის შეფასების პროცესი განხორციელდა იშიკავას დიაგრამის საშუალებით და ქვემოდან ზემოთ და ზემოდან ქვემოთ მიდგომების გაერთიანებით. **შედეგები:** გამოთვლილი იქნა ვაშლის ნარჩენში ურსოლისა და ოლეანოლის მჟავების შემცველობა (მგ/გ) გაფართოებული განუსაზღვრელობის მნიშვნელობით, რომელიც შეადგენს 7.06 ± 0.647 მგ/გ (k=1.96; P=95%) და 4.70 ± 0.422 მგ/გ (k=1.96; P=95%), შესაბამისად. გამოვლინდა განუსაზღვრელობაში მონაწილე ფაქტორების ექვსი წყარო, რომლებმაც გავლენა მოახდინა გასაზომზე. **განსჯა:** A ტიპის სტანდარტული განუსაზღვრელობა 3-ჯერ ნაკლებია, ვიდრე B ტიპის სტანდარტული განუსაზღვრელობა ორივე საანალიზო ნივთიერებისთვის. შედეგებმა აჩვენებს, რომ B ტიპის სტანდარტული განუსაზღვრელობა არის მთავარი მონაწილე და ვალიდირებული მეთოდის გაფართოებული განუსაზღვრელობის სიდიდე არ შეიცვლება იდენტური პირობებში ანალიზიდან ანალიზამდე. **დასკვნები:** ამ კვლევაში აღწერილი მეთოდოლოგია კარგად ხსნის მეთოდის ვალიდაციის მონაცემების გამოყენებით ჰიბრიდული მიდგომის დეტალებსა და პრაქტიკულ ასპექტებს და გვთავაზობს ნაბიჯ-ნაბიჯ ინსტრუქციას როგორ შევაფასოთ რაოდენობრივი განსაზღვრის მეთოდის გაზომვის განუსაზღვრელობა.

საკვანძო სიტყვები: *გაზომვის განუსაზღვრელობა, მესქ, ურსოლის მჟავა, ოლეანოლის მჟავა*

1. INTRODUCTION

Apple pomace, as a waste material of the apple processing industry containing approximately 25% of the processed apple, represents a low-cost and rich source of fruit-derived bioactive compounds with valuable properties, including pentacyclic triterpenoids regioisomeric triterpene acids - ursolic acid (UA) and oleanolic acid (OA). These bioactive compounds have attracted much attention due to their unique and strong biological, a wide variety of approved pharmacological activities, including anti-cancer, chemopreventive, hepatoprotective, antiviral, antibacterial, anti-inflammatory, anticardiovascular, antiatherosclerostic, antidiabetic, antioxidant, immunomodulatory and gastroprotective properties. UA and OA are also utilized in preparing food supplements and important ingredients of cosmetic formulations and sports supplements. It has been reported that UA can stimulate muscle growth and enhance the epidermal permeability barrier recovery in the skin. The UA and OA chemical structures are given in Figures 1 and 2, respectively (Rubashvili *et al*., 2020; Liese *et al.,* 2015; Khwaza *et al*., 2020; Jin *et al*., 2016; Woźniak *et al*., 2015; Kashyap *et al*., 2016; Alvarado *et al.,* 2015). Due to the wide range of applications in pharmaceutical and nutraceutical industries, these bioactive

compounds have a high commercial value. Therefore, an efficient, selective, and high-yield extraction to obtain UA and OA from raw plant materials and quantitative determination of these compounds in the mentioned material and the extracted product using a suitable analytical method has great significance and practicability. Consequently, there is a need to develop and validate a new, reliable, and suitable method obtained with the combination of an extraction procedure to isolate UA and OA from apple processing waste material as a dry powdered form and an analytical procedure for the quantitative determination of these analytes in the mentioned material.

The authors of the present paper have developed a new, selective, reproducible, and high-yield extraction method by ultrasound-assisted technique for obtaining UA and OA from apple pomace and an effective, specific, sensitive, and rapid high-performance liquid chromatography (HPLC) analytical procedure to determine these target compounds quantitatively. Based on both procedures, a new combined method has been developed and validated (Rubashvili *et al.*, 2020). Analytical results are not complete unless their measurement uncertainty accompanies them. Measurement uncertainty of the analytical method may originate from many possible sources, including sample preparation, matrix effects, purity of chemical reference substances, method validation, and uncertainty associated with the analytical instrument calibration (Jebali *et al*., 2020).

The ISO/IEC 17025 requirements for evaluation of measurement uncertainty are fulfilled if the results are obtained by following the described analytical procedure and reporting instructions, provided that all uncertainty contributors are under control (testing is performed by qualified personnel using suitable reference standards and calibrated/qualified equipment, system suitability criteria are satisfied and the repeatability is evaluated against pre-defined acceptance criteria) (OMCL guideline).

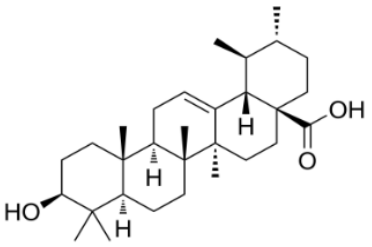

Figure 1. The chemical structure of UA.

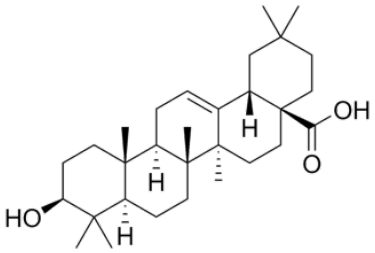

Figure 2. The chemical structure of OA.

For consistent interpretation of the measurement results, it is necessary to evaluate the confidence that can be placed in the presentation of an analytical result, which the indication of the data quality must accompany. Therefore, method validation is an essential component of the measures, and the laboratory should implement it to produce reliable analytical data. Besides common method performance characteristics obtained in the validation process, testing laboratories shall have and apply procedures for estimating the uncertainty of measurements. This means that the analytical result cannot be viewed only as a separate value (ISO/IEC 17025; Ellison *et al*., 2012; Rubashvili and Tsitsishvili, 2015; Senila *et al.,* 2014).

The measurement uncertainty is estimated mainly by a top-down or bottom-up approach. In the top-down approach, the major sources of uncertainty are identified and evaluated, while in the bottom-up approach, all the uncertainty sources are systematically evaluated, and only those with significant contributions are used to derive the measurement uncertainty. The top-down approach is time-consuming and requires extensive knowledge of the analytical procedure, but it enables the identification of significant uncertainty sources and, consequently, the reduction of total measurement uncertainty. Another relatively quick and easy way of uncertainty estimation is the in-house validation that includes determining the method performance parameters (Senila *et al.,* 2014; Rubashvili and Tsitsishvili, 2015).

According to Eurachem/CITAC Guides, OMCL, and EA guidelines, the bottom-up approach applies to cases with limited or no method performance data. The uncertainty arising from each source is evaluated by replicate measurements and then combined using statistical processes. The top-down approach applies to cases where method performance data are available. The combined contribution to the uncertainty is estimated using method

performance data: certified reference materials, validation study data, collaborative study data (establishment of chemical reference standards or validation of new test method), proficiency testing study data, and control charts, providing that the available performance data are used for the estimation of measurement uncertainty of the selected test/method, namely: comparable precision, satisfactory performance (system suitability) and quality control results compliant with the established analytical acceptance criteria (OMCL guideline; Eurachem guide; EA guideline; Barwick and Ellison, 2000; Barwick, 2012; Eurolab Technical Report; ISO guide 98-3; JCGM 100:2008 guide; Senila *et al.,* 2014).

The purpose of the present work was to estimate detailed measurement uncertainty for the developed and validated analytical HPLC method combined with the ultrasound-assisted extraction (UAE) procedure for the quantitative determination of UA and OA in apple pomace as an apple processing agroindustrial waste material. A hybrid approach is used as the most useful and convenient method for measurement uncertainty obtained with a combination of those as mentioned earlier - bottom-up and top-down approaches.

2. MATERIALS AND METHODS:

2.1. Materials

Local apple fruit manufacturers provided Apple pomace as an apple processing waste material. The raw material was dried in a laboratory room under controlled conditions (the temperature - 20-25 ºC and the relative humidity - 30-60 %) and protected from direct sunlight. The sample was ground manually to be powdered and stored in a refrigerator before extraction (Rubashvili *et al.,* 2020).

The certified analytical standards of OA and UA, the HPLC grade acetonitrile and methanol, the analytical grade potassium dihydrogen phosphate, sodium hydroxide, hydrochloride acid, anhydrous formic acid, absolute ethanol and ethyl acetate were purchased from Sigma-Aldrich (Germany).

2.2. Instrumentation

The HPLC-grade purified water was prepared using Milli Q Advantage A10 purification system (France). The UAE used the dual-frequency ultrasonic bath DW-5200DTS (bath-type) (China). The chromatographic analysis was performed using LC-20AD Prominence Shimadzu HPLC System (Japan). Analytical balance ALX-210 (USA) and pH-meter Hanna Instruments HI 2211 (USA) were used to prepare solutions. All the measuring equipment was appropriately calibrated. The experiment was carried out in a controlled area (temperature, t=22±3 ºC, relative humidity, RH=45±15 %).

2.3. Extraction Procedure

The ultrasound frequency was 25 kHz; the temperature was controlled at 25±2 ºC during ultrasonication; ethanol and ethylacetate were selected as non-toxic and the best extraction solvents. The two-stage UAE was carried out by adding 10 g of the powdered dried sample of apple pomace and 100 mL of solvent in a 200 mL extraction vessel equipped with a digital temperature controller for 20 minutes. After both extraction stages, the crude extract solutions were centrifuged at 4000 rpm for 10 minutes, and then the obtained supernatants were collected to evaporate under airflow to remove the organic solvent. Then 50 mL of purified water was added to the obtained wet powder containing OA and UA and mixed vigorously for a few minutes. In order to remove water-soluble impurities, the obtained suspension was heated at 50 ºC for 30 minutes and then centrifuged at 4000 rpm for 10 minutes, and the precipitate was dried. In order to remove non-polar impurities, n-hexane was added to the dried powder, and the obtained suspension was stirred for 1 hour and then centrifuged at 4000 rpm for 10 minutes. The precipitate was dried and then dissolved in hot alkaline ethanol - a mixture of ethanol and strong sodium hydroxide solution 90:10 v/v (pH~10). Then the pH value of this solution was adjusted to 7.0±0.05 with hydrochloride acid solution, and the obtained solution was allowed to stand for 24 hours. The crystalline solid was separated from the solution through centrifugation and then dried under air flow to obtain an extracted product (Rubashvili *et al.*, 2020).

2.4. Analytical Procedure

The analytical procedure was developed using the HPLC column - Agilent SB-C18 4.6×250 mm, 5 µm (USA) with an isocratic elution of mobile phase (MP) containing a mixture of phosphate buffer solution pH 6.0 (6.8 g/L potassium dihydrogen phosphate solution adjusted to pH 6.0 with strong sodium hydroxide solution), acetonitrile and methanol (20:30:50 v/v) filtered through PVDF 0.45 µm membrane filters and degassed; The flow rate of mobile phase was 1.0 mL/min; The UV-spectrophotometric detection was performed at the wavelength - 210 nm; The injected volume was 20 µL; The column temperature was maintained at 35 °C. The

analytical data were reported using HPLC system software (Rubashvili *et al.*, 2020).

2.5. Standard and Sample Preparation

The analytical standards of UA and OA were diluted in a mixture of anhydrous formic acid and methanol 2:98 v/v (diluent) as the standard solution at the concentration – 0.25 mg/mL (10 mg of standard dissolved in 50 mL of diluent). Both standard solutions were mixed 1:1 v/v, and the obtained solution was used as the standard solution at the concentration - 0.125 mg/mL of each analyte.

To prepare the test solution, the dried extracted product (approx. 10 mg) was transferred to a 50 mL volumetric flask, diluted to volume with the diluent, and mixed well. The obtained solution was filtered through a 0.45 µm PVDF microporous membrane filter.

2.6. Calculations

The concentration of UA/OA - C_S, mg/mL in the test solution was calculated by Equation 1:

$$C_s = \frac{A_{st} \times W_{st} \times P}{A_s \times V_{St} \times 100} \quad \text{(Eq. 1)}$$

Where, A_S – The peak area of UA/OA obtained with the test solution; A_{St} – The peak area of UA/OA obtained with the standard solution; W_{St} – The weight of the standard of UA/OA, mg; V_{St} – The dilution of the standard of UA/OA, mL; P – The purity of the standard of UA/OA, %.

The content of UA/OA – X_i, mg per 1 g of the dry sample of raw material (apple pomace) was calculated using Equation 2:

$$X_i = \frac{A_s \times W_{st} \times V_2 \times W_1 \times P}{A_{st} \times W_s \times W \times V_{St} \times 100} \quad \text{(Eq. 2)}$$

Where W - the weight of the dry sample of the raw material (apple pomace), g.

2.7. Measurement Uncertainty Evaluation

The process of measurement uncertainty evaluation was performed in four steps: in the first step, the measurand was identified; in the second step, uncertainty contributors and sources were identified by the Ishikawa diagram; in the third step, the quantification of uncertainty was performed by a combination of bottom-up and top-down approaches. After that, the standard uncertainty arising from each source was evaluated by replicate measurements and method performance data based on the method validation study (Rubashvili *et al.*, 2020; Meyer; 2003); at the last step, the combined standard uncertainty was calculated; In order to obtain an expanded uncertainty of the method, the coverage factor – k=1.96 was used as a multiplier of the combined standard uncertainty at the level of confidence of 95 % for normally distributed data and k=1.65 for rectangular (uniform) distribution data (OMCL guideline).

All the calculations were performed using the validated Microsoft Excel spreadsheet software.

2.7.1 Standard Uncertainty of the Repeatability of the Method

The standard uncertainty of the repeatability of the method, considered as A-type uncertainty of the method, was evaluated by calculating the standard deviation of the contents of UA/OA – X_i, mg per 1 g of the dry sample of apple pomace (for 6 individual determinations). The content of each analyte was calculated using Equation 2.

The standard uncertainty – u_A of the repeatability of the method (A-type uncertainty) by Equation 3:

$$u_A = \frac{SD}{\sqrt{n}} \quad \text{(Eq. 3)}$$

Where n – is the number of individual determinations; SD – the standard deviation of the contents of UA/OA in the apple pomace, mg/g.

In order to calculate the expanded uncertainty, the normal distribution was checked with the calculation of d-criteria using Equations 4, and 5:

$$s^* = \sqrt{\frac{1}{n}\sum_{i=1}^{n}(X_i - X)^2} \quad \text{(Eq. 4)}$$

$$d = \frac{\sum_{i=1}^{n}|X_i - X|}{n \times S^*} \quad \text{(Eq. 5)}$$

Where S* – the dispersion value; the d-criteria of the normal distribution should be from 0.7153 to 0.9073 for six individual determinations (n=6).

2.7.2 Standard Uncertainty of Standard Preparation

The combined relative standard uncertainty of standard preparation – u_{st}/X was

calculated as follows:

The relative standard uncertainty of analytical balance - Equation 6 calculated $u(W_{St})/W_{St}$ with rectangular distribution:

$$\frac{u(W_{St})}{W_{St}} = \frac{\Delta_B}{W_{St}\times\sqrt{3}} \quad \text{(Eq. 6)}$$

where Δ_B - the standard uncertainty of the analytical balance from the calibration certificate; W_{St} - the standard UA/OA weight, mg.

The relative standard uncertainty of the standard purity $u(P_{St})/P_{St}$ was calculated using Equation 7:

$$\frac{u(P_{St})}{P_{St}} = \frac{\Delta_P}{P_{St}\times\sqrt{3}} \quad \text{(Eq. 7)}$$

Where Δ_P - the standard uncertainty of analytical standard of UA/OA from the quality certificate; W_{St} - the weight of standard of UA/OA, mg.

The relative standard uncertainty of the molar mass of UA/OA (Molecular formula: $C_{30}H_{48}O_3$) u(M)/M was calculated using Equation 8:

$$\frac{u(M)}{M} = \frac{\sqrt{30\times0.0006^2+3\times0.00021^2+48\times0.0000784^2}}{456.7\times\sqrt{3}} \quad \text{(Eq. 8)}$$

Where M - is the molar mass of UA/OA, 456.7 g/mol.

The relative standard uncertainty of the mass of standard - $u(m_{St})/W_{St}$ was calculated by Equation 9:

$$\frac{u(m_{St})}{W_{St}} = \sqrt{(\frac{u(W_{St})}{W_{St}})^2 + (\frac{u(P_{St})}{P_{St}})^2 + (\frac{u(M)}{M})^2} \quad \text{(Eq. 9)}$$

The relative standard uncertainty of the used volumetric glassware - Equation 10 calculated $u(V_{St}G)/V_{St}i$ with triangular distribution:

$$\frac{u(V_{St}G)i}{V_{St}i} = \frac{\Delta_V}{V_{St}i\times\sqrt{6}} \quad \text{(Eq. 10)}$$

Where ΔV - the standard uncertainty of the glassware from the calibration certificate, mL; V_{St} - the measured dilution volume of standard, mL.

The relative standard uncertainty of the temperature effect of the volumetric glassware - $u(V_{St}T)i/V_{St}i$ with rectangular distribution was calculated by Equation 11:

$$\frac{u(V_{St}T)i}{V_{St}i} = \frac{V_E}{V_{St}i\times\sqrt{3}} \quad \text{(Eq. 11)}$$

Where V_T - the expansion of the volume, mL was calculated by Equation 12:

$$\Delta_V = V_{St}i \times \Delta t \times \frac{0.00021}{1} \quad \text{(Eq. 12)}$$

Where, Δt – the half value of the temperature range in the laboratory room, ºC.

The relative standard uncertainty of the dilution volume of standard - $u(V_{St})i/V_{St}i$ was calculated by Equation 13:

$$\frac{u(V_{St})i}{V_{St}i} = \sqrt{(\frac{u(V_{St}G)i}{V_{St}i})^2 + (\frac{u(V_{St}T)i}{V_{St}i})^2} \quad \text{(Eq. 13)}$$

The combined relative standard uncertainty of standard preparation expressed as the uncertainty of the concentration of UA/OA in standard solution - u_{St}/X was calculated by Equation 14:

$$\frac{u_{St}}{X} = \sqrt{(\frac{u(m_{St})}{W_{St}})^2 + \left(\sum_{i=1}^{k}\frac{u(V_{St})i}{V_{St}i}\right)^2} \quad \text{(Eq. 14)}$$

2.7.3 Standard Uncertainty of Sample Preparation

The combined relative standard uncertainty of sample preparation expressed as the uncertainty of the concentration of UA/OA in test solution – u_s/X was calculated as follows:

The relative standard uncertainty of the repeatability of weighting - $u(W_{rep})/W_s$ with rectangular distribution was calculated using Equation 15:

$$\frac{u(W_{rep})}{W_S} = \frac{SD}{W_S\times\sqrt{3}} \quad \text{(Eq. 15)}$$

Where SD - the standard deviation of the extracted product weights (n=6), mg, which was calculated using Equation 16:

$$SD = \sqrt{\frac{1}{(n-1)}\sum_{j=1}^{n}(W_i - W_S)^2} \quad \text{(Eq. 16)}$$

Where, W_i - the weight of each sample of the extracted product, mg.

The relative standard uncertainty of analytical balance - Equation 17 calculated $u(W_S)/W_S$ with rectangular distribution:

$$\frac{u(W_S)}{W_S} = \frac{\Delta_B}{W_S \times \sqrt{3}} \quad \text{(Eq. 17)}$$

The relative standard uncertainty of the mass of the sample of the extracted product - $u(m_S)/W_S$ was calculated using Equation 18:

$$\frac{u(m_S)}{W_S} = \sqrt{(\frac{u(W_S)}{W_S})^2 + (\frac{u(W_{rep})}{W_S})^2} \quad \text{(Eq. 18)}$$

The relative standard uncertainty of the used volumetric glassware – Equation 19 calculated $u(V_SG)/V_Si$ with triangular distribution:

$$\frac{u(V_SG)i}{V_Si} = \frac{\Delta_V}{V_Si \times \sqrt{6}} \quad \text{(Eq. 19)}$$

Where ΔV - the standard uncertainty of the glassware from the calibration certificate, mL; V_S - the measured dilution volume of the extracted product, mL sample.

The relative standard uncertainty of the temperature effect of the volumetric glassware - $u(V_ST)i/V_Si$ with rectangular distribution was calculated by Equation 20:

$$\frac{u(V_ST)i}{V_Si} = \frac{V_E}{V_Si \times \sqrt{3}} \quad \text{(Eq. 20)}$$

Where V_T - the expansion of the volume, mL was calculated by Equation 21:

$$\Delta_V = V_Si \times \Delta t \times \frac{0.00021}{1} \quad \text{(Eq. 21)}$$

Where, Δt – the half value of the temperature range in the laboratory room, ºC.

The relative standard uncertainty of the dilution volume of the sample - $u(V_S)i/V_Si$ using Equation 22:

$$\frac{u(V_S)i}{V_Si} = \sqrt{(\frac{u(V_SG)i}{V_Si})^2 + (\frac{u(V_ST)i}{V_Si})^2} \quad \text{(Eq. 22)}$$

The combined relative standard uncertainty of sample preparation – Equation 23 calculated u_S/X:

$$\frac{u_S}{X} = \sqrt{(\frac{u(m_S)}{W_S})^2 + \left(\sum_{i=1}^{k}\frac{u(V_S)i}{V_Si}\right)^2} \quad \text{(Eq. 23)}$$

2.7.4 Standard Uncertainty of the mass of the apple pomace

The combined relative standard uncertainty of the mass of the apple pomace – u(m)/W was calculated as follows:

The relative standard uncertainty of the repeatability of weighting balance - the Equation 24 calculated $u(W_{rep})/W$ with rectangular distribution:

$$\frac{u(W_{rep})}{W} = \frac{SD}{W \times \sqrt{3}} \quad \text{(Eq. 24)}$$

Where SD - the standard deviation of the weights of the apple pomace samples (n=6), g, which was calculated using Equation 25:

$$SD = \sqrt{\frac{1}{(n-1)}\sum_{j=1}^{n}(W_i - W)^2} \quad \text{(Eq. 25)}$$

The relative standard uncertainty of analytical balance - Equation 26 calculated u(W)/W with rectangular distribution:

$$\frac{u(W)}{W} = \frac{\Delta_B}{W \times \sqrt{3}} \quad \text{(Eq. 26)}$$

The combined relative standard uncertainty of the mass of the apple pomace – u(m)/W was calculated using Equation 27:

$$\frac{u(m)}{W} = \sqrt{(\frac{u(W_{rep})}{W})^2 + \left(\frac{u(W)}{W}\right)^2} \quad \text{(Eq. 27)}$$

2.7.5 Measurement Uncertainty of the Accuracy of the Method

In order to evaluate the standard uncertainty of the accuracy of the method - u_R, the

mean recovery value – R (R, %/100) and the relative standard deviation (RSD, %) of the percentage recoveries (n=3) were used based on the accuracy study of the combined method (Rubashvili *et al.*, 2020). Equation 28 calculated the standard uncertainty of the accuracy of the combined method:

$$u_R = \frac{RSD}{100\times\sqrt{3}} \qquad \text{(Eq. 28)}$$

2.7.6 Standard Uncertainty of Analytical Equipment - HPLC

The combined relative standard uncertainty of analytical equipment – HPLC system – u_E/A was calculated with rectangular distribution was calculated using Equation 29:

$$\frac{u(E)}{A} = \sqrt{\left(\frac{\Delta_E}{A_{St}\times\sqrt{3}}\right)^2 + \left(\frac{\Delta_E}{A_S\times\sqrt{3}}\right)^2} \qquad \text{(Eq. 29)}$$

Where ΔE - is the standard uncertainty of the HPLC system from the calibration certificate.

2.7.7 Combined Standard Uncertainty and Expanded Uncertainty of the Method

Combined B-type standard uncertainty – u_B was calculated using Equation 30:

$$u_B = X \times \sqrt{(c_1 \times \frac{u_{St}}{X})^2 + (c_2 \times \frac{u_S}{X})^2 + (c_3 \times \frac{u(m)}{W})^2 + (c_4 \times u_R)^2 + (c_5 \times \frac{u(E)}{A})^2} \qquad \text{(Eq. 30)}$$

Where c_i - the sensitivity coefficient was considered equal to 1 (Eurachem guide).

Equation 31 calculated the combined standard uncertainty of the combined method - u:

$$u = \sqrt{{u_A}^2 + {u_B}^2} \qquad \text{(Eq. 31)}$$

Equation 32 calculated the expanded uncertainty of the combined method - U:

$$U = u \times k \qquad \text{(Eq. 32)}$$

Where k - the coverage coefficient equals 1.96 for normal distribution and 1.65 for rectangular distribution, based on the calculated results of d-criteria for both analytes.

3. RESULTS AND DISCUSSION:

The measurement of the method was the content of UA/OA in the apple processing waste material (apple pomace), expressed in mg/g calculated by Equation 2. Each parameter that affects the value of the measurand is shown as a cause and effect Ishikawa diagram (Figure 3) (OMCL guideline; Ellison and Barwick,1998).

3.1. Results

The first source affected the measurand – the content of UA/OA in apple pomace (mg/g) was uncertainty arising from the repeatability of the method, which was carried out by preparing and injecting a standard solution with six replicates and six test solutions into the HPLC system by the validated method. Based on the obtained analytical data, the contents of UA/OA – X_i, mg/g in the samples of the apple pomace were calculated using Equation 2; Then, the standard deviation (n=6) of the contents of each analyte was used to evaluate the standard uncertainty of the repeatability of the method – u_A (A-type uncertainty) using Equation 3. The obtained results are given in Table 1.

Table 1. *The results of the repeatability and A type standard uncertainty*

№	The content of UA in apple pomace, mg/g	The content of OA in apple pomace, mg/g
1	6.93	4.49
2	7.39	4.64
3	6.86	4.71
4	7.34	4.99
5	7.01	4.74
6	6.83	4.66
Average	**7.06**	**4.70**
SD	**0.24**	**0.16**
n	**6**	**6**
u_A	**0.099**	**0.067**
d-Criteria	**0.9019**	**0.8990**

The second source that affected the measurand was uncertainty arising from standard preparation, which was calculated by the combined relative standard uncertainty of standard preparation – u_{st}/X (Equation 14). This source includes the following contributors: 1) the

relative standard uncertainty of analytical balance - $u(W_{St})/W_{St}$ (Equation 6); 2) the relative standard uncertainty of the standard purity $u(P_{St})/P_{St}$ (Equation 7); 3) the relative standard uncertainty of the molar mass of UA/OA - u(M)/M (Equation 8); 4) the relative standard uncertainty of the mass of standard - $u(m_{St})/W_{St}$ (Equation 9); 5) the relative standard uncertainty of the used volumetric glassware - $u(V_{St}G)/V_{St}i$ (Equation 10); 6) the relative standard uncertainty of the temperature effect of the volumetric glassware - $u(V_{St}T)i/V_{St}i$ (Equation 13). The obtained results of the combined relative standard uncertainty of standard preparation are given in Table 2.

The third source was evaluated by the combined relative standard uncertainty of sample preparation - u_s/X, which was calculated using Equation 23. This contains the following contributors: 1) the relative standard uncertainty of the repeatability of weighting - $u(W_{rep})/W_s$ (Equation 15); 2) the relative standard uncertainty of analytical balance (Equation 17); 3) the relative standard uncertainty of the mass of the sample of the extracted product - $u(m_S)/W_S$ (Equation 18); The relative standard uncertainty of the dilution volume of the sample - $u(V_S)i/V_Si$ (Equation 22). The results are given in Table 3.

The combined relative standard uncertainty of the mass of the apple pomace – u(m)/W calculated using Equation 27 was one of the determined main sources that affected the measurand. The source combines two contributors: 1) the relative standard uncertainty of the repeatability of weighting balance $u(W_{rep})/W$ (Equation 24) and 2) the relative standard uncertainty of analytical balance u(W)/W (Equation 26). The results are shown in Table 4.

The accuracy of the method was contributed to the value of the expanded uncertainty of the method. The standard uncertainty of the accuracy of the method - u_R was calculated using Equation 28 and is shown in Table 5.

Table 5. *The results of the accuracy of the method*

Parameter	UA	OA
R, %	96.85	4.70
RSD, % (n=3)	1.75	0.53
u_R	0.01	0.003

The last source that affected the measurand was uncertainty arising from analytical equipment – HPLC system. This source was evaluated by calculating the combined relative standard uncertainty of analytical equipment – u_E/A (Equation 29). The obtained results are given in Table 6.

Table 7. *The values of standard uncertainties and expanded uncertainty of the combined method expressed in mg/g*

Parameter	UA	OA
u_A	0.099	0.067
u_B	0.315	0.205
u	0.330	0.215
k	1.96	1.96
U	0.647	0.422

The values of the combined B-type standard uncertainty – u_B, the combined standard uncertainty – u, and the expanded uncertainty of the method – U calculated using Equations 30, 31, 32, respectively, are shown in Table 7. Based on the calculated results of d-criteria for both analytes, normal distribution of analytical data appeared in both cases. Accordingly, 1.96 was used as the coverage coefficient – k to calculate the expanded uncertainty value.

The content of each test compound expressed in mg per 1 g of the dry sample of the agroindustrial waste material (apple pomace) was calculated. The obtained results indicate that the content of UA and OA, mg/g in apple pomace varies from 6.86 to 7.39 mg/g and from 4.49 to 4.99 mg/g, respectively; the average content of UA and OA with the value of the expanded uncertainty is 7.06 ± 0.647 mg/g (k=1.96; P=95%) and 4.70 ± 0.422 mg/g (k=1.96; P=95%), respectively.

3.2. Discussion

The measurement uncertainty of the method includes all the uncertainties arising from each individual source and contributor determined by the cause and effect Ishikawa diagram and affected the measurand – the content of UA and OA in apple pomace expressed in mg per 1 g. There are observed six sources of all the contributors: 1) uncertainty of standard preparation; 2) uncertainty of sample preparation; 3) uncertainty of the accuracy of the method; 4) uncertainty of the repeatability of the method; 5) uncertainty of the mass of apple pomace sample,

and 6) uncertainty of the analytical equipment. Each source was evaluated, and the results show that all the contributors contributed to the combined standard uncertainty arising from both extraction and chromatographic analytical procedures. All the uncertainty sources equally affect the measurement of the method. The A-type standard uncertainty value was 3 times less than the B-type standard uncertainty for both analytes. The results show that B-type standard uncertainty is a major contributor and equals approximately 95 % of the combined standard uncertainty for both analytes. Therefore, the value of the expanded uncertainty of the validated method will not change from test to test in the same laboratory conditions by using the same equipment, instruments, and reagents during the routine intra-day or inter-day analyses, which confirms the suitability and robustness of the validated method.

4. CONCLUSIONS:

The hybrid approach used in the measurement uncertainty of the analytical method fully ensures a detailed assessment of uncertainty and consideration of all contributors. Furthermore, it is possible to reliably use the value of the expanded uncertainty calculated by this approach based on the method validation data in routine analyses so that the measurement uncertainty is not needed to calculate for each routine analysis. The presented work explains well the details and practical aspects of this approach and proposes the step-by-step methodology of measurement uncertainty according to Eurachem and EA guidelines which can be used to evaluate measurement uncertainty for other analytical HPLC methods. The proposed validated method with measurement uncertainty can be applied successfully to control ursolic and oleanolic acids in apple peel, apple pomace, any apple processing agroindustrial waste material, and the dry extracted product obtained from apple pomace.

5. DECLARATIONS

5.1. Study Limitations

The study is limited to the sample size and methods utilized, and no further limitations were known at the time of the study.

5.2. Funding source

The Shota Rustaveli National Science Foundation supported the research within the framework of fundamental research project #21-4196.

5.3. Competing Interests

The authors declare that there are no conflicts of interest in this publication.

7. REFERENCES:

1. Rubashvili, I; Tsitsagi, M; Zautashvili, M; Chkhaidze, M; Ebralidze, K; Tsitsishvili, V. (2020). Extraction and analysis of oleanolic acid and ursolic acid from apple processing waste materials using ultrasound-assisted extraction technique combined with high-performance liquid chromatography. *Revue Roumaine de Chimie,* 65(10), 919-928. DOI: 10.33224/rrch.2020.65.10.07

2. Liese, J; Abhari, B.A; Fulda, S. (2015). Smac mimetic and oleanolic acid synergize to induce cell death in human hepatocellular carcinoma cells. *Cancer Letters,* 365, 47-56. DOI: 10.1016/j.canlet.2015.04.018

3. Khwaza, V; Oyedeji, O.O; Aderibigbe, B.A. (2020). Ursolic Acid-Based Derivatives as Potential Anti-Cancer Agents: An Update. *International Journal of Molecular Sciences,* 21, 5920. DOI: 10.3390/ijms21165920

4. Jin, H; Pi, J; Yang, F; Wu, C; Cheng, X; Bai, H; Chen, Z.W. (2016). Ursolic acid-loaded chitosan nanoparticles induce potent anti-angiogenesis in tumor. *Biotechnological products and process engineering,* 100, 6643-6652. DOI: 10.1007/s00253-016-7360-8

5. Woźniak, L; Skąpska, S; Marszałek, K. (2015). Ursolic Acid--A Pentacyclic Triterpenoid with a Wide Spectrum of Pharmacological Activities. *Molecules,* 20(11), 20614–20641. DOI: 10.3390/molecules201119721

6. Kashyap, D; H. S. Tuli, H. S; Sharma, A. K. (2016). Ursolic acid (UA): A metabolite with promising therapeutic potential. *Life Sciences,* 146, 201-213. DOI: 10.1016/j.lfs.2016.01.017

7. Alvarado, H. L; Abrego, G; Garduño-Ramirez, M.L; Clares, B; Garcia, M. L; Calpena, A. C. (2015*).* Design and optimization of oleanolic/ursolic acid-loaded nanoplatforms for ocular anti-inflammatory applications*. Nanomedicine: Nanotechnology, Biology and Medicine*, 11(3) 521-530. DOI: 10.1016/j.nano.2015.01.004

8. Jebali, S; Bahri, S; Latrous, L. (2020). Estimation of measurement uncertainty and validation of RP-HPLC for simultaneous determination of fve antihistamines in pharmaceutical formulations. *Accreditation and Quality Assurance*, 25,147–159. DOI: 10.1007/s00769-019-01422-7

9. PA/PH/OMCL (18) 145 R1 CORR. (2020). Evaluation of Measurement Uncertainty (Core Document). ISO/IEC 17025:2017. (2017). General requirements for the competence of testing and calibration laboratories. https://www.edqm.eu/documents/52006/128968/omcl-evaluation-of-measurement-uncertainty-core-document.pdf/b9b88e44-e831-4221-9926-d8c6e8afe796?t=1628491784923

10. Ellison, S.L.R; Rosslein, M; Williams, A. (2012). Quantifying uncertainty in analytical measurement. EURACHEM/ CITAG Guide CG4. Third edition. Eurachem/CITAC. https://www.eurachem.org/images/stories/Guides/pdf/QUAM2012_P1.pdf

11. Rubashvili, I; Tsitsishvili, V. (2015) Quantitative Estimation of volatile N-nitrosamines in Tobacco Smoke Using Validated GC-MS Method and its Uncertainty Evaluation, Illustrated by determination of N-nitrosomethylethylamine. *The Bulletin of the Georgian National Academy of Sciences*, 9(1), 85-92.

12. Senila, M; Drolc, A; Pintar, A; Senila, L; Levei, E. (2014). Validation and measurement uncertainty evaluation of the ICP-OES method for the multi-elemental determination of essential and nonessential elements from medicinal plants and their aqueous extracts 1 Validation and measurement. *Journal of Analytical Science and Technology*, 5(37), 1-9.

13. EA-4/16 G:2003. (2003). EA guidelines on the expression of uncertainty in quantitative testing. https://european-accreditation.org/wp-content/uploads/2018/10/ea-4-16-g-rev00-december-2003-rev.pdf

14. Barwick V; Ellison, S. (2000). VAM Project 3.2.1, Part (d): protocol for uncertainty evaluation from validation data. In: Development and harmonisation of measurement uncertainty principles, LGC/VAM/1998/088, TEDDINGTON. http://www.demarcheiso17025.com/private/Protocol%20for%20uncertainty%20evaluation%20from%20validation%20data.pdf

15. Barwick V. (2012). The top down “approach to uncertainty estimation”. Evaluating measurement uncertainty in clinical chemistry, LGC/R/2010/17, UK. http://www.demarcheiso17025.com/private/Evaluating%20measurement%20uncertainty%20in%20clinical%20chemistry.pdf

16. Eurolab. (2002). Measurement uncertainty in testing, a short introduction on how to characterise accuracy and reliability of results including a list of useful references, Technical Report No. 1. https://www.eurolab.org/pubs-techreports

17. Ellison, S; Barwick, V. (1998). Using

Validation data for ISO measurement uncertainty estimation. Part 1: principles of an approach using cause and efect analysis. *Analyst,* 123, 1387–1392. DOI: 10.1039/A706946D

18. ISO Guide 98-3, Uncertainty of measurement - Part 3: Guide to the expression of uncertainty in measurement (GUM). https://www.iso.org/standard/50461.html

19. Evaluation of measurement data - Guide to the expression of uncertainty in measurement, JCGM 100:2008. https://www.bipm.org/documents/20126/2071204/JCGM_100_2008_E.pdf/cb0ef43f-baa5-11cf-3f85-4dcd86f77bd6

20. Meyer, V.R. (2003). measurement uncertainty of liquid chromatographic analyses visualized by ishikawa diagrams. *Journal of Chromatographic Science,* 41, 439-443.

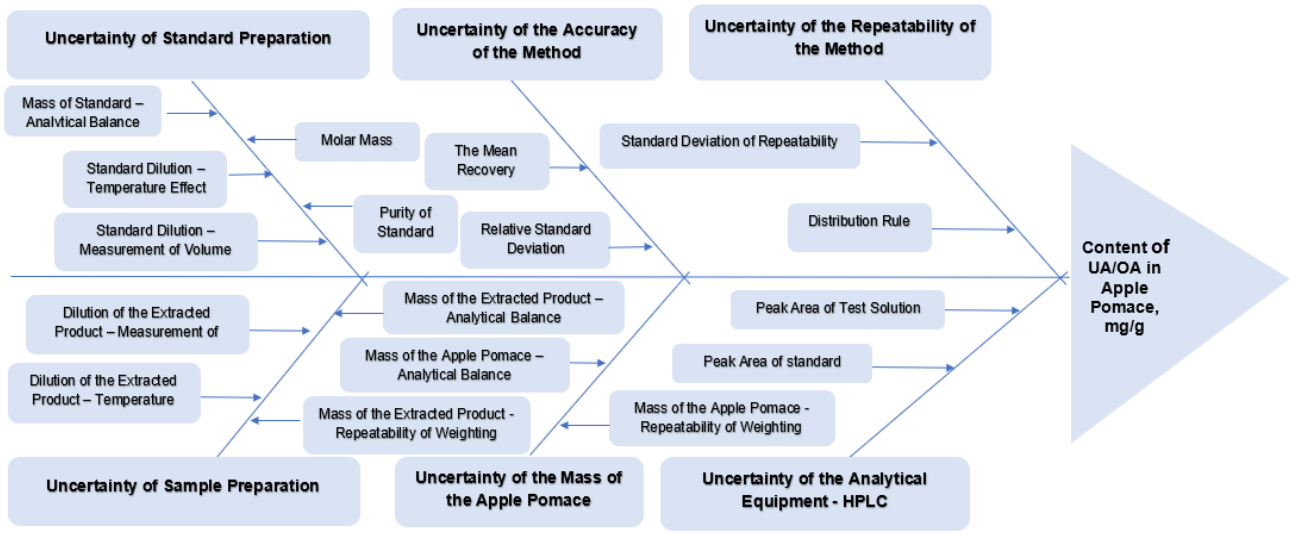

Figure 3. The cause and effect ishikawa diagram.

Table 2. *The budget of evaluation of measurement uncertainty of standard preparation*

№	Contributor	Value	Type	Unit	Relative Standard Uncertainty of Contributor	Distribution	Sensitivity Coefficient	Relative Standard Uncertainty
Ursolic Acid								
1	Mass of Standard - Analytical Balance - $u(W_{St})/W_{St}$	10.5	B	mg	0.00055	Rectangular	1	
2	Purity of Standard - $u(P_{St})/P_{St}$	96	B	%	0.00107	Rectangular	1	0.00121
3	Molar Mass - u(M)/M	456.7	B	g/mol	0.000004	Rectangular	1	
4	Dilution of Standard – Measurement of Volume - $u(V_{St}G)/V_{St}i$	50	B	mL	0.00049	Triangular	1	
5	Dilution of Standard - Temperature Effect - $u(V_{St}T)i/V_{St}i$	50	B	mL	0.00036	Rectangular	1	0.00576
6	Dilution of Standard – Measurement of Volume - $u(V_{St}G)/V_{St}i$	5	B	mL	0.000572	Triangular	1	
7	Dilution of Standard - Temperature Effect - $u(V_{St}T)i/V_{St}i$	5	B	mL	0.00036	Rectangular	1	
Combined relative standard uncertainty – u_{st}/X								0.00588
Oleanolic Acid								
1	Mass of Standard - Analytical Balance - $u(W_{St})/W_{St}$	12.5	B	mg	0.00046	Rectangular	1	
2	Purity of Standard - $u(P_{St})/P_{St}$	98	B	%	0.00075	Rectangular	1	0.00088
3	Molar Mass - u(M)/M	456.7	B	g/mol	0.000004	Rectangular	1	
4	Dilution of Standard – Measurement of Volume - $u(V_{St}G)/V_{St}i$	50	B	mL	0.00049	Triangular	1	
5	Dilution of Standard - Temperature Effect - $u(V_{St}T)i/V_{St}i$	50	B	mL	0.00036	Rectangular	1	0.00576
6	Dilution of Standard – Measurement of Volume - $u(V_{St}G)/V_{St}i$	5	B	mL	0.000572	Triangular	1	
7	Dilution of Standard - Temperature Effect - $u(V_{St}T)i/V_{St}i$	5	B	mL	0.00036	Rectangular	1	
Combined relative standard uncertainty – u_{st}/X								0.00583

Table 3. *The budget of evaluation of measurement uncertainty of sample preparation*

№	Contributor	Value	Type	Unit	Relative Standard Uncertainty of Contributor	Distribution	Sensitivity Coefficient	Relative Standard Uncertainty
Ursolic Acid								
1	Mass of Sample - Analytical Balance - $u(W_S)/W_S$	11.8	B	mg	0.00049	Rectangular	1	0.04329
2	Repeatability of Weighting - $u(W_{rep})/W_s$	11.8	A	mg	0.043328	Rectangular	1	
3	Dilution of Sample - Measurement of Volume - $u(V_SG)/V_Si$	50	B	mL	0.00049	Triangular	1	0.00061
4	Dilution of Sample - Temperature Effect - $u(V_{St}T)i/V_{St}i$	50	B	mL	0.00036	Rectangular	1	
Combined relative standard uncertainty – u_s/X								0.04329
Oleanolic Acid								
1	Mass of Sample - Analytical Balance - $u(W_S)/W_S$	11.8	B	mg	0.00049	Rectangular	1	0.04329
2	Repeatability of Weighting - $u(W_{rep})/W_s$	11.8	A	mg	0.043328	Rectangular	1	
3	Dilution of Sample - Measurement of Volume - $u(V_SG)/V_Si$	50	B	mL	0.00049	Triangular	1	0.00061
4	Dilution of Sample - Temperature Effect - $u(V_{St}T)i/V_{St}i$	50	B	mL	0.00036	Rectangular	1	
Combined relative standard uncertainty – u_s/X								0.04329

Table 4. *The budget of evaluation of measurement uncertainty of the mass of apple pomace*

№	Contributor	Value	Type	Unit	Relative Standard Uncertainty of Contributor	Distribution	Sensitivity Coefficient	Relative Standard Uncertainty
Ursolic Acid								
1	Mass of Sample - Analytical Balance - u(W)/W	10.38	B	g	0.0000006	Rectangular	1	0.00409
2	Repeatability of Weighting - $u(W_{rep})/W$	10.38	A	g	0.00409	Rectangular	1	
Combined relative standard uncertainty – u(m)/W								0.00409
Oleanolic Acid								
1	Mass of Sample - Analytical Balance - u(W)/W	10.38	B	g	0.0000006	Rectangular	1	0.00409
2	Repeatability of Weighting - $u(W_{rep})/W$	10.38	A	g	0.00409	Rectangular	1	
Combined relative standard uncertainty – u(m)/W								0.00409

Table 6. *The budget of evaluation of measurement uncertainty of analytical equipment - HPLC*

№	Contributor	Value	Type	Unit	Relative Standard Uncertainty of Contributor	Distribution	Sensitivity Coefficient	Relative Standard Uncertainty
Ursolic Acid								
1	Peak area of the standard solution - HPLC	1781997.00	B	mAU	0.00029	Rectangular	1	0.00042
2	Peak area of the test solution - HPLC	2345089.83	B	mAU	0.00029	Rectangular	1	
Combined relative standard uncertainty – u_E/A								0.00042
Oleanolic Acid								
1	Peak area of the standard solution - HPLC	3230243.17	B	mAU	0.00029	Rectangular	1	0.00042
2	Peak area of the test solution - HPLC	2349147.33	B	mAU	0.00029	Rectangular	1	
Combined relative standard uncertainty – u_E/A								0.00042

PERIÓDICO TCHÊ QUÍMICA
NOTA EDITORIAL

FERRAMENTA PARA CRIAÇÃO DE RESUMOS

ABSTRACT MAKER TOOL (A. M. T.)

DE BONI, Luis Alcides Brandini[1*]

[1] Periódoco Tchê Química. Brazil.

** Corresponding author*
e-mail: journal.tq@gmail.com

There are different ways that the authors can present the abstract of a manuscript. However, with the evolution of the journal and the passing of time, the Periodico Tchê Química adopted the structured format of the abstract.

The structured abstract is intended to be comprehensive, providing a logical order for the presentation of scientific communication. It also provides the readers with a summary of the research background, objectives, methods, results, and conclusions. It is not complicated to do, but frequently the authors may forget to include parts of its content; therefore, this tool was developed, so the authors can enjoy the writing of the abstract in a very straightforward way.

To access the AMT environment at tchequimica.com, please click on the highlighted icon from Figures 1 or 2, or type the URL < https://www.tchequimica.com/en/abstract_maker.php >.

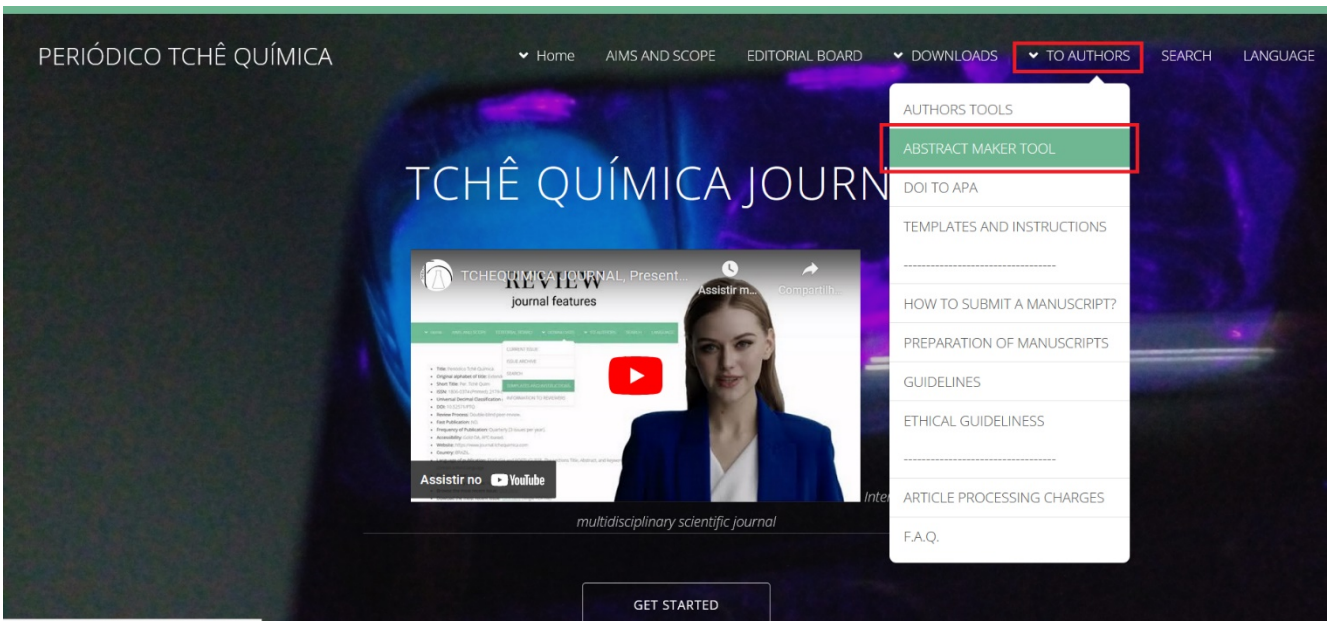

Figure 1. Locating the AMT link on the navigation bar.

DOI: NO DOI REQUIRED

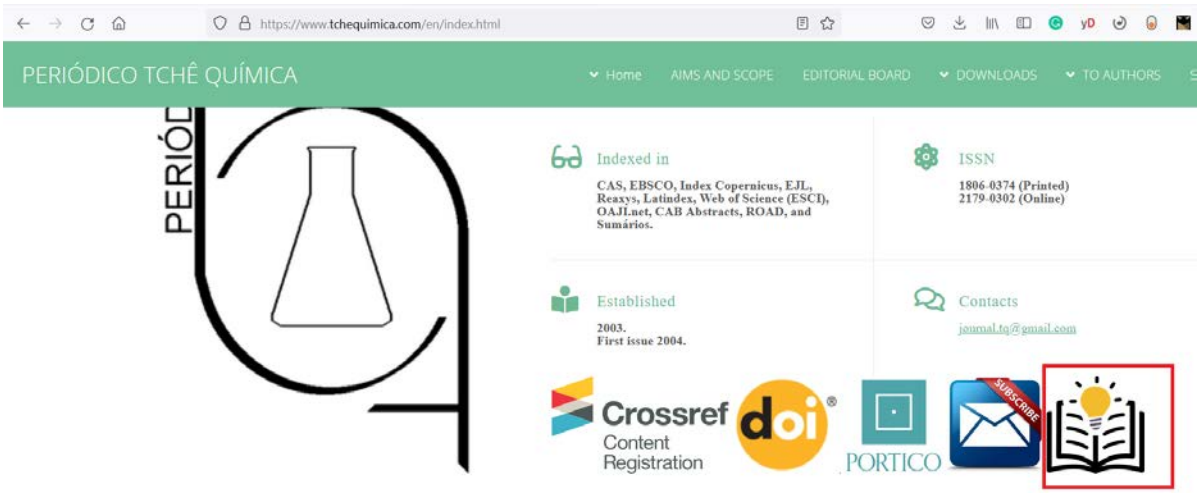

Figure 2. Locating the AMT icon at the website.

When exploring the environment of the A. M. T. (script version 1.3), the authors will initially find a collection of text boxes to include the proper text (background, aims…), as in Figure 3.

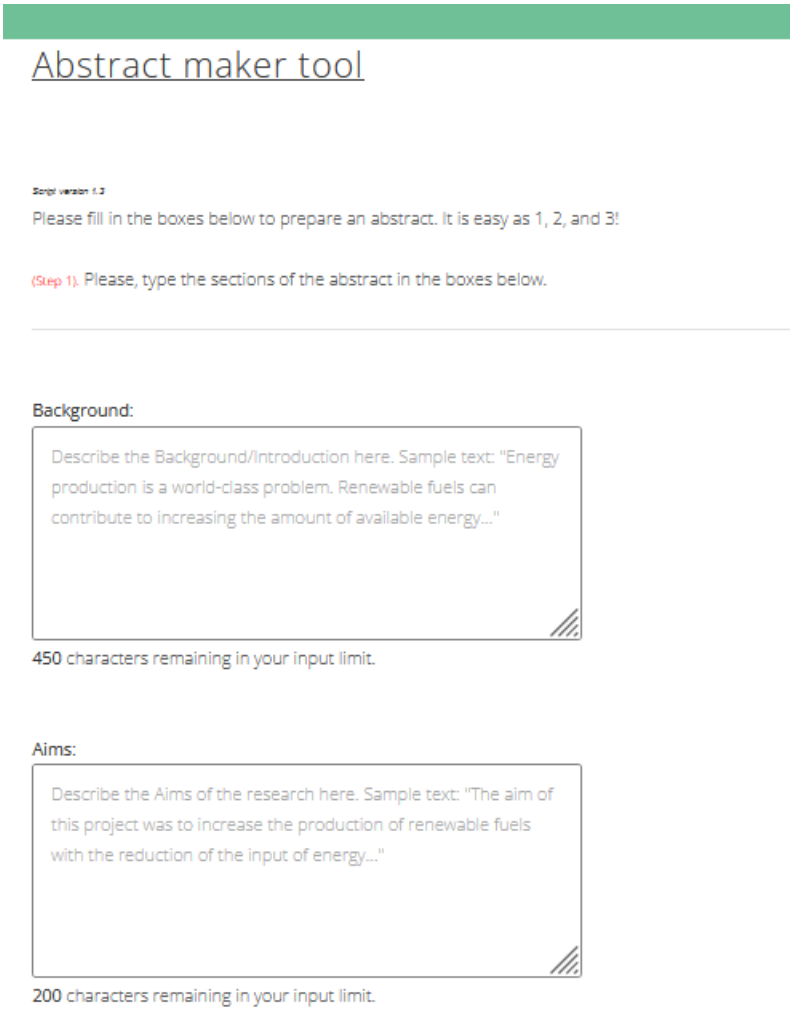

Figure 3. Textfield introduction areas for the abstract maker tool.

If the authors have a browser with a dictionary or spellchecker installed, recommendations for text corrections will be made available instantaneously.

After completing the text boxes, the authors will locate a submission button, as in Figure 4. It is expected that the authors press the submit button.

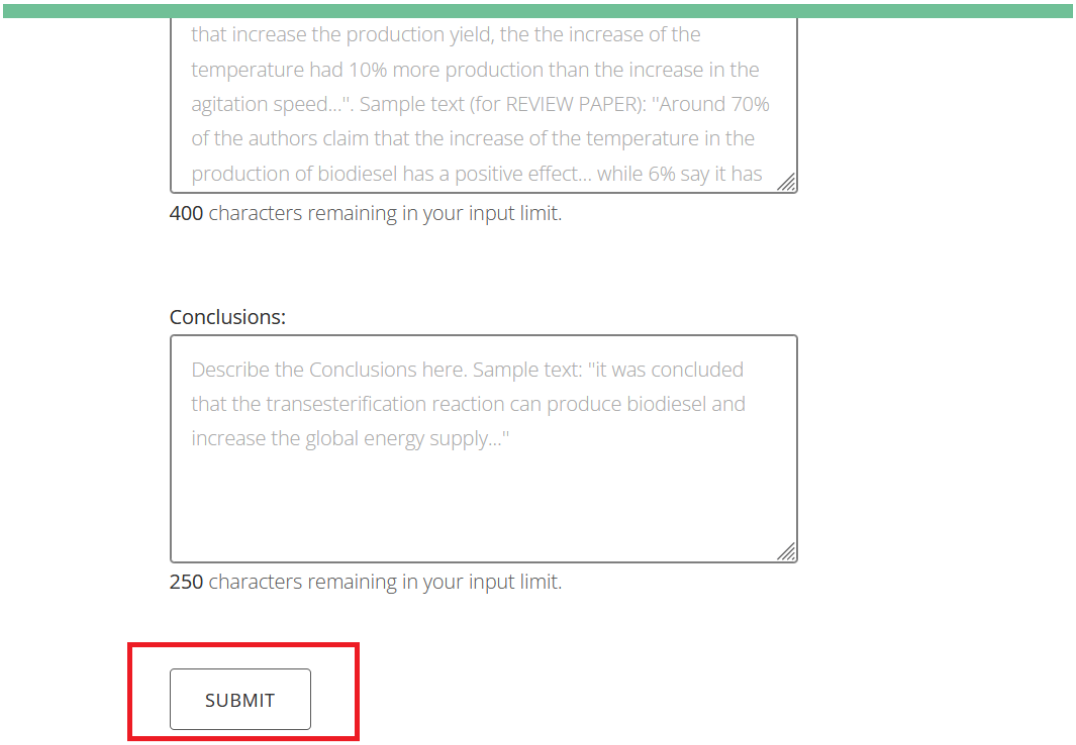

Figure 4. Submit button to generate the text paragraph.

After pressing the submit button, the authors should go to step 2. In step 2, it is possible to see the abstract generated with the previously informed text, according to Figure 5.

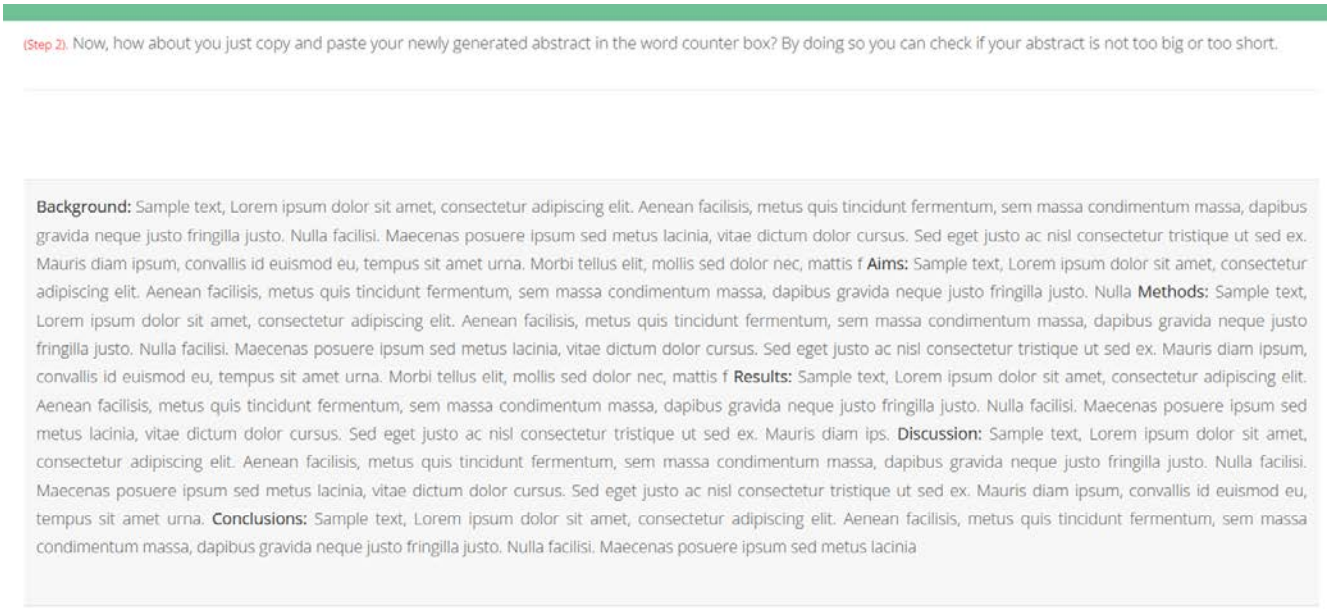

Figure 5. Paragraph preview.

As a final step, the authors can copy and paste the text into a word counter box, Figure 6. In this box, the authors can measure the abstract size if it is too extensive or too short. For example, the Southern Journal of Sciences recommends that the abstract section should have around 250 and 350 words. The word counter box also allows text edition, making the adjustments faster.

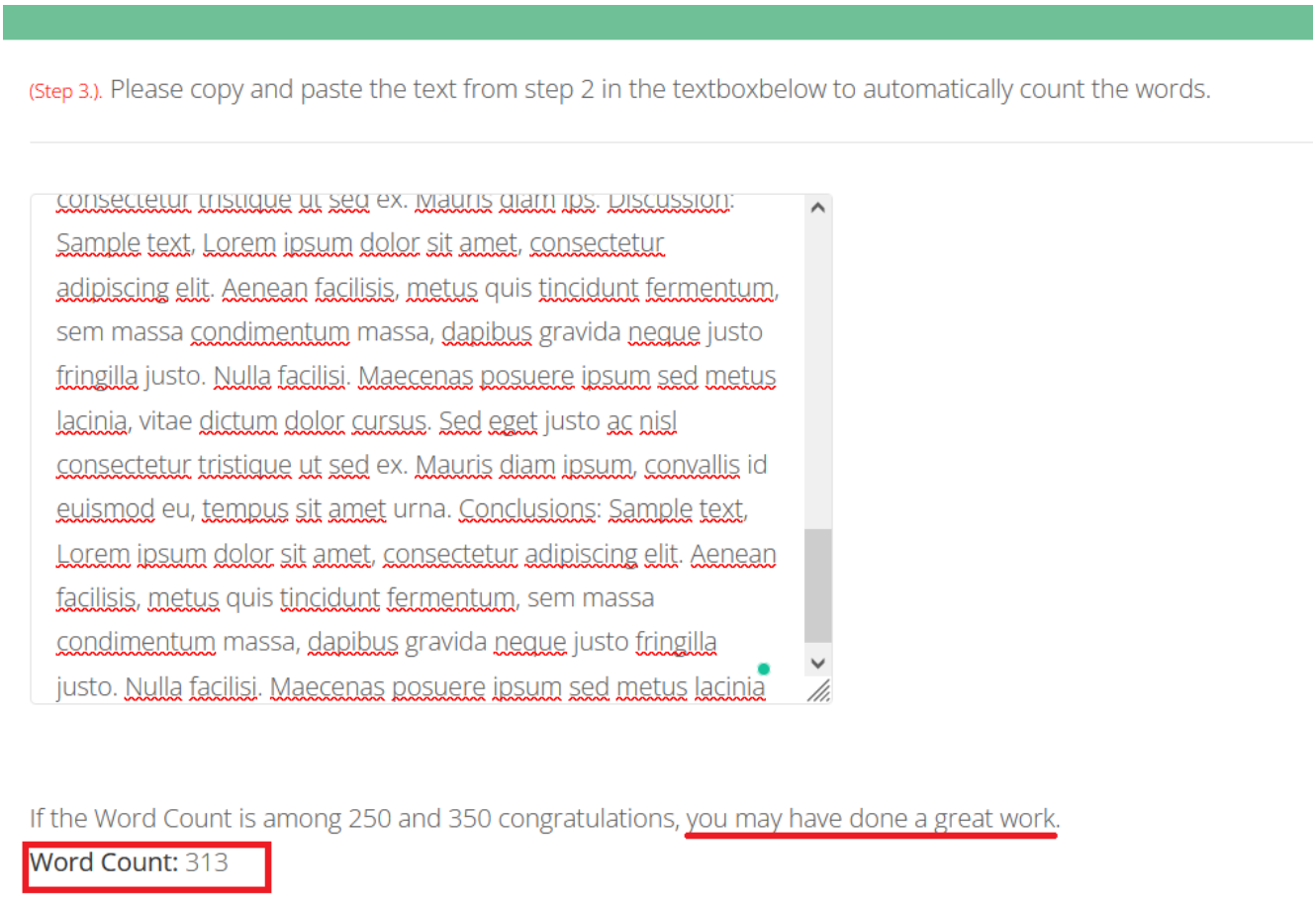

Figure 6. Word counter box.

If the authors are satisfied with the results, they can copy and paste the abstract directly into the journal template file. Therefore, this tool assists the authors in the production of a complete, proportional, and structured abstract, making the submission and review process faster. The tool is freely available at https://www.tchequimica.com/en/abstract_maker.php.

NOVA INTERFACE PARA APRESENTAÇÃO DO JORNAL E PRODUTOS RELACIONADOS

NEW INTERFACE FOR PRESENTING THE NEWSPAPER AND RELATED PRODUCTS

DE BONI, Luis Alcides Brandini[1*]

[1] Periódoco Tchê Química. Brazil.

** Corresponding author*
e-mail: journal.tq@gmail.com

Please scan the codes to see the results.

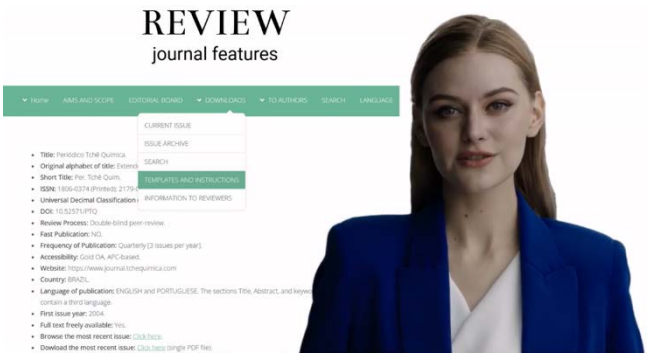

SCAN ME

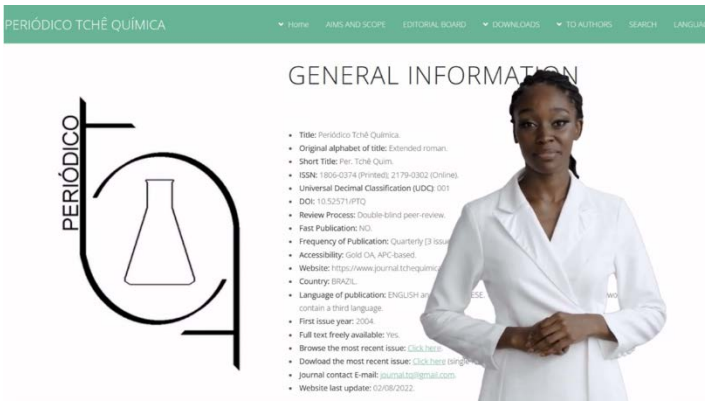

SCAN ME

VIDEO ABSTRACTS

Supplement material of this edition

Click on the image		Scan the code
	SEROPREVALENCE OF COVID-19 IGG ANTIBO… Background: Estimation of seroprevalence of COVID-19 antibodies can be used to more…	
	EFFECT OF AMAZON CACTUS AS A NATURAL … Background: Brazil suffers from a lack of basic sanitation in many regions, intensified in the…	
	SYNTHESIS, DOCKING STUDY, AND BIOLOGIC… Background: 4-aminoantipyrine is one of the pyrazolone derivatives, it has been exposed to a…	
	USE OF RGB AS A QUANTITATIVE METHOD AP… Background: The use of alternatives for teaching analytical chemistry in undergraduate studies has…	
	MEASUREMENT UNCERTAINTY EVALUATION … Background: Apple pomace represents a low-cost and rich source of bioactive compounds with…	
	IN SILICO STUDIES OF DITERPENES EXTRACT… Introduction: HIV, whose viral multiplication is associated with three enzymes. Reverse…	